CANADIAN THESES ON MICROFICHE

THÈSES CANADIENNES SUR MICROFICHE

NOTICE

The quality of this microfiche is heavily dependent upon the quality of the original thesis submitted for microfilming. Every effort has been made to ensure the highest quality of reproduction possible.

If pages are missing, contact the university which granted the degree.

Some pages may have indistinct print especially if the original pages were typed with a poor typewriter ribbon or if the university sent us an inferior photocopy.

Previously copyrighted materials (journal articles, published tests, etc.) are not filmed.

Reproduction in full or in part of this film is governed by the Canadian Copyright Act, R.S.C. 1970, c. C-30. Please read the authorization forms which accompany this thesis.

AVIS

La qualité de cette microfiche dépend grandement de la qualité de la thèse soumise au microfilmage. Nous avons tout fait pour assurer une qualité supérieure de reproduction.

S'il manque des pages, veuillez communiquer avec l'université qui a conféré le grade.

La qualité d'impression de certaines pages peut laisser à désirer, surtout si les pages originales ont été dactylographiées à l'aide d'un ruban usé ou si l'université nous a fait parvenir une photocopie de qualité inférieure.

Les documents qui font déjà l'objet d'un droit d'auteur (articles de revue, examens publiés, etc.) ne sont pas microfilmés.

La reproduction, même partielle, de ce microfilm est soumise à la Loi canadienne sur le droit d'auteur, SRC 1970, c. C-30. Veuillez prendre connaissance des formules d'autorisation qui accompagnent cette thèse.

THIS DISSERTATION HAS BEEN MICROFILMED EXACTLY AS RECEIVED

LA THÈSE A ÉTÉ MICROFILMÉE TELLE QUE NOUS L'AVONS REÇUE

Canadä

O 315-19438-3

PERMISSION TO MICROFILM — AUTORISATION DE MICROFILMER

• Please print or type — Écrire en lettres moulées ou dactylographier

Full Name of Author — Nom complet de l'auteur

Sabah Yacoub MANSOUR

Date of Birth — Date de naissance

Oct. 15, 1942

Country of Birth — Lieu de naissance

IRAQ

Permanent Address — Résidence fixe

c/o DEPT. OF ELECTRICAL ENGINEERING
UNIVERSITY OF ALBERTA
EDMONTON, ALBERTA, T6G 2E1

Title of Thesis — Titre de la thèse

POWER SYSTEMS ECONOMIC DISPATCH
USING NETWORK LOSS MODELS

University — Université

ALBERTA

Degree for which thesis was presented — Grade pour lequel cette thèse fut présentée

Ph.D. ELECTRICAL ENGINEERING

Year this degree conferred — Année d'obtention de ce grade

1985

Name of Supervisor — Nom du directeur de thèse

DR. D.H. Kelly and Dr. D.O. Koval

Date

Jan. 24, 1985

Signature

THE UNIVERSITY OF ALBERTA

POWER SYSTEMS ECONOMIC DISPATCH USING NETWORK LOSS MODELS

by

SABAH YACOUB MANSOUR

©

A THESIS

SUBMITTED TO THE FACULTY OF GRADUATE STUDIES AND RESEARCH

IN PARTIAL FULFILMENT OF THE REQUIREMENTS FOR THE DEGREE

OF DOCTOR OF PHILOSOPHY

DEPARTMENT OF ELECTRICAL ENGINEERING

EDMONTON, ALBERTA

SPRING 1985

THE UNIVERSITY OF ALBERTA

RELEASE FORM

NAME OF AUTHOR   SABAH YACOUB MANSOUR

TITLE OF THESIS   POWER SYSTEMS ECONOMIC DISPATCH USING NETWORK
LOSS MODELS

DEGREE FOR WHICH THESIS WAS PRESENTED   DOCTOR OF PHILOSOPHY

YEAR THIS DEGREE GRANTED   1985

Permission is hereby granted to the UNIVERSITY OF ALBERTA

to reproduce single copies of this thesis and to lend or sell

such copies for private, scholarly or scientific purposes only.

The author reserves other publication rights, and neither

the thesis nor extensive extracts from it may be printed or

otherwise reproduced without the author's written permission.

(Signed) ....

PERMANENT ADDRESS:

DEPT. OF ELECTRICAL ENGINEERING

UNIVERSITY OF ALBERTA

EDMONTON, ALBERTA, CANADA

DATED .....Nov. 2.....19 84

THE UNIVERSITY OF ALBERTA

FACULTY OF GRADUATE STUDIES AND RESEARCH

The undersigned certify that they have read, and recommend to the
Faculty of Graduate Studies and Research, for acceptance, a thesis
entitled POWER SYSTEMS ECONOMIC DISPATCH USING NETWORK LOSS MODELS
submitted by SABAH YACOUB MANSOUR, in partial fulfilment of the
requirements for the degree of Doctor of Philosophy in Electrical
Engineering.

....
Joint Supervisor

....
Joint Supervisor

....

....

....

....
External Examiner

Date : Nov 2, 1984

ABSTRACT

This thesis deals with the definition and evaluation of the economic operating conditions of electrical power systems. Two new methods are proposed for the solution of the optimum economic dispatch problem in electric power utilities. The two new methods presented have been rigorously tested and found to be quite successful. The first method is suitable for small power networks which contain a small number of generation buses. The second method is an extension of the first, formulated using diakoptical techniques to handle large power system networks. The use of network tearing techniques in the second method minimizes computational time, storage and numerical errors.

In the proposed methods, the constrained fuel cost function minimization procedure is based on the evaluated power loss model (or models) of the power system under consideration. The loss model parameters of a particular network are evaluated with a high degree of accuracy by the ridge regression estimation technique from a set of load flow studies of the power system. These base load flow solutions are obtained for different load and voltage levels which define a feasible operating region through which a search is conducted for the optimal solution.

The cost function used in the above methods, relates the total fuel cost to the active power generations of the individual power plants. The network loss models that are investigated in this thesis are the active power loss model which relates the network total active power losses to active power generations, and the active-reactive power loss model. The latter model is divided into two separate submodels. The first submodel relates the network total active and reactive power

losses to the active and reactive powers of the generation buses of the network. The second submodel treats the purely reactive sources of the network which are expressed as functions of the network total reactive load demand. The advantages of the separation of sources are discussed in this thesis.

Based on the evaluated network model (or models), the economic dispatch conditions of the power system under consideration, are obtained for different system load levels. The accuracy of the evaluated loss models and the validity of the economic dispatch solutions are verified in this thesis. The proposed methods are simple to implement and produce accurate dispatch solutions for different system load levels. These methods can handle ill-conditioned situations and are not sensitive to load flow mismatches in comparison to other optimal methods. The methods are suitable for on-line economic dispatch of power systems as the bulk of the computational effort can be done off-line. The proposed methods are used to evaluate the economic dispatch schedules of common standard test systems.

ACKNOWLEDGEMENTS

TABLE OF CONTENTS

x

LIST OF TABLES

LIST OF FIGURES

CHAPTER I

INTRODUCTION

The problem of minimizing the total fuel costs in electric power systems has long been of concern to utilities. In recent years, the growth of computing capability along with sharp increases in fuel costs, have increased interest in this aspect of power system operation. The literature documents various approaches to this complex problem. In this thesis, new approaches to evaluate the economic dispatch schedules of a power system using network loss models are presented and tested.

1.1 The Electric Power System

A typical power system basically consists of a complex transmission network which interconnects the sources of energy (i.e., generation plants) to the load centers which are scattered throughout a large geographical area. A functional diagram of a typical power system is shown in Figure 1.1. The transmission network configuration is dependent upon the available energy sources and the geographical location of the load centers.

1.2 Power System Operation

The optimum economic operation of transmission and distribution of electrical energy depends on the delivery system configuration, the nature and patterns of energy utilization and sources of electrical energy (e.g., thermal, nuclear, hydro, wind, solar, geothermal, etc.). A power system is required to operate optimally with respect to economy, security and environmental constraints (1,2). Various mathematical tools have been developed for the analysis of power systems. The analytical tools that are of concern in this thesis, are those used to determine the economic dispatch schedules of power systems. The base

1

G₁ ·········· Gₘ

Generating
plants

TRANSMISSION NETWORK

BULK POWER SUBSTATION

SUBTRANSMISSION NETWORK

SUBSTATION (DISTRIBUTION)

LOAD DEMAND
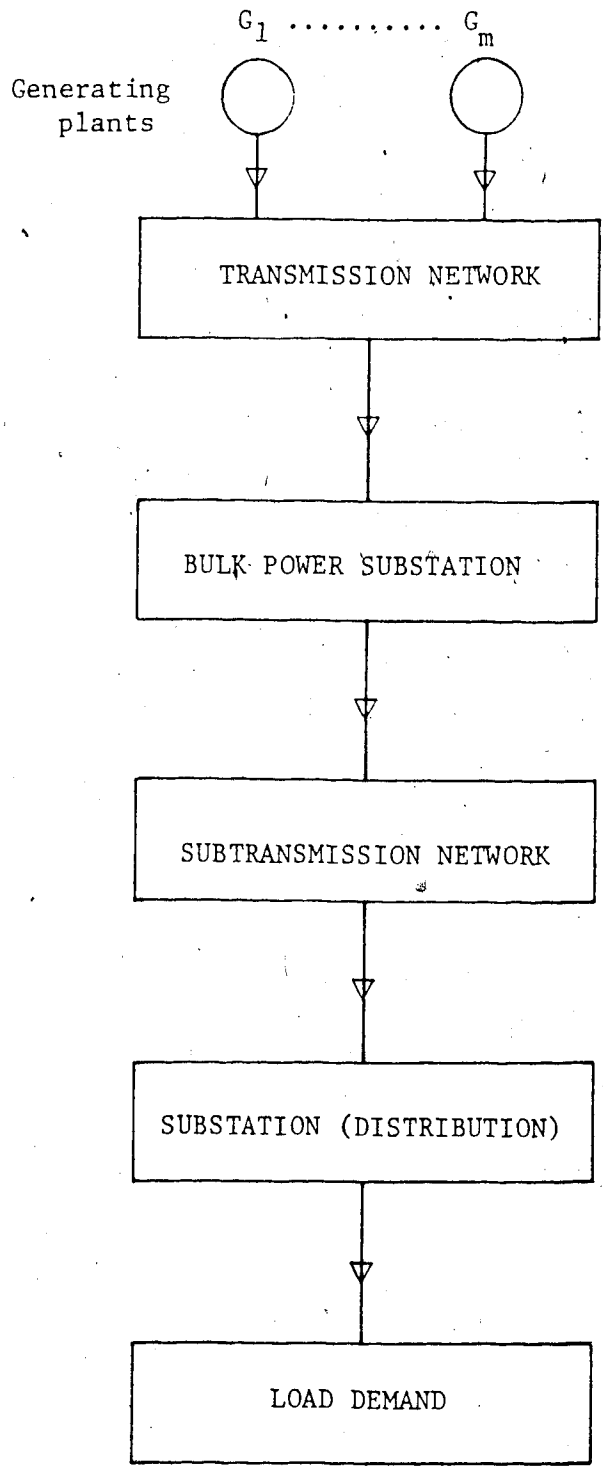
Figure 1.1 Functional diagram of a

typical power system

for the use of these dispatch methods is the load flow algorithm

(3-8). This algorithm basically solves the nodal equations of the

network taking into account the non-linear relationship between the

currents and power flows. The algorithm provides a complete solution

of the steady state voltages, active and reactive power flows in the

system.

1.3 The Economic Dispatch Problem

The direction of research is to develop simple, fast and efficient

algorithms to economically schedule power system generations for given

load demands. Various methods to solve the economic dispatch problem

in electric power systems are documented in the literature (9-16). The

classical method (1), uses the B-coefficient loss model to represent

the transmission network in the cost function minimization procedure.

This method is simple but involves many assumptions and refinements

can be cumbersome. Optimal load flow techniques (17-21), promise accurate

dispatch solutions, but these methods are sensitive to load flow mis-

matches and may have convergence problems. In recent years, new

approaches to the economic dispatch problem have been developed (22-24).

In these methods, the network loss model coefficients are evaluated by

least squares or similar methods from load flow results of the power

system. These methods produce accurate dispatch solutions for small

power networks operating at nominal loads. Brief descriptions of the

classical approach, the optimal load flow technique and the least

squares based economic dispatch method, and discussions of their

computational problems and limitations are presented in the next section.

The final part of this chapter outlines the research objectives of

this thesis.

1.3.1 The Classical Economic Dispatch Method

The Classical method is a Lagrange multiplier approach to the fuel cost minimization problem. The approach uses the B-coefficient method to evaluate the power system losses. This loss evaluation is the weak point in the method. In this approach the system total active power loss is expressed as a quadratic function of generator powers. The coefficients of the quadratic model are assumed to be constant. This constancy depends upon the following assumptions:

1. the voltages and angles at the source nodes remain constant;

2. the power factor at each source remains constant;

3. the ratio of load currents to the total current remain constant.

With these assumptions, the network can be reduced to a radial equivalent with a single equivalent load node (1,4). Since the above assumptions are not strictly true, the loss coefficients will only be valid over a small range of loadings in the region of the base case. Various methods to counter this problem, such as the use of sensitivity parameters or re-evaluation of the loss coefficients coupled with load flows and dispatch solutions have been used. However, such approaches require considerable computational effort for each case under consideration. The mathematical formulation of the classical method for the evaluation of the economic dispatch schedules of a thermal power system is given below.

1.3.1.1 The Classical Dispatch Method - Formulation

The power network is represented by the following B-coefficient

model:

$$P_L = P_G^T \cdot B \; P_G \qquad\qquad (1.1)$$

where,

P_L - the network total active power losses in MW

P_G - the network active power generation vector in MW

B - the B-coefficient matrix

To obtain the economic dispatch schedules of the power system under consideration; a cost function F_0 is minimized subject to the net active power balance using the Lagrangian formulation as given below:

minimize F_0 subject to:

$$P_D + P_L - \sum_{i=1}^{m} P_{Gi} = 0.0 \qquad\qquad (1.2)$$

where,

F_0 - a cost function relating the total operating cost to active power generations in $/h

P_D - the network total active load demand in MW

P_{Gi} - the active power generation of the ith generating unit in MW

m - the number of generating units of the power system

Using the Lagrangian formulation, the constrained minimization problem is converted into an unconstrained minimization problem as given below:

$$F_A = F_0 + \lambda_p \left[P_D + P_L - \sum_{i=1}^{m} P_{Gi} \right] \qquad (1.3)$$

where,

F_A - the augmented (Lagrangian) cost function

λ_p - Lagrange type multiplier

Equation 1.3 may be written in compact form as:

$$F_A = F_0(\underline{U}) + \lambda_p [F(\underline{U})] \qquad (1.4)$$

where

$\underline{U}$ - the control vector

The economic dispatch solution of the power system under consideration is obtained by differentiating equation 1.4 with respect to the control variables and λ_p and equating the resulting set of equations to zero. A suitable numerical method can be used to solve for the economic generation requirements of the power system.

1.3.2 The Optimal Load Flow Technique

In this method, the ordinary load flow program is modified to optimize the active or active-reactive powers of all generators. The generator powers are not specified as fixed quantities as in the case of

ordinary load flow, but the minimum and maximum limits of the generator outputs are specified instead. The cost coefficients of each generating unit are also specified. Based on this information and other system data and if the source voltages are specified as fixed values, the algorithm optimally allocates the active power generations of all generators (i.e., active dispatch). The solution in this case gives a set of unique reactive power generations. If the generator voltages are specified to lie between some practical permissible limits instead of fixed values, the algorithm will give the economic active and reactive power generations of all generators (i.e., active-reactive dispatch).

Although optimal load flow techniques promise accurate dispatch solutions, they have inherent problems due to the nature of limit constraints which can introduce drastic changes in the cost function when limit violations occur. This often requires deceleration of the solution process for stable convergence. In addition, the minimum of the cost function is generally so flat that small mismatches in the load flow solution can cause large shifts in the apparent minimum. The mathematical formulation of the optimal load flow method is given in a compact form below.

1.3.2.1 The Optimal Load Flow Technique - Formulation

The cost function F_0 is minimized subject to the steady state power flow equations of the system (equality constraints) and the source voltage and power constraints (inequality constraints) as given by the following equations:

$$\text{minimize } F_0 = F_0 \ (\underline{X}, \ \underline{U}) \tag{1.5}$$

subject to:

$$f(\underline{X}, \ \underline{U}) = \underline{0} \tag{1.6}$$

and,

$$\underline{h}(\underline{X}, \ \underline{U}) \le \underline{0} \tag{1.7}$$

where,

$\underline{X}$ - the state vector

$\underline{U}$ - the control vector

Equations 1.6 and 1.7 are the equality and the inequality constraints respectively. Equation 1.6 is essentially the load flow equation of the power system in compact form. The constrained problem is transformed into an unconstrained optimization problem using the Lagrange-Kuhn-Tucker formulation as given below:

$$F_A = F_0(\underline{X}, \ \underline{U}) + \underline{\lambda}^T \ [\ \underline{f}(\underline{X}, \ \underline{U})] + \underline{\mu}^T \ [\ \underline{h}(\underline{X}, \ \underline{U})] \tag{1.8}$$

or

$$F_A = F_0(\underline{X}, \underline{U}) + \underline{\lambda}^T[\underline{f}(\underline{X}, \underline{U})]$$

$$+ \underline{\mu}_{Xmin}^T[\underline{X}_{min} - \underline{X}]$$

$$+ \underline{\mu}_{Xmax}^T[\underline{X} - \underline{X}_{max}]$$

$$+ \underline{\mu}_{Umin}^T[\underline{U}_{min} - \underline{U}]$$

$$+ \underline{\mu}_{Umax}^T[\underline{U} - \underline{U}_{max}] \qquad\qquad (1.9)$$

where,

F_A - Lagrange-Kuhn-Tucker function.

$\underline{\lambda}$ - Lagrange type multiplier vector.

$\underline{\mu}$ - Kuhn-Tucker multiplier vector.

T - stands for transpose.

The Kuhn-Tucker multiplier vector $\underline{\mu} = \underline{0}$ if the constraints are not violated and $\underline{\mu} > \underline{0}$, if the constraints are violated. The optimum conditions are obtained by differentiating equation 1.8 with respect to $\underline{X}$, $\underline{U}$, $\underline{\lambda}$ and $\underline{\mu}$ and equating the resulting set of equations to zero. This set of equations is usually solved using the Newton-Raphson iterative method (3, 7, 17), with sparsity directed elimination (25) to minimize storage.

1.3.3 The Least Squares Based Economic Dispatch Methods

The least squares based optimization methods, take advantage of

the basic simplicity of the classical approach. Parameter estimation techniques are used for improved evaluation of the network loss model coefficients (22-24). The economic dispatch solutions are very sensitive to the accuracy of the evaluated network power loss model or models (the active and/or active-reactive power loss models). References (22-24) suggest the use of some parameter estimation techniques to evaluate the transmission network loss model parameters. These estimation techniques are, the weighted least squares (26, 27), Gauss-Newton or Bard algorithm (28), Marquardt algorithm (29), and the Powell regression algorithm (30). The base data (i.e., observations) required for the application of the above parameter estimation techniques are obtained from a number of load flow solutions of the power system. These load flow studies are carried out by varying the active power generations using one fixed load level (the peak of nominal load of the system) with fixed source voltage levels.

Using the loss models evaluated by the above mentioned estimation algorithms, the corresponding economic dispatch solutions are obtained for nominal loads of the system tested. All four parameter estimation routines arrive at almost the same economic dispatch schedules. The choice between the four estimation routines is based on computational time and storage requirements. Based on this criteria, the weighted least squares method and the Powell regression algorithm are preferred over the other two routines. While the Powell regression algorithm produces almost identical results to the weighted least squares method, it requires initial parameter estimates for solution. This however, is not a serious problem as initial guesses can be easily obtained using the

ordinary least squares estimator. Since the two routines give almost

identical results, the published report suggests the use of weighted

least squares method.

The work described above produces satisfactory economic dispatch

solutions for small power systems with a small number of generation

buses operating at their nominal loads. As will be seen later, the

parameters of the network loss model are functions of voltages, phase.

angles, impedances and the load patterns of the network and hence are

not constant. In the cost function minimization procedure using loss

models, the absolute minimum of the cost function for a given load is

very sensitive to the accuracy of the estimated loss model parameters.

To ensure accurate economic dispatch solutions for different system

els with minimum computational cost and numerical errors, the

g factors must be considered.

NETWORK LOAD VARIATIONS

In order to obtain accurate economic dispatch solutions for

erent load levels of a power system, the loss model coefficients

t be evaluated considering the effects of load variations. A net-

rk loss model evaluated using nominal loading will only give an

accurate dispatch solution when the network is operating at this nominal

load.

2. SOURCE VOLTAGE VARIATIONS

If the voltage variations are not taken into consideration at light

and heavy load periods when the base load flow data is obtained, the

economic dispatch solutions will have voltage profiles that are outside

the acceptable operating limits.

3. ILL-CONDITIONING

Ill-conditioning, if encountered in the least squares parameter
estimation process, will result in unstable parameter estimates and
hence will yield erroneous dispatch solutions. Ill-conditioning occurs
when the explanatory variables become highly non-orthogonal. In such
cases slight changes in the observable data will result in large changes
in the parameter estimates (27).

4. PROBLEMS ASSOCIATED WITH PURELY REACTIVE SOURCES - ACTIVE-REACTIVE
    MODEL

In the active-reactive power loss model, the active and reactive
power losses are expressed as functions of all active and reactive
generation sources of the network. A network containing a small number
of generation buses and a small number of purely reactive sources, will
have a large loss model (large in the sense of the number of parameters
the model contains). In such cases, two problems are encountered in
the parameter estimation procedure, namely:

1. a large number of load flow results are required,
    an added cost.

2. a tendency to develop ill-conditioning in the evaluation
    of parameters.

5. LARGE POWER NETWORKS

In both the active and active-reactive power loss models, the
number of parameters to be evaluated depends upon the number of
generation buses of the network. In the evaluation of large models, the

two problems mentioned in 4 above cannot be avoided (i.e., large

increase in the load flow results required and the problem of ill-

conditioning).

In this thesis the above five problems are addressed and remedied.

1.4 Research Objectives

The objective of this thesis is to develop a new approach to the

economic dispatch problem using network loss models that can provide

accurate dispatch solutions with acceptable voltage profiles for all

power system operating load patterns (e.g., light load and heavy loads).

The method should also be able to handle ill-conditioned situations

that may arise in the network loss model evaluation process. The

method should also be extended to handle large power networks containing

a large number of generation buses without excessive computational cost,

which is a problem of many existing methods. Finally, the method should

maintain the simplicity of the classical approach.

1.5 Scope of Thesis

The thesis is divided into two major parts. The first part deals

with small power systems (i.e., systems containing a small number of

generation buses). The second part treats large power system networks

where diakoptical techniques are used in the loss model parameter

estimation procedure. In both parts, computational results are presented

for standard IEEE and other test systems.

The various power system models used are presented in Chapter II.

Chapter III is devoted to the description of the parameter estimation

technique which is used to evaluate the power network models. Chapter

IV presents the loss model based optimization algorithms used to solve

for the economic active and active-reactive dispatch conditions of power

systems. In Chapter V, the optimization algorithms are applied to small

model power systems where the economic dispatch solutions of the model

systems are evaluated. Chapter VI outlines the diakoptical active and

active-reactive power loss models that are used to represent large

power systems and the diakoptical economic dispatch procedures. In

Chapter VII, the diakoptical loss model based optimization algorithms

are applied to evaluate the economic dispatch conditions of some model

power systems. Chapter VIII is devoted to the discussion of the work

presented in this thesis. This chapter also includes the conclusions

and suggestions for further research work in the area of optimum economic

dispatch of power systems.

CHAPTER II

POWER SYSTEM MODELS

In this thesis, the power systems studied are assumed to consist of thermal generation sources and an interconnected transmission network. For the purpose of evaluating the economic dispatch conditions, each of the above power system subdivisions is represented by a mathematical model. The thermal generation source model is presented next followed by the network power loss models.

2.1 The Thermal Generation Source Model

The thermal generation source model used is the familiar second order function which relates the total fuel cost to the active power generation of the individual power plants (31). The model is given by the following equation:

$$F_0 = \sum_{i=1}^{m} \alpha_{si} + \beta_{si} P_{Gsi} + \gamma_{si} P_{Gsi}^2 \qquad (2.1)$$

where,

F_0 - the total fuel cost in $/h

P_{Gsi} - the active power generation of the ith thermal unit in MW

α_{si}, β_{si} and γ_{si} - the cost coefficients of the ith thermal unit in $/h , $/MWh and $h/(MWh)^2 respectively

The cost coefficients of a particular generator are usually evaluated by the method of least squares from measured performance data. Typical generator coefficients used in this thesis are given in Table 2.1 (31).

Other coefficients will be given as used.

Generator Size, (MW)	α $/h	β $/(MWh)	γ $h/(MWh)^2$
50	49.92	10.06	0.01030
200	173.61	8.67	0.00230
400	300.84	8.14	0.00150
600	462.28	8.28	0.00530
800	751.39	7.48	0.00099
1200	1130.80	7.47	0.00067

Table 2.1 Cost Coefficients of Coal

Fired Plants

2.2   The Network Power Loss Models

The network power loss models used in this thesis are listed

below (31):

1.   the active power loss model

2.   the active-reactive power loss model

The detailed mathematical formulation of the above two models can be

found in Appendix A.   The active power loss model is presented in the

next section followed by the active-reactive power loss model.

2.2.1 The Active Power Loss Model

The active power loss model used is assumed to be a quadratic function relating the system total active power losses to the aggregate active power generated. The model may be written in compact form as:

$$P_L = K_{L0} + \underline{B}_0^T \underline{P}_G + \underline{P}_G^T \underline{B}\, \underline{P}_G \qquad (2.2)$$

where,

P_L — the network total active power losses in per unit

$\underline{P}_G$ — the active power generation vector of the system in per unit

K_{L0}, $\underline{B}_0$ and $\underline{B}$ — the parameters of the loss model in per unit, which are to be determined

The parameters of equation 2.2 are functions of voltages, phase angles, impedances and the load patterns of the transmission network. These parameters are not constant since the complex voltages vary with system load. The coefficient matrix $\underline{B}$ is a square symmetric matrix (as will be seen later, the matrix $\underline{B}$ may become rectangular in the piecewise loss model formulation). The number of parameters to be evaluated for the active power loss model (equation 2.2), is given by:

$$NC = (NG + 2)(NG + 1)/2 \qquad (2.3)$$

where,

NC - the number of parameters

NG - the number of generation buses in the network

2.2.1.1 The Active Power Loss Model-Multiple Generators

In power system networks, having more than one generator feeding a generation bus, equation 2.2 is modified by using the connection matrix concept. The binary elements of this connection matrix are 0's and 1's, where the number 1 represents a connection and 0 represents no connection. The modified active power loss model can be written as:

$$P_L = K_{LO} + \underline{B}_0^T \, \underline{C}_G^T \, \underline{P}_G + \underline{P}_G^T \, \underline{C}_G \, \underline{B} \, \underline{C}_G^T \, \underline{P}_G \qquad (2.4)$$

where,

$\underline{C}_G$ - the connection matrix with elements of 0's and 1's

The number of parameters in equation 2.4, can be evaluated from equation 2.3. To illustrate the use of the connection matrix concept, consider the simple power system shown in Figure 2.1. As seen in Figure 2.1, bus number 1 is fed by one generator P_{G1}, while bus number 2 is fed by two generators P_{G2} and P_{G3}. The connection matrix $\underline{C}_G$ for this simple example is given by:

$$\underline{C}_G = \quad
\begin{array}{c|c|c}
 & \text{Bus No.1} & \text{Bus No.2} \\
\hline
P_{G1} & 1 & 0 \\
\hline
P_{G2} & 0 & 1 \\
\hline
P_{G3} & 0 & 1 \\
\end{array}
\qquad (2.5)$$
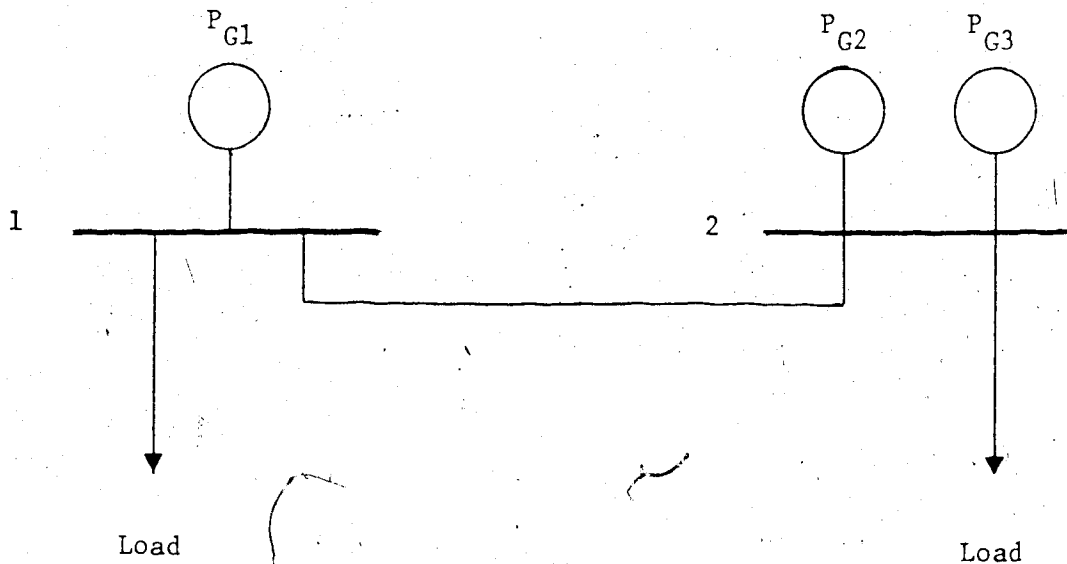
Figure 2.1 A Two Bus Power System

2.2.1.2 The Active Power Loss Model Parameter Estimation - Set Up

The active power loss model given by equation 2.2 or 2.4 above, may be written in the following format for the purpose of the parameter estimation procedure:

$$\underline{Y} = \underline{A} \underline{x} \tag{2.6}$$

In equation 2.6, the vector $\underline{Y}(n \times 1)$ has the following elements:

$$\underline{Y} = [P_{L1} \ P_{L2} \ \cdots \cdots \ P_{Ln}]^T \tag{2.7}$$

where,

P_{Li} — the total active power losses of the ith observation (the ith load flow result).

n — the number of observations (number of load flow result), where n>NC

The observation matrix $\underline{A}$ (nxp) where p = NC, is given by:

$$\underline{A} = \begin{bmatrix} \underline{A}_1 \\ \underline{A}_2 \\ \cdot \\ \cdot \\ \cdot \\ \underline{A}_n \end{bmatrix} \tag{2.8}$$

where,

$$\underline{A}_i = [\underline{a}_1 \ \underline{a}_2 \ \cdots \cdots \ \underline{a}_{m-1} \ \underline{a}_m] \tag{2.9}$$

where,

$$\underline{a}_1 = 1.0 \tag{2.10}$$

$$\underline{a}_2 = [P_{G1} \ P_{G2} \ \cdots \cdots \ P_{Gm}] \tag{2.11}$$

$$\underline{a}_3 = [P_{G1}^2 \ 2P_{G1} \ P_{G2} \ \cdots \cdots \ 2P_{G1} \ P_{Gm}] \tag{2.12}$$

$$\underline{a}_{m-1} = [P_{Gm-1}^2 \ 2P_{Gm-1} \cdot P_{Gm}] \tag{2.13}$$

$$\underline{a}_m = [P_{Gm}^2] \qquad\qquad (2.14)$$

where,

P_{Gi} - the active power generation injected into bus i

The vector equation given by 2.9, corresponds to the result of the ith load flow solution of the power system under consideration. The coefficient vector $\underline{x}$(pxl) is given by:

$$\underline{x}^T = [\ \underline{x}_1^T \ \underline{x}_2^T \ \underline{x}_3^T \ ] \qquad\qquad (2.15)$$

where,

$$\underline{x}_1^T = K_{L0} \qquad\qquad (2.16)$$

$$\underline{x}_2^T = [B_{01} \ B_{02} \ \cdots\cdots \ B_{0m}] \qquad\qquad (2.17)$$

and,

$$\underline{x}_3^T = [\underline{z}_1^T \ \underline{z}_2^T \ \cdots\cdots \ \underline{z}_{m-1}^T \ \underline{z}_m^T] \qquad\qquad (2.18)$$

where,

$$\underline{z}_1^T = [B_{11} \ B_{12} \ \cdots\cdots \ B_{1m}] \qquad\qquad (2.19)$$

$$\underline{z}_2^T = \begin{bmatrix} B_{22} & B_{23} & \cdots\cdots & B_{2m} \end{bmatrix} \qquad (2.20)$$

$$\vdots$$

$$\underline{z}_{m-1}^T = \begin{bmatrix} B_{m-1,m-1} & B_{m-1,m} \end{bmatrix} \qquad (2.21)$$

$$\underline{z}_m^T = \begin{bmatrix} B_{m,m} \end{bmatrix} \qquad (2.22)$$

2.2.2 The Active-Reactive Power Loss Model

The active-reactive power loss model used in this thesis is divided into two separate submodels. In the first submodel, the total active and reactive power losses of the network are taken as functions of the active and reactive powers of the generation buses of the network. The second submodel relates the purely reactive source powers (voltage regulated bus reactive powers) to the total reactive load demand of the power system (32-34). The advantages gained by this formulation are:

1. the number of load flow results required to evaluate the active-reactive loss model parameters is reduced significantly which results in significant savings in computational cost

2. the possibility of encountering the problem of ill-conditioning is minimized in the parameter estimation procedure

The network active-reactive power loss submodel is given next, followed by the purely reactive source submodel.

2.2.2.1 The Network Active-Reactive Power Loss Submodel

The real and imaginary parts of the transmission network active-

reactive submodel are assumed to have quadratic forms as given by the following equations (see Appendix A for details):

$$P_L = K_{LOP} + [E_{PP}^T \ E_{PQ}^T] \begin{bmatrix} P_G \\ Q_G \end{bmatrix}$$

$$+ [P_G^T \ Q_G^T] \begin{bmatrix} A_{PGG} & - B_{PGG} \\ B_{PGG} & A_{PGG} \end{bmatrix} \begin{bmatrix} P_G \\ Q_G \end{bmatrix} \qquad (2.23)$$

and,

$$Q_L = K_{LOQ} + [E_{QP}^T \ E_{QQ}^T] \begin{bmatrix} P_G \\ Q_G \end{bmatrix}$$

$$+ [P_G^T \ Q_G^T] \begin{bmatrix} A_{QGG} & -B_{QGG} \\ B_{QGG} & A_{QGG} \end{bmatrix} \begin{bmatrix} P_G \\ Q_G \end{bmatrix} \qquad (2.24)$$

where,

P_L, Q_L - the network total active and reactive power losses in per unit respectively

P_G, Q_G - the active and reactive power generation vectors in per unit respectively

K_{LOP}, E_{PP}, E_{PQ}, A_{PGG} and B_{PGG} - the parameters of P_L in per unit

K_{LOQ}, E_{QP}, E_{QQ}, A_{QGG} and B_{QGG} - the parameters of Q_L in per unit

The parameters of P_L and Q_L are functions of voltages, phase angles,

impedances and the load patterns of the network. As in the case of the active power loss model, these parameters are not constant since the network complex nodal voltages vary with system loads. The coefficient matrices $\underline{A}_{PGG}$ and $\underline{A}_{QGG}$ are square symmetric matrices. The matrices $\underline{B}_{PGG}$ and $\underline{B}_{QGG}$ are skew symmetric matrices with zero diagonal elements. The matrices $\underline{A}_{PGG}$, $\underline{A}_{QGG}$, $\underline{B}_{PGG}$ and $\underline{B}_{QGG}$ may become rectangular as will be seen later in the network piecewise loss model analysis. The number of parameters of the submodels P_L and Q_L to be evaluated for a particular network is given by:

$$NC_P = NC_Q = (NG + 1)^2 \qquad (2.25)$$

where,

NC$_P$, NC$_Q$ – the number of parameters of P_L and Q_L respectively

NG – the number of active-reactive generation buses in the network

In the case of more than one generator supplying a generation bus, the active-reactive submodel is modified using the connection matrix concept as was done for the active power loss model. The modified active-reactive submodel will have the same number of parameters as that of the original case (i.e., as given by equation 2.25).

2.2.2.2 The Active-Reactive Power Loss Model Parameter Estimation – Set Up

For the parameter estimation procedure, equations 2.23 and 2.24 may be written in the following partitioned matrix equation:

$$\begin{bmatrix} \underline{A}_P & \underline{0} \\ \underline{0} & \underline{A}_Q \end{bmatrix} \begin{bmatrix} \underline{x}_P \\ \underline{x}_Q \end{bmatrix} \qquad (2.26)$$

or given load flow results (observations) of the power system under consideration, the vectors $\underline{Y}_P$(nx1) and $\underline{Y}_Q$(nx1) are given by the following:

$$\underline{Y}_P = [P_{L1} \ P_{L2} \ \cdots\cdots \ P_{Ln}]^T \qquad (2.27)$$

and,

$$\underline{Y}_Q = [Q_{L1} \ Q_{L2} \ \cdots\cdots \ Q_{Ln}]^T \qquad (2.28)$$

where

P_{Li}, Q_{Li} - the network total active and reactive power losses
of the ith load flow result of the system

n   - the number of load flow results required to evaluate
the parameters of P_L and Q_L. $n>NC_P$ and $n>NC_Q$.

The observation submatrices $\underline{A}_P$ and $\underline{A}_Q$ are identical (i.e., $\underline{A}_P = \underline{A}_Q$).
The elements of these submatrices are combinations of active and reactive
power generations of the network as given below:

$$\underline{A}_P = \underline{A}_Q = \begin{bmatrix} \underline{A}_1 \\ \underline{A}_2 \\ \vdots \\ \underline{A}_n \end{bmatrix} \qquad (2.29)$$

where,

$$\underline{A}_i = [\underline{a}_1 \ \underline{a}_2 \ \cdots \ \underline{a}_{m-1} \ \underline{a}_m \ \underline{b}_1 \ \underline{b}_2 \ \cdots \ \underline{b}_{m-1}] \qquad (2.30)$$

where,

$$\underline{a}_1 = 1.0 \qquad (2.31)$$

$$\underline{a}_2 = [P_{G1} \ P_{G2} \ \cdots \ P_{Gm}] \qquad (2.32)$$

$$\underline{a}_3 = [Q_{G1} \ Q_{G2} \ \cdots \ Q_{Gm}] \qquad (2.33)$$

$$\underline{a}_4 = [(P_{G1}^2 + Q_{G1}^2) \ 2(P_{G1} \cdot P_{G2} + Q_{G1} \cdot Q_{G2}) \ \cdots \ 2(P_{G1} \cdot P_{Gm} + Q_{G1} \ Q_{Gm})] \qquad (2.34)$$

$$\underline{a}_5 = [(P_{G2}^2 + Q_{G2}^2) \ 2(P_{G2} \cdot P_{G3} + Q_{G2} \cdot Q_{G3}) \ \cdots \ 2(P_{G2} \cdot P_{Gm} + Q_{G2} \cdot Q_{Gm})] \qquad (2.35)$$

$$\vdots$$

$$\underline{a}_{m-1} = [(P_{Gm-1}^2 + Q_{Gm-1}^2) \ 2(P_{Gm-1} \cdot P_{Gm} + Q_{Gm-1} \cdot Q_{Gm})] \qquad (2.36)$$

$$\underline{a}_m = [(P_{Gm}^2 + Q_{Gm}^2)] \qquad (2.37)$$

$$\underline{b}_1 = [-2(P_{G1} \ Q_{G2} - P_{G2} \cdot Q_{G1}) - 2(P_{G1} \ Q_{G3} - P_{G3} \cdot Q_{G2}) \ \cdots$$

$$\cdots \ -2(P_{G1} \cdot Q_{Gm} - P_{Gm} \ Q_{G1})] \qquad (2.38)$$

$$\vdots$$

$$\underline{b}_{m-1} = [-2(P_{Gm-1} \cdot Q_{Gm} - P_{Gm} \cdot Q_{Gm-1})] \qquad (2.39)$$

where,

m – the number of active-reactive generation buses of the network

The coefficient vector $\underline{x}_p$ (p×1), where $p = NC_p$, is given by:

$$\underline{x}_p^T = [\underline{x}_1^T \ \underline{x}_2^T \ \underline{x}_3^T \ \cdots \ \underline{x}_{m-1}^T \ \underline{x}_m^T \ \underline{X}_1^T \ \underline{X}_2^T \ \cdots \ \underline{X}_{m-1}^T] \tag{2.40}$$

where,

$$\underline{x}_1^T = K_{LOP} \tag{2.41}$$

$$\underline{x}_2^T = [E_{PP1} \ E_{PP2} \ \cdots \ E_{PPm}] \tag{2.42}$$

$$\underline{x}_3^T = [E_{PQ1} \ E_{PQ2} \ \cdots \ E_{PQm}] \tag{2.43}$$

$$\underline{x}_4^T = [A_{P11} \ A_{P12} \ \cdots \ A_{P1m}] \tag{2.44}$$

$$\underline{x}_5^T = [A_{P22} \ A_{P23} \ \cdots \ A_{P2m}] \tag{2.45}$$

$$\vdots$$

$$\underline{x}_{m-1}^T = [A_{Pm-1,m-1} \ A_{Pm-1,m}] \tag{2.46}$$

$$\underline{x}_m^T = [A_{Pm,m}] \tag{2.47}$$

$$\underline{X}_1^T = [B_{P12} \ B_{P13} \ \cdots \ B_{P1m}] \tag{2.48}$$

$$\underline{x}_2^T = [B_{P23} \ B_{P24} \ \ldots \ B_{P2m}] \tag{2.49}$$

$$\vdots$$

$$\underline{x}_{m-1}^T = [B_{Pm-1,m}] \tag{2.50}$$

In a similar fashion, the elements of the coefficient vector $\underline{x}_Q$(px1) can be written as was done for $\underline{x}_P$.

2.2.2.3 The Network Purely Reactive Source Submodel

As previously discussed, there are advantages in separating the purely reactive sources from the active-reactive generation sources. The purely reactive source powers may be modeled in terms of the total reactive load demand as given by:

$$Q_{Gvi} = f(Q_D) \tag{2.51}$$

where,

Q_{Gvi} - the ith purely reactive power of the network in per unit

Q_D - the total reactive load demand of the network in per unit

The relationship of equation 2.51, may be linear or non-linear. In the modeling process, the limits of these sources are constrained as follows:

$$Q_{Gvi \ min} \leq Q_{Gvi} \leq Q_{Gvi \ max} \tag{2.52}$$

2.3 Data for Loss Model Parameter Estimation

The parameters of the network loss models are evaluated from a data set characterizing the power system. This data set is obtained from a series of load flow studies of the system. It was observed that evaluating the power system loss model using load flow results obtained for two different load levels (e.g., 50% and 100% of the nominal system load), resulted in improved economic dispatch solutions for different load levels as opposed to the results based on load flow solutions of one load level (35). The evaluation of more than one set of parameters of the loss model (i.e., one set of parameters per load level), would be a very expensive procedure, which in practice would be unacceptable. In this thesis, one set of parameters of the loss model of the system under consideration is evaluated from a set of load flow solutions, which are carried out over a wide range of system load levels with varying active and reactive power generations and varying source voltage levels at light and heavy load periods. This set of parameters resulted in accurate dispatch solutions for different load levels of the system (36). In practice, historical load flow solutions of a power system obtained at different load levels can be used, if available, with the objective of obtaining loss model parameters which best fit the system over the whole range of operation.

The parameter estimation technique used in this thesis, is the ridge regression algorithm which is discussed in detail in the next chapter.

CHAPTER III

THE NETWORK LOSS MODEL PARAMETER

ESTIMATION TECHNIQUE

In this chapter, a detailed description is given of the parameter estimation technique used to evaluate the models of the power systems considered in this thesis. This parameter estimation technique is known as the ridge regression algorithm (37, 38). The ridge regression estimation routine provides better parameter estimates than the parameter estimation techniques mentioned in Chapter I (39).

Inaccuracies in the evaluated network loss models can cause the economic dispatch solution to deviate significantly from the optimal solution. This can be seen by examining the quadratic thermal cost function given by equation 2.1. This function, at a specific load level, shows a broad and indistinct minimum for active power generations obtained from load flow studies of the system. In other words $\partial F_0 / \partial P_{Gi}$ is very small for a wide range about the minimum.

3.1 The Ridge Regression Estimation Algorithm

Based on a given observation data (load flow results or actual measurement of the system), least squares or similar estimation methods, may or may not result in stable parameter estimates depending on the condition of the observed data. An estimate is stable if small changes in the observable data do not result in large changes in the parameter estimates. Unstable parameter estimates are encountered when the explanatory variables become highly non-orthogonal, resulting in severely ill-conditioned situations. In such cases, least squares or similar methods, are not expected to give meaningful solutions. The ridge

estimator is an algorithm that can handle ill-conditioned situations where it provides stable parameter estimates, and well-conditioned cases where it reduces to ordinary least squares estimation.

In statistical least squares theory, there exists a true vector $\underline{x}$ such that:

$$Y = \underline{A}\ \underline{x} + \underline{e} \qquad\qquad (3.1)$$

where,

$\underline{Y}$ - (nx1) vector of observations on a response variable. The elements of this vector in this work are the total active or active-reactive power losses of the network.

$\underline{A}$ - (nxp) matrix of observations on p explanatory variables. The elements of this matrix are functions of active or active-reactive power generations of the system.

$\underline{x}$ - (px1) vector of regression coefficients. The elements of this vector are the network loss model parameters which are to be evaluated.

$\underline{e}$ - (nx1) error vector with $E(\underline{e}) = \underline{0}$, and $E(\underline{e}\ \underline{e}^T)= \sigma^2\ \underline{I}$, assuming that the elements of $\underline{e}$ have the same variance σ^2. $\underline{I}$ is a unit matrix.

The least squares estimator is obtained by forming an objective scalar function as given by:

$$J = [\underline{Y} - \underline{A}\ \underline{x}]^T\ [\underline{Y} - \underline{A}\ \underline{x}] \qquad\qquad (3.2)$$

where,

J - the scalar objective function.

The minimization of a scalar with respect to a vector is obtained when,

$$\frac{\partial J}{\partial \underline{x}} = \underline{0} \ , \tag{3.3}$$

and the Hessian of J is positive semi-definite or:

$$\left| \frac{\partial^2 J}{\partial \underline{x}^2} \right| \geq \underline{0} \ . \tag{3.4}$$

Differentiating J given by equation 3.2 with respect to the vector $\underline{x}$ and equating the result to zero, and if the inverse of $\underline{A}^T \underline{A}$ exists, gives:

$$\hat{\underline{x}} = [\underline{A}^T \underline{A}]^{-1} \underline{A}^T \underline{Y} \tag{3.5}$$

where,

$\hat{\underline{x}}$ - an estimate of $\underline{x}$ that minimizes the sum of square error.

If L is the distance from $\hat{\underline{x}}$ to $\underline{x}$, then,

$$L^2 = [\hat{\underline{x}} - \underline{x}]^T [\hat{\underline{x}} - \underline{x}] \tag{3.6}$$

and,

$$E(L^2) = E[(\hat{\underline{x}} - \underline{x})^T (\hat{\underline{x}} - \underline{x})] \tag{3.7}$$

$$= \sigma^2[\text{Trace } (A^T A)^{-1}] \tag{3.8}$$

and,

$$E[\hat{\underline{x}}^T x] = \hat{\underline{x}}^T \hat{x} + \sigma^2[\text{Trace } (\underline{A}^T \underline{A})] \tag{3.9}$$

where,

    E - the expected value

    Trace - a trace of a matrix is the sum of its diagonal elements

If the eigenvalues of $\underline{A}^T\underline{A}$ are given by:

$$\lambda_i \; ; \; i = 1, 2, \ldots, p, \tag{3.10}$$

where,

$$\lambda_{max} = \lambda_1 \geq \lambda_2 \ldots \geq \lambda_p = \lambda_{min} \tag{3.11}$$

then,

$$E(L^2) = \sigma^2 \sum_{i=1}^{p} 1/\lambda_i . \tag{3.12}$$

The mean square error is then given by:

$$E[(\hat{\underline{x}} - \underline{x})^T (\hat{\underline{x}} - \underline{x})] = \sigma^2 \sum_{i=1}^{p} 1/\lambda_i . \tag{3.13}$$

If one or more of the eigenvalues of $\underline{A}^T\underline{A}$ are small, the mean square error in equation 3.13 becomes large which will result in unstable parameter estimate vector $\hat{\underline{x}}$. In such cases, least squares estimates will be inaccurate. The ridge estimator on the other hand minimizes the mean square error and produces stable estimates. Let $\underline{X}$ be any estimate, then,

$$\psi = [\underline{Y} - \underline{A}\,\underline{X}]^T [\underline{Y} - \underline{A}\,\underline{X}] \tag{3.14}$$

$$= [\underline{Y} - \underline{A}\,\hat{\underline{x}}]^T [\underline{Y} - \underline{A}\,\hat{\underline{x}}]$$

$$+ [\underline{X} - \hat{\underline{x}}]^T \underline{A}^T\underline{A}[\underline{X} - \hat{\underline{x}}] \tag{3.15}$$

$$= \psi_{min} + \psi_0 \tag{3.16}$$

If $\underline{A}^T\underline{A}$ has large eigenvalues, ψ will be minimum, however, if one or more of these eigenvalues are small, ψ moves away from ψ_{min}. The ridge trace is a path that moves in a direction that minimizes the length of the vector $[\underline{X} - \hat{\underline{x}}]$. The ridge estimator may be derived as follows:

minimize $\underline{X}^T\underline{X}$ subject to:

$$[\underline{X} - \hat{\underline{x}}]^T \underline{A}^T\underline{A}[\underline{X} - \hat{\underline{x}}] = \psi_0 \tag{3.17}$$

An augmented (Lagrangian) function F can be formed as:

$$F = \underline{X}^T\underline{X} + (1/k)[(\underline{X}-\hat{\underline{x}})^T\underline{A}^T\underline{A}(\underline{X}-\hat{\underline{x}}) - \psi_0]$$ (3.18)

where,

   $1/k$ - a Lagrange type multiplier

Differentiating equation 3.18 with respect to $\underline{X}$ gives:

$$\frac{\partial F}{\partial \underline{X}} = 2\underline{X} + (1/k)\ [2(\underline{A}^T\underline{A})\underline{X} - 2(\underline{A}^T\underline{A})\ \hat{\underline{x}}]$$ (3.19)

Equating equation 3.19 to zero and rearranging gives:

$$[\underline{A}^T\underline{A} + k\ \underline{I}]\ \underline{X} = \underline{A}^T\underline{A}\ \hat{\underline{x}}$$ (3.20)

Equation 3.20 reduces to:

$$\underline{X} = \hat{\underline{x}}* = [\underline{A}^T\underline{A} + k\ \underline{I}]^{-1}\ \underline{A}^T\underline{Y}$$ (3.21)

where,

   $\hat{\underline{x}}*$ - the value of $\underline{X}$ that minimizes the sum of squares error

Equation 3.21 is known as the ridge estimator. The value of k must satisfy the equality constraint given by equation 3.17. The value of k is chosen to lie between 0 and 1.0, after scaling the matrix $\underline{A}$ (see

Appendix B for matrix scaling) such that:

1. it is the smallest value that makes $\hat{x}$ stable

2. it gives a value of mean square error close to the minimum value

3. it makes the variance-covariance matrix of $\hat{x}$ approximately orthogonal

The ridge trace or path, may be interpreted as follows: If the squared length of the vector $\underline{X}$ is fixed at C^2, then $\underline{x}^*$ is the value of $\underline{X}$ that minimizes the function given by:

$$F = [\underline{Y} - \underline{A}\ \underline{X}]^T [\underline{Y} - \underline{A}\ \underline{X}] + 1/k\ [\underline{X}^T\underline{X} - C^2] \qquad (3.22)$$

An iterative ridge regression procedure can be easily generated as follows:

$$\hat{\Delta\underline{x}}^{(\nu)} = [\underline{A}^T\underline{A} + k\ \underline{I}]^{-1}\ \underline{A}^T\ \Delta\underline{Y}^{(\nu)}, \qquad (3.23)$$

where,

$\hat{\Delta\underline{x}}^{(\nu)}$ — the correction vector at iteration ν

$\Delta\underline{Y}^{(\nu)}$ — the error vector

The updated vector at the $(\nu+1)$th iteration is given by:

$$\overset{(\nu+1)}{\hat{\underline{x}}} = \overset{(\nu)}{\hat{\underline{x}}} + \overset{(\nu)}{\Delta\hat{\underline{x}}} \tag{3.24}$$

The iterative process is terminated when:

$$\left|\Delta\hat{\underline{x}}\right| \leq \varepsilon \tag{3.25}$$

where,

ε - some desired tolerance

The optimum value of k that stabilizes the estimate vector $\hat{\underline{x}}$ can be easily determined by solving equation 3.21 iteratively with respect to k between 0.0 and 1.0, after scaling the observation matrix $\underline{A}$ to unit column lengths.

3.2 The Condition Number and the Condition Index of a Matrix

The condition of a given matrix can be examined by evaluating the singular values (or the eigenvalues) of the matrix. The matrix that is of concern here, is the square symmetric matrix $[\underline{A}^T\underline{A} + k\ \underline{I}]$ of equation 3.20. The singular values of this matrix can be evaluated by factorizing the matrix using the singular value decomposition (SVD) technique (27, 40) as given below:

Let,

$$\underline{D} = [\underline{A}^T\underline{A} + k\ \underline{I}] , \tag{3.26}$$

The matrix $\underline{D}$ in factored form may be written as:

$$\underline{D} = \underline{U} \ \underline{S} \ \underline{U}^T \qquad\qquad (3.27)$$

where,

$\quad \underline{U}$ - (pxp) orthogonal matrix, whose columns are the eigenvectors

$\qquad$ of $\underline{D} \ \underline{D}^T$ or $\underline{D}^T \underline{D}$

$\quad \underline{S}$ - (pxp) diagonal matrix whose elements are the singular

$\qquad$ values of $\underline{D}$

Since $\underline{U}$ is an orthogonal matrix, then

$$\underline{U}^T \underline{U} = \underline{U} \ \underline{U}^T = \underline{I} \qquad\qquad (3.28)$$

and,

$$||\underline{U}|| = 1 \qquad\qquad (3.29)$$

where,

$\quad \underline{I}$ - (pxp) unit matrix

$\quad ||\cdot||$ - Euclidean norm.

The matrix $\underline{S}$ may be written as:

$$\underline{S} = \begin{bmatrix} S_1 & - & - & - & - & - & 0 \\ 0 & S_2 & & & & & \vdots \\ \vdots & & \ddots & & & & \vdots \\ \vdots & & & \ddots & & & \vdots \\ 0 & - & - & - & - & \cdot & S_p \end{bmatrix} \qquad (3.30)$$

where,

S_i - the ith singular value of $\underline{D}$. $S_i \geq 0$ for $i=1, i, \ldots, p$.

Taking the norm of equation 3.27 gives:

$$||\underline{D}|| = ||\underline{U}\ \underline{S}\ \underline{U}^T|| \leq ||\underline{S}|| \qquad (3.31)$$

and,

$$||\underline{S}|| = ||\underline{U}^T\ \underline{S}\ \underline{U}|| \leq ||\underline{D}|| \qquad (3.32)$$

hence,

$$||\underline{D}|| = ||\underline{S}|| , \qquad (3.33)$$

similarly,

$$= ||\underline{S}^{-1}|| \qquad (3.34)$$

The norm of the matrix $\underline{S}$ is defined as:

$$||\underline{S}|| = \underset{1 \le i \le p}{\text{Max}} \ S_i = S_{max} \qquad (3.35)$$

and,

$$||\underline{S}^{-1}|| = \underset{1 \le i \le p}{\text{Max}} \ S_i^{-1} = 1/S_{min} \qquad (3.36)$$

$$\text{for } S_i \ne 0$$

The condition number of the matrix $\underline{D}$ is defined as:

$$\text{Cond } (\underline{D}) = ||\underline{D}|| \ ||\underline{D}^{-1}|| \qquad (3.37)$$

or,

$$\text{Cond } (\underline{D}) = \frac{S_{max}}{S_{min}} \ge 1 \qquad (3.38)$$

where,

$$||\underline{D}|| = [\sum_{i=1}^{p} \sum_{j=1}^{p} D_{ij}^2]^{\frac{1}{2}} \qquad (3.39)$$

or,

$$||\underline{D}|| = [\text{trace } (\underline{D}^T\underline{D})]^{\frac{1}{2}} \qquad (3.40)$$

It can be seen from above that the singular values of $\underline{D}$ are also its eigenvalues. A very well-conditioned matrix will have a condition number approaching 1.0.

Another useful index which is used to determine the severity of ill-conditioning, is the condition index which is defined as:

$$\eta_i = \frac{S_{max}}{S_i} \geq 1 \tag{3.41}$$

where,

η_i - the condition index of the matrix $\underline{D}$, for i=1, i, ..., p.

The largest value of η_i for some i, is the matrix condition number. The condition index gives an indication of the dependencies among the matrix columns. It is difficult to draw a line on how large is "large" with regards to the condition number of a matrix. Experience shows (40) that after scaling the matrix to unit column lengths, a condition number of 10 to 30, indicates weak to moderate column dependices. However, this cannot be taken as a definite measure. From the computational experience gained in the preparation of this thesis, indices larger than 30 resulted in stable loss model parameter estimates and consequently in satisfactory dispatch solutions. The ridge estimator adjusts the small singular values of the matrix $\underline{D}$ and for the proper value of k gives small and satisfactory condition indices.

3.3 The Ridge Regression Computational Procedure

The various computational steps taken to evaluate the parameters of

all loss models used in this thesis by the ridge regression estimation
technique are given below:

1. read in the power system data obtained from n load flow
    solutions ($n \geq p+1$), where p is the number of parameters
    of the loss model under consideration. Also read in the
    ridge increment Δk, k_{max} and the maximum number of
    iterations.

2. compute the elements of the observation matrix $\underline{A}$ and form
    the vector $\underline{Y}$(i.e., $\underline{Y} = \underline{A}\,\underline{x} + \underline{e}$).

3. scale the matrix $\underline{A}$ and the vector $\underline{Y}$ to have unit
    column lengths.

4. form the scaled equivalent of $\underline{A}^T\underline{A}$ and of $\underline{A}^T\underline{Y}$ and begin
    the ridge regression process.

5. set ridge $k = 0.0$.

6. factorize the matrix $\underline{D}$ using the singular value decomposition
    technique and compute the condition number.

7. check if $k \leq k_{max}$. If yes, go to 8, if not go to 18.

8. check if Cond ($\underline{D}$) $\leq$ 50 and/or if the inverse of $\underline{D}$ exists.
    If yes go to 9, if not go to 17.

9. set iteration count $\nu=1$.

10. solve for $\hat{\underline{x}}$ from $\hat{\underline{x}} = [\underline{A}^T\underline{A} + k\,\underline{I}]^{-1}\,\underline{A}^T\underline{Y}$.

11. compute $\hat{\underline{Y}}$ using the computed $\hat{\underline{x}}$ and calculate the error vector
    $\Delta\hat{\underline{y}}$ from:

    $$\hat{\underline{Y}} = \underline{A}\,\hat{\underline{x}} \quad \text{and} \quad \Delta\hat{\underline{Y}} = \hat{\underline{Y}} - \underline{Y}.$$

12. compute $\Delta\hat{x}$ from:

$$\Delta\hat{\underline{x}} = [\underline{A}^T \underline{A} + k \underline{I}]^{-1} \underline{A}^T \Delta\underline{Y}$$

13. check if $|\Delta\hat{\underline{x}}| \leq$ some desired tolerance, if convergence is achieved go to 18, if not go to 14.

14. check if $\nu \geq \nu_{max}$. If yes go to 17, if not go to 15.

15. update the iteration count ν by one (i.e., $\nu = \nu+1$).

16. update the estimate vector $\underline{x}$ by $\Delta\underline{x}$ (i.e., $\hat{\underline{x}}^{(\nu+1)} = \hat{\underline{x}}^{(\nu)} + \Delta\hat{\underline{x}}^{(\nu)}$) and go to 11.

17. update the ridge k by the increment Δk and go to 6.

18. print out the estimated parameter vector $\hat{\underline{x}}$, the computed power loss vector $\hat{\underline{Y}}$, the error vector $\Delta\hat{\underline{Y}}$, condition indices and the condition number.

19. stop.

The above computational steps are summarized in the flow chart shown in Figure 3.1.

```
┌─────────────────────────────────────┐
│  Read in data from load flow studies,│
1 │  Δk, k_max  and ν_max.               │
└─────────────────────────────────────┘
                  ▽

┌─────────────────────────────────────┐
│  Compute the elements of A and form  │
2 │         the vector Y.                │
└─────────────────────────────────────┘
                  ▽

┌─────────────────────────────────────┐
│   Scale A and Y to unit column       │
3 │          lengths                     │
└─────────────────────────────────────┘
                  ▽

┌─────────────────────────────────────┐
4 │  Form the scaled A^T A and A^T Y     │
└─────────────────────────────────────┘
                  ▽

┌─────────────────────────────────────┐
5 │         Set ridge  k = 0.0           │
└─────────────────────────────────────┘
                  ▽
                 ( A )
```
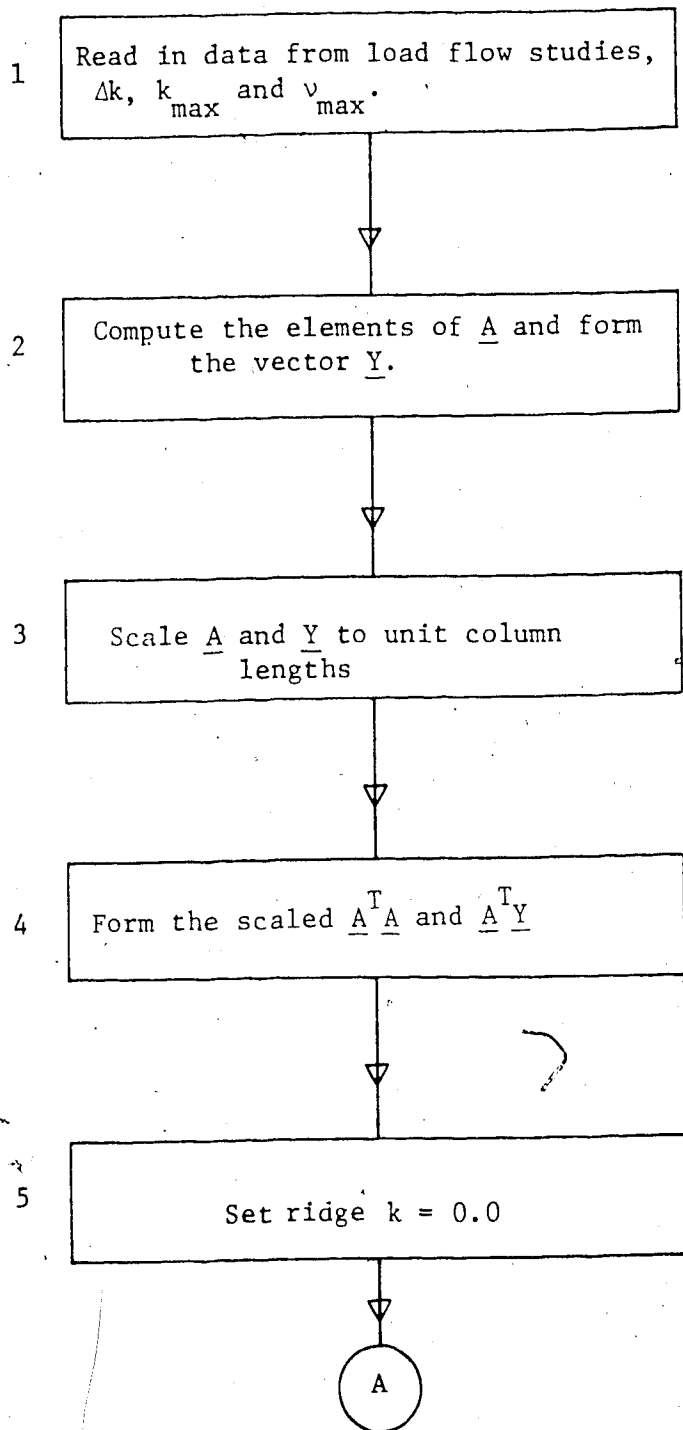
Figure 3.1 The Ridge Regression Estimation

Algorithm Flow Chart
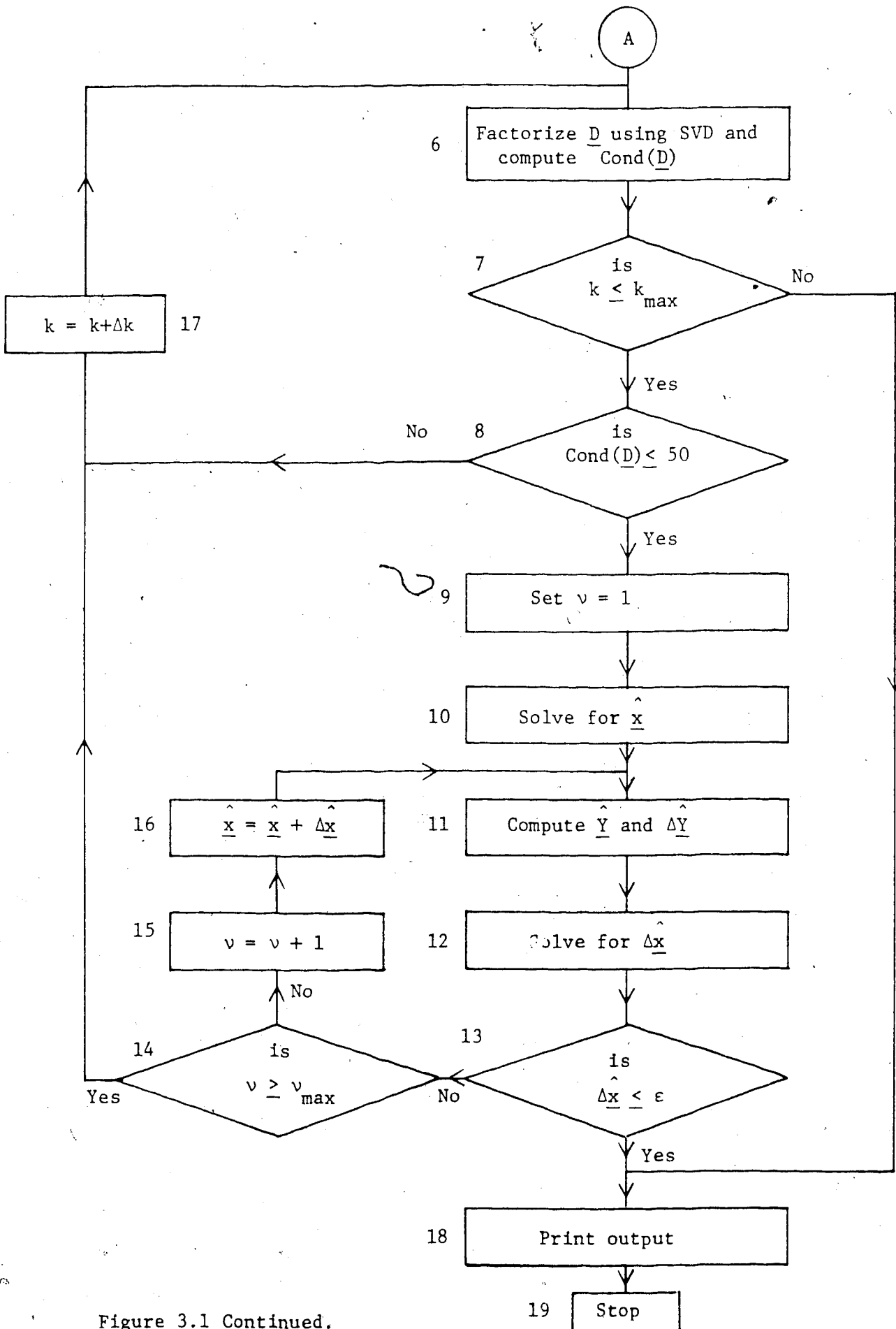
Figure 3.1 Continued.

CHAPTER IV

THE OPTIMIZATION PROCEDURE

FOR ECONOMIC GENERATION SCHEDULING

The active and active-reactive dispatch procedures used to solve

for the economic operating conditions of a given power system, are

discussed in detail in this chapter. The optimization methods are based

on the network loss models given in Chapter II. In these methods, the

thermal cost function is minimized subject to the net active or active-

reactive power balance and the system source constraints, observing

the Kuhn-Tucker optimality conditions (7, 31, 41). The active dispatch

procedure will be considered first, followed by the active-reactive

dispatch procedure.

4.1   The Optimization Procedure-Active

The fuel cost function given by equation 2.1 in Chapter II

(repeated here for convenience), is minimized using the Lagrange-Kuhn-

Tucker formulation as given by the following equations:

minimize

$$F_0 = \sum_{i=1}^{m} \alpha_{si} + \beta_{si} P_{Gsi} + \gamma_{si} P_{Gsi}^2 \qquad (4.1)$$

subject to:

$$h_p(P_{Gsi}) = P_D + P_L - \sum_{i=1}^{m} P_{Gsi} = 0.0 \qquad (4.2)$$

and,

$$g_p(P_{Gsi}) \leq 0.0 \tag{4.3}$$

Equation 4.3 can be written as:

$$P_{Gsi\ min} - P_{Gsi} \leq 0.0 \tag{4.4}$$

$$P_{Gsi} - P_{Gsi\ max} \leq 0.0 \tag{4.5}$$

The Lagrange-Kuhn-Tucker function is formed to convert the constrained problem into an unconstrained optimization problem as given by:

$$F_A = F_0 + \lambda_p \left[P_D + P_L - \sum_{i=1}^{m} P_{Gsi} \right]$$

$$+ \sum_{i=1}^{m} \mu_{pi\ min} \left[P_{Gsi\ min} - P_{Gsi} \right]$$

$$+ \sum_{i=1}^{m} \mu_{pi\ max} \left[P_{Gsi} - P_{Gsi\ max} \right] \tag{4.6}$$

where,

F_A — the Lagrange-Kuhn-Tucker function.

P_D — the network total active load demand.

P_L — the network total active power losses

P_{Gsi} — the active power generation of the ith unit.

λ_p — Lagrange type multiplier.

μ_{pi} — Kuhn-Tucker multiplier .

m — the number of generating units in the system

The optimum economic dispatch conditions are obtained by differentiating equation 4.6 with respect to P_{Gsi}; $i=1,2,\ldots m$, λ_p and μ_p's and setting the set of equations to zero. This set of equations can be written as:

$$\frac{\partial F_A}{\partial P_{Gsi}} = f_{pi} = \frac{\partial F_0}{\partial P_{Gsi}} + \lambda_p \frac{\partial h_p}{\partial P_{Gsi}}$$

$$+ \mu_{pi\ min} \frac{\partial g_{p\ min}}{\partial P_{Gsi}} + \mu_{pi\ max} \frac{\partial g_{p\ max}}{\partial P_{Gsi}} = 0.0 \qquad (4.7a)$$

$$\frac{\partial F_A}{\partial \lambda_p} = f_{pD} = h_p\ (P_{Gsi}) = 0.0 \qquad (4.7b)$$

$$\frac{\partial F_A}{\partial \mu_{pi\ min}} = g_{p\ min}\ (P_{Gsi}) = 0.0 \qquad (4.7c)$$

$$\text{for } \mu_{pi\ min} > 0 \text{ or } \mu_{pi\ min} = 0.0 \qquad (4.7d)$$

$$\frac{\partial F_A}{\partial \mu_{pi\ max}} = g_{p\ max}\ (P_{Gsi}) = 0.0 \qquad (4.7e)$$

$$\text{for } \mu_{pi\ max} > 0 \text{ or } \mu_{pi\ max} = 0.0 \qquad (4.7f)$$

The Lagrange multipliers are active (i.e., can either be positive or negative but non zero). The Kuhn-Tucker multipliers on the other hand, can only be active or inactive (i.e., either positive or zero). The search for the minimum of F_0 is carried out in a feasible region bounded

by the above constraints. The base load flow results used to evaluate the network loss models, describe a feasible operating region of the power system under consideration. If during the search for the minimum of F_0, the minimum falls inside the feasible region, the Kuhn-Tucker multipliers will all be zero (inactive) and can be disregarded. If however, the minimum of F_0 lies on the boundary of the feasible region, one or more of the Kuhn-Tucker multipliers will be positive (active). The inequality constraints in this case are treated as equality constraints.

The set of equations given by equation 4.7 are solved for the economic dispatch schedules of a given power system using the Newton-Raphson method (3, 7, 31) which is described in general terms in Section 4.3. The economic active-reactive dispatch formulation is presented next.

4.2 The Optimization Procedure - Active-Reactive

The fuel cost function given by equation 4.1, is minimized using the Lagrange-Kuhn-Tucker formulation as given by the following equation:

$$\text{minimize} \quad F_0 = \sum_{i=1}^{m} \alpha_{si} + \beta_{si} P_{Gsi} + \gamma_{si} P_{Gsi}^2$$

subject to:

$$h_p(P_{Gsi}) = P_D + P_L - \sum_{i=1}^{m} P_{Gsi} = 0.0 \qquad (4.8)$$

$$h_q(Q_{Gsi}) = Q_D + Q_L - \sum_{i=1}^{m} Q_{Gsi} - \sum_{j=1}^{n} Q_{Gvj} - \sum_{k=1}^{r} Q_{Shk} = 0.0 \quad (4.9)$$

and,

$$g_p(P_{Gsi}) \leq 0.0 \qquad (4.10)$$

$$g_q(Q_{Gsi}) \leq 0.0 \qquad (4.11)$$

Equations 4.10 and 4.11, may be written as:

$$P_{Gsi\,min} - P_{Gsi} \leq 0.0 \qquad (4.12)$$

$$P_{Gsi} - P_{Gsi\,max} \leq 0.0 \qquad (4.13)$$

and,

$$Q_{Gsi\,min} - Q_{Gsi} \leq 0.0 \qquad (4.14)$$

$$Q_{Gsi} - Q_{Gsi\,max} \leq 0.0 \qquad (4.15)$$

The Lagrange-Kuhn-Tucker function is formed as:

$$F_A = F_0 + \lambda_p \left[P_D + P_L - \sum_{i=1}^{m} P_{Gsi} \right]$$

$$+ \lambda_q \left[Q_D + Q_L - \sum_{i=1}^{m} Q_{GSi} - \sum_{j=1}^{n} Q_{Gvj} - \sum_{k=1}^{r} Q_{Shk} \right]$$

$$+ \sum_{i=1}^{m} \mu_{pi\,min} \left[P_{Gsi\,min} - P_{Gsi} \right]$$

$$+ \sum_{i=1}^{m} \mu_{pi \; max} \left[P_{Gsi} - P_{Gsi \; max} \right]$$

$$+ \sum_{i=1}^{m} \mu_{qi \; min} \left[Q_{Gsi \; min} - Q_{Gsi} \right]$$

$$+ \sum_{i=1}^{m} \mu_{qi \; max} \left[Q_{Gsi} - Q_{Gsi \; max} \right] \qquad (4.16)$$

where,

F_A - the augmented function

P_D, Q_D - the total active and reactive load demand of the system

P_L, Q_L - the total active and reactive power losses of the system

P_{Gsi}, Q_{Gsi} - the active and reactive powers of the ith 'generating' unit

Q_{Gvj} - the purely reactive generation power at the jth bus of the network

Q_{Shk} - the shunt purely reactive power at the kth node

λ_p, λ_q - Lagrange type multipliers

μ_{pi}, μ_{qi} - Kuhn-Tucker multipliers

m - the number of thermal generation units in the network

n - the number of purely reactive sources in the network

r - the number of shunt reactive powers of the system

The optimum economic active-reactive dispatch conditions are obtained by differentiating equation 4.16 with respect to P_{Gsi}, Q_{Gsi}, i=1,2,...,m,

λ_p, λ_q, μ'_{ps} and μ'_{qs} and equating the resulting equations to zero. This set of equations can be written as:

$$\frac{\partial F_A}{\partial P_{Gsi}} = f_{pi} = \frac{\partial F_0}{\partial P_{Gsi}} + \lambda_p \frac{\partial h_p}{\partial P_{Gsi}} + \lambda_q \frac{\partial h_q}{\partial P_{Gsi}}$$

$$+ \mu_{pi\ min} \frac{\partial g_{p\ min}}{\partial P_{Gsi}} + \mu_{pi\ max} \frac{\partial g_{p\ max}}{\partial P_{Gsi}} = 0.0 \qquad (4.17a)$$

$$\frac{\partial F_A}{\partial Q_{Gsi}} = f_{qi} = \frac{\partial F_0}{\partial Q_{Gsi}} + \lambda_p \frac{\partial h_p}{\partial Q_{Gsi}} + \lambda_q \frac{\partial h_q}{\partial Q_{Gsi}}$$

$$+ \mu_{qi\ min} \frac{\partial g_{q\ min}}{\partial Q_{Gsi}} + \mu_{qi\ max} \frac{\partial g_{q\ max}}{\partial Q_{Gsi}} = 0.0 \qquad (4.17b)$$

$$\frac{\partial F_A}{\partial \lambda_p} = f_{pD} = h_p(P_{Gsi}) = 0.0 \qquad (4.17c)$$

$$\frac{\partial F_A}{\partial \lambda_q} = f_{qD} = h_q(Q_{Gsi}) = 0.0 \qquad (4.17d)$$

$$\frac{\partial F_A}{\partial \mu_{pi\ min}} = 0.0 \quad \text{for } \mu_{pi\ min} > 0 \text{ or } \mu_{pi\ min} = 0.0 \qquad (4.17e)$$

$$\frac{\partial F_A}{\partial \mu_{pi\ max}} = 0.0 \quad \text{for } \mu_{pi\ max} > 0 \text{ or } \mu_{pi\ max} = 0.0 \qquad (4.17f)$$

$$\frac{\partial F_A}{\partial \mu_{qi\ min}} = 0.0 \quad \text{for } \mu_{qi\ min} > 0 \text{ or } \mu_{qi\ min} = 0.0 \qquad (4.17g)$$

$$\frac{\partial F_A}{\partial \mu_{qi\ max}} = 0.0 \quad \text{for } \mu_{qi\ max} > 0 \text{ or } \mu_{qi\ max} = 0.0 \qquad (4.17h)$$

In a similar fashion to that of the active case, the set of equations 4.17 are solved by the Newton-Raphson iterative method which is given next.

4.3   The Newton-Raphson Method

Consider the general vector valued function given by:

$$\underline{f} = \underline{f}\ (\underline{x}) = \underline{0} \qquad (4.18)$$

The Newton-Raphson iterative algorithm can be derived by expanding the function given by equation 4.18, using Taylors series expansion about an initial vector $\underline{x}^{(0)}$ as given below:

$$\underline{f} = \underline{0} = \underline{f}(\underline{x}^{(0)}) + \left.\frac{\partial \underline{f}(\underline{x})}{\partial \underline{x}}\right|_{\underline{x}^{(0)}} \Delta\underline{x}^{(0)} + \text{ higher order terms} \qquad (4.19)$$

If the higher order terms are neglected the updating vector $\Delta\underline{x}$ at

iteration (ν) is given by:

$$\Delta\underline{x}^{(\nu)} = - \underline{J}^{-1} \Big|_{\underline{x}^{(\nu)}} \underline{f}(\underline{x})^{(\nu)} \tag{4.20}$$

where,

$$\underline{J} = \frac{\partial}{\partial \underline{x}} [\underline{f}(\underline{x})] \tag{4.21}$$

where,

$\underline{J}$ – the Jacobian matrix.

The updated vector $\underline{x}$ at the $(\nu+1)$th iteration is given by:

$$\underline{x}^{(\nu+1)} = \underline{x}^{(\nu)} + \Delta\underline{x}^{(\nu)} \tag{4.22}$$

The iterative process is continued until convergence is achieved to some desired tolerance. The Newton-Raphson method is used to solve the set of equations of 4.7 and 4.17 for the economic active or active-reactive dispatch conditions of the system under consideration. The Newton-Raphson based optimization algorithms, minimizing the thermal cost function are given next.

4.4   The Newton-Raphson Based Optimization Algorithm - Active

The Newton-Raphson technique is applied to the set of equations given by 4.7 to evaluate the optimum economic active dispatch schedules of a given power system. In this case, the elements of the vectors $\underline{f}$, $\Delta\underline{x}$ and the matrix $\underline{J}$ are given below:

$$\underline{f} = \begin{bmatrix} f_{p1} & f_{p2} & \cdots & f_{pm} & f_{pD} \end{bmatrix}^T \qquad (4.23)$$

The Jacobian matrix is given by (subscript s is dropped).

$$\underline{J} = \begin{bmatrix} \dfrac{\partial f_{p1}}{\partial P_{G1}} & \dfrac{\partial f_{p1}}{\partial P_{G2}} & \cdots & \dfrac{\partial f_{p1}}{\partial P_{Gm}} & \dfrac{\partial f_{p1}}{\partial \lambda_p} \\[2ex] \dfrac{\partial f_{p2}}{\partial P_{G1}} & \dfrac{\partial f_{p2}}{\partial P_{G2}} & \cdots & \dfrac{\partial f_{p2}}{\partial P_{Gm}} & \dfrac{\partial f_{p2}}{\partial \lambda_p} \\[2ex] \vdots & & & & \\[2ex] \dfrac{\partial f_{pm}}{\partial P_{G1}} & \dfrac{\partial f_{pm}}{\partial P_{G2}} & \cdots & \dfrac{\partial f_{pm}}{\partial P_{Gm}} & \dfrac{\partial f_{pm}}{\partial \lambda_p} \\[2ex] \dfrac{\partial f_{pD}}{\partial P_{G1}} & \dfrac{\partial f_{pD}}{\partial P_{G2}} & \cdots & \dfrac{\partial f_{pD}}{\partial P_{Gm}} & 0 \end{bmatrix} \qquad (4.24)$$

The increment vector $\Delta \underline{x}$ is given by:

$$\Delta \underline{x} = \begin{bmatrix} \Delta P_{G1} & \Delta P_{G2} & \cdots & \Delta P_{Gm} & \Delta \lambda_p \end{bmatrix}^T \qquad (4.25)$$

The initial guesses for this algorithm are obtained by neglecting the power losses in the system as given by the following equations:

$$F_A = F_0 + \lambda_p \left[P_D - \sum_{i=1}^{m} P_{Gsi} \right] \qquad (4.26)$$

$$\frac{\partial \overset{*}{F}_A}{\partial P_{Gsi}} = \beta_{si} + 2\gamma_{si}\, P_{Gsi} - \lambda_p = 0.0 \tag{4.27}$$

Solving equation 4.27 for λ_p and P_{Gsi} gives:

$$\lambda_p = [2P_D + (\sum_{i=1}^{m} \beta_{si}/\gamma_{si})]/[\sum_{i=1}^{m} \gamma_{si}]^{-1} \tag{4.28}$$

and,

$$P_{Gsi} = [\lambda_p - \beta_{si}]/[2\gamma_{si}] \tag{4.29}$$

$$\text{for } i = 1, 2, \ldots, m$$

The computational procedure for the evaluation of the optimum active dispatch schedules of a power system is summarized in a flow chart given in Figure 4.1.

4.5 The Newton-Raphson Based Optimization Algorithm – Active-Reactive

The elements of the vectors $\underline{f}$, $\Delta\underline{x}$ and the matrix $\underline{J}$ in the Newton-Raphson formulation for the evaluation of the optimum active-reactive conditions of a power system are given below:

$$\underline{f} = [f_{p1}\, f_{p1}\, \cdots\, f_{pm}\, f_{q1}\, f_{q2}\, \cdots\, f_{qm}\, f_{pD}\, f_{qD}]^T \tag{4.30}$$

The Jacobian matrix is given by (subscript "s" is dropped):

$$
\underline{J} = \begin{bmatrix}
\dfrac{\partial f_{p1}}{\partial P_{G1}} & \dfrac{\partial f_{p1}}{\partial P_{G2}} & \cdots & \dfrac{\partial f_{p1}}{\partial P_{Gm}} & \dfrac{\partial f_{p1}}{\mu Q_{G1}} & \dfrac{\partial f_{p1}}{\mu Q_{G2}} & \cdots & \dfrac{\partial f_{p1}}{\partial Q_{Gm}} & \dfrac{\partial f_{p1}}{\partial \lambda_p} & \dfrac{\partial f_{p1}}{\partial \lambda_q} \\[2.2em]
\dfrac{\partial f_{p2}}{\partial P_{G1}} & \dfrac{\partial f_{p2}}{\partial P_{G2}} & \cdots & \dfrac{\partial f_{p2}}{\partial P_{Gm}} & \dfrac{\partial f_{p2}}{\partial Q_{G1}} & \dfrac{\partial f_{p2}}{\partial Q_{G2}} & \cdots & \dfrac{\partial f_{p2}}{\partial O_{Gm}} & \dfrac{\partial f_{p2}}{\partial \lambda_p} & \dfrac{\partial f_{p1}}{\partial \lambda_q} \\[2.2em]
\dfrac{\partial f_{pm}}{\partial P_{G1}} & \dfrac{\partial f_{pm}}{\partial P_{G2}} & \cdots & \dfrac{\partial f_{pm}}{\partial P_{Gm}} & \dfrac{\partial f_{pm}}{\partial Q_{G2}} & \dfrac{\partial f_{pm}}{\partial Q_{G2}} & \cdots & \dfrac{\partial f_{pm}}{\partial Q_{Gm}} & \dfrac{\partial f_{pm}}{\partial \lambda_p} & \dfrac{\partial f_{pm}}{\partial \lambda_p} \\[2.2em]
\dfrac{\partial f_{q1}}{\partial P_{G1}} & \dfrac{\partial f_{q1}}{\partial P_{G2}} & \cdots & \dfrac{\partial f_{q1}}{\partial P_{Gm}} & \dfrac{\partial f_{q1}}{\partial Q_{G1}} & \dfrac{\partial f_{q1}}{\partial Q_{G2}} & \cdots & \dfrac{\partial f_{q1}}{\partial Q_{Gm}} & \dfrac{\partial f_{q1}}{\partial \lambda_p} & \dfrac{\partial f_{q1}}{\partial \lambda_q} \\[2.2em]
\dfrac{\partial f_{qm}}{\partial P_{G1}} & \dfrac{\partial f_{qm}}{\partial P_{G2}} & \cdots & \dfrac{\partial f_{qm}}{\partial P_{Gm}} & \dfrac{\partial f_{qm}}{\partial Q_{G1}} & \dfrac{\partial f_{qm}}{\partial Q_{Gm}} & \cdots & \dfrac{\partial f_{qm}}{\partial Q_{Gm}} & \dfrac{\partial f_{qm}}{\partial \lambda_p} & \dfrac{\partial f_{qm}}{\partial \lambda_q} \\[2.2em]
\dfrac{\partial f_{pD}}{\partial P_{G1}} & \dfrac{\partial f_{pD}}{\partial P_{G2}} & \cdots & \dfrac{\partial f_{pD}}{\partial P_{Gm}} & \dfrac{\partial f_{pD}}{\partial Q_{G1}} & \dfrac{\partial f_{pD}}{\partial Q_{G2}} & \cdots & \dfrac{\partial f_{pD}}{\partial Q_{Gm}} & 0 & 0 \\[2.2em]
\dfrac{\partial f_{qD}}{\partial P_{G1}} & \dfrac{\partial f_{qD}}{\partial Q_{G2}} & \cdots & \dfrac{\partial f_{qD}}{\partial P_{Gm}} & \dfrac{\partial f_{qD}}{\partial Q_{G1}} & \dfrac{\partial f_{qD}}{\partial Q_{G2}} & \cdots & \dfrac{\partial f_{qD}}{\partial Q_{Gm}} & 0 & 0
\end{bmatrix}
\tag{4.31}
$$

The increment vector $\Delta \underline{x}$ is given by:

$$
\Delta \underline{x} = \begin{bmatrix} \Delta P_{G1} & \Delta P_{G2} & \cdots & \Delta P_{Gm} & \Delta Q_{G1} & \Delta Q_{G2} & \cdots & \Delta Q_{Gm} & \Delta \lambda_p & \Delta \lambda_q \end{bmatrix}^T
\tag{4.32}
$$

Similarly, the initial guesses for this algorithm are obtained by neglecting the power losses. Initial guesses for λ_p and P_{Gsi} are as given by equations 4.28 and 4.29 respectively. The reactive power generations are approximated as:

$$Q_{Gsi} = P_{Gsi} \ (Q_D/P_D) \tag{4.33}$$

The initial guess for λ_q is either taken as 1.0 or calculated from:

$$\lambda_q = \lambda_p \left[(\partial P_L/\partial Q_{Gsi})/(1 - \partial Q_L/\partial P_{Gsi}) \right] \tag{4.34}$$

The computational procedure for this algorithm is given in the flow chart of Figure 4.1.
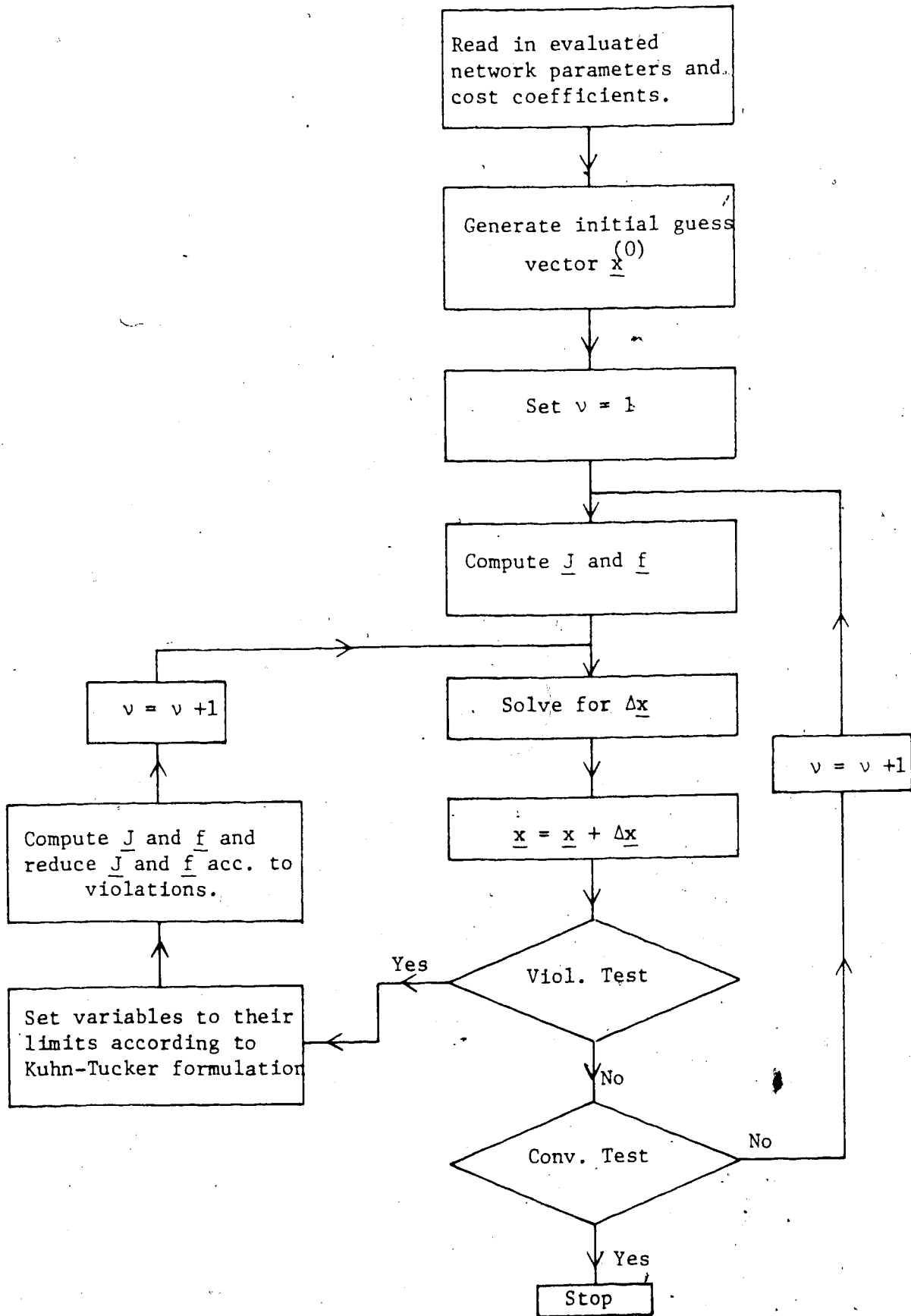
Figure 4.1 The Optimization Procedure - Flow Chart

CHAPTER V

APPLICATION OF LOSS MODEL BASED ECONOMIC DISPATCH

METHODS TO MODEL POWER SYSTEMS

In this chapter, the ridge regression estimation procedure is applied to evaluate the active and active-reactive power loss models of some sample power systems. Based on the evaluated loss models, the economic active and active-reactive dispatch schedules of the power systems are evaluated. The accuracy of the estimated loss model parameters and the validity of the dispatch solutions are also verified in this chapter.

The ridge regression based optimization procedures used in this chapter are suitable for the evaluation of dispatch solutions of small power systems with a small number of generation buses, as the system loss models are evaluated for the entire networks in one estimation process. Large power networks containing a large number of generation buses are analyzed in a piecewise manner as will be seen later.

To illustrate the parameter estimation, and the economic dispatch procedures, the IEEE 14 bus test system (42), is studied in detail in this chapter. Other standard test systems were also studied, namely the 5 bus (3) and the IEEE 30 bus (42) test systems. Since the economic dispatch solutions of these systems were obtained in a similar fashion to the IEEE 14 bus system, the results of the 5 and 30 bus test systems are presented in Appendix C.

The parameters of the active, active-reactive loss models and the purely reactive models of the above systems were evaluated from data sets characterizing the power systems. The data set for each of these power systems was obtained by performing a number of load flow studies

of the system for different system load and voltage levels that cover

the entire operating range of the power systems. This data set forms a

feasible operating region of the power system, through which a search

for the optimal solution is conducted.

5.1 The Active Power Loss Model and the Active Dispatch Results

This section presents the parameter estimates obtained for the

active power loss model and the economic dispatch schedules of the

IEEE 14 bus test system.

5.1.1 The IEEE 14 Bus Test System-Active Power Loss Model

The single line diagram of the IEEE 14 bus test system is shown

in Figure 5.1. The system particulars are given in Tables 5.1, 5.2,

5.3 and 5.4 respectively. The power system has two active-reactive

generation buses, 1 and 13, and three purely reactive generation

sources at buses 4, 6 and 14. The system also has one purely shunt

reactive source at bus number 7. On the basis of equation 2.3, the

number of parameters to be evaluated for the active power loss model

of this system is 6. A minimum of seven load flow results are required,

which were carried out for increments of 10 to 100% of the system

nominal load of 259+j73.5 MVA. Using the load flow results obtained,

the parameters of the active power loss model of this system were

evaluated by the iterative ridge regression procedure. The results

obtained are presented in Table 5.5. The parameters of t░░░░░░and

of all other tables are rounded off to six decimal places░░░░░░░l

data to eight decimal places.

5.1.2 The IEEE 14 Bus Test System – Economic Active Dispatch

The thermal generation unit capacities used in the evaluation of

the economic dispatch schedules of the IEEE 14 bus test system are
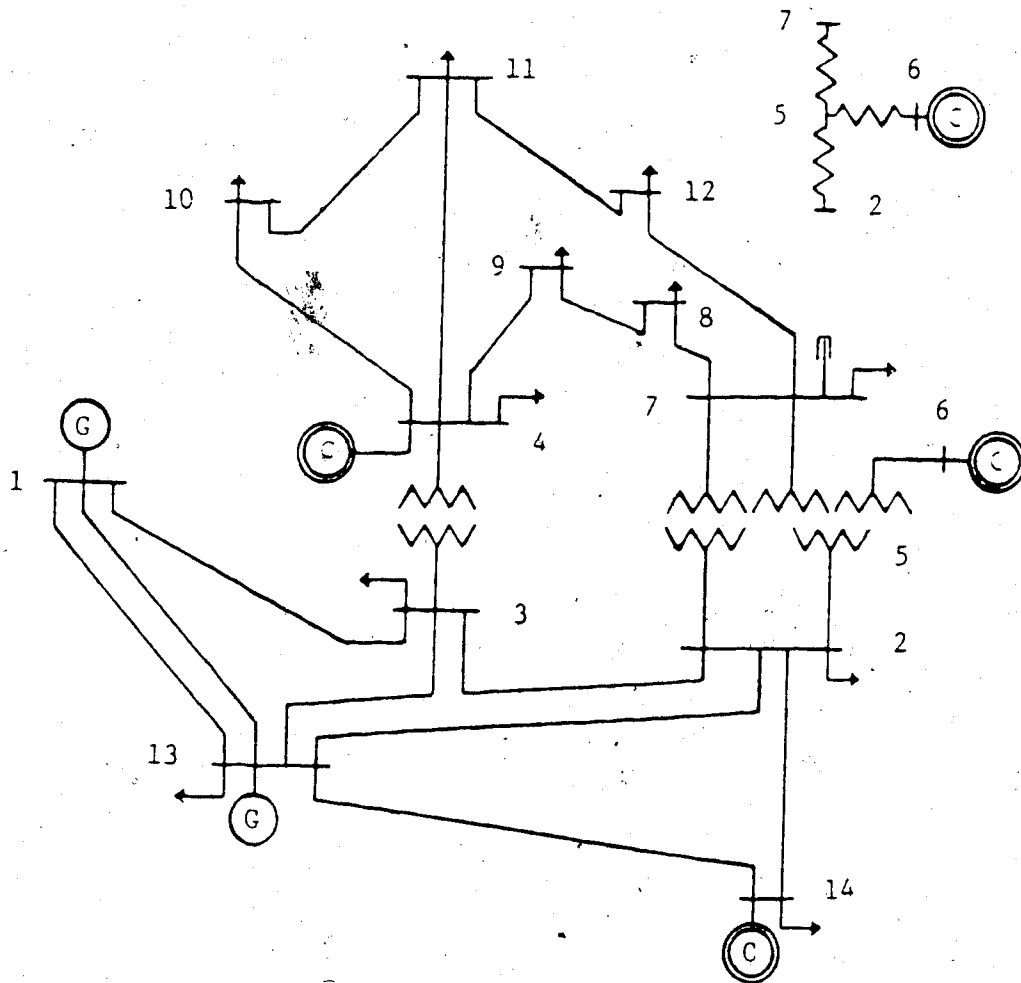
Figure 5.1 The IEEE 14 Bus Test System

Bus No.	Voltage* p.u.	Angle Degrees	Generation MW	Load** MW	MVAR
***					
1	1.06	0.0	0.0	0.0	0.0
2	1.00	0.0	0.0	47.80	-3.90
3	1.00	0.0	0.0	7.60	1.60
4	1.00	0.0	0.0	11.20	7.50
5	1.00	0.0	0.0	0.0	0.0
6	1.00	0.0	0.0	0.0	0.0
7	1.00	0.0	0.0	29.50	16.60
8	1.00	0.0	0.0	9.00	5.80
9	1.00	0.0	0.0	3.50	1.80
10	1.00	0.0	0.0	6.10	1.60
11	1.00	0.0	0.0	13.50	5.80
12	1.00	0.0	0.0	14.90	5.00
13	1.00	0.0	40.0	21.70	12.70
14	1.00	0.0	0.0	94.20	19.00

* - initial values, ** tot·l load = 259+j73.5 MVA, *** slack bus

Table 5.1 The IEEE 14 Bus Test System Operating Conditions

Bus No.	Voltage p.u.	MVAR Capability	
		Min	Max
4	1.070	-6.00	24.00
6	1.090	-6.00	24.00
13	1.045	-40.00	50.00
14	1.010	0.00	40.00

Table 5.2 The IEEE 14 Bus Test System Voltage Regulated Bus Data

Send Bus	End Bus	Resistance	Reactance	Line Charging
1	13	.01938	.05917	.02640
13	14	.04699	.19797	.02190
13	2	.05811	.17632	.01870
1	3	.05403	.22304	.02460
13	3	.05695	.17388	.01700
14	2	.06701	.17103	.01730
2	3	.01335	.04211	.00640
3	4	.	.25202	.
2	5	.	.20912	.
5	6	.	.17615	.
2	7	.	.55618	.
5	7	.	.11001	.
7	8	.03181	.08450	.
4	9	.09498	.19890	.
4	10	.12291	.25581	.
4	11	.06615	.13027	.
7	12	.12711	.27038	.
8	9	.08205	.19207	.
10	11	.22092	.19988	.
11	12	.17093	.34802	.

Table 5.3 The IEEE 14 Bus Test System Line Impedances in
p.u. on 100 MVA Base

Transformer Data		
Send Bus	End Bus	Tap Setting
2	5	0.978
2	7	0.969
3	4	0.932

Shunt Data	
Bus No.	Susceptance
7	0.190

Table 5.4 The IEEE 14 Bus Test System Transformer

and Shunt Data

given in Table 5.6, for coal fired plants. The cost coefficients of

these plants are given in Table 2.1. Based on the evaluated active

power loss model of this system for ridge k = 0.039 (Table 5.5), the

economic active dispatch solutions were obtained as shown in Table 5.7.

The dispatch solutions in Table 5.7, were fed back into the load flow

program and the solution obtained for all system loads considered. These

results are shown in brackets in Table 5.7 for comparison. The load

flow solutions were carried out to validate the accuracy of the evaluated

loss model and the accuracy of the dispatch solutions. The load flow

Parameter	Ridge k=0.0		Ridge k=0.039	
	Estimated Value	Condition Index	Estimated Value	Condition Index
K_{L0}	-0.000040	1	-0.005096	1
B_{01}	0.014069	2	0.012278	2
B_{02}	-0.054198	5	0.005811	5
B_{11}	0.020589	35	0.017185	11
B_{12}	0.004957	69	0.006991	11
B_{22}	0.054078	679	0.011829	11
Condition Number	679		11	
Mean Square Error	39.56		4.82	

Table 5.5 The Active Power Los Model Parameters of the

IEEE 14 Bus Test System in p.u. on 100 MVA Base

Generator No.	Generator Size (MW)	Source Constraints		Bus No.
		(MW)	(MVAR)	
1	200	$5 \leq P_{G1} \leq 200$	$-80 \leq Q_{G1} \leq 50$	1
2	200	$5 \leq P_{G13} \leq 200$	$-40 \leq Q_{G13} \leq 50$	13

Table 5.6 The IEEE 14 Bus Test System Generator Sizes – Coal

solutions based on the economic dispatch results gave voltage profiles that had voltage levels which were within the voltage limits of the feasible operating region of the power system. Samples of the voltage profiles obtained for light and heavy loads are shown in Table 5.7

5.1.3 The IEEE 14 Bus Test System-Active Power Dispatch : Multiple Generators

The case of more than one generator feeding one generation bus of the power system, is presented in this section. The IEEE 14 bus test system shown in Figure 5.1, is considered to be fed by one generator at bus 1 and by two generators at bus 13. The size of the individual coal fired units used in the dispatch procedure are listed in Table 5.9 (see Table 2.1 for cost coefficients). Using the active power loss model with the parameters of Table 5.5 for $k = 0.039$, the economic dispatch solution was obtained for the nominal load of the system of 259+j73.5 MVA as shown in Table 5.10. The load flow solution based on the economic dispatch result is shown in brackets in Table 5.10 for comparison. The load flow voltage profile obtained is shown in Table 5.11.

5.1.4 Discussion of the IEEE 14 Bus Results - Active Model

As seen from Table 5.5, the parameter estimates obtained for $k=0.0$, resulted in a high value for the condition number (679) which indicates that data used for the loss coefficient evaluation was ill-conditioned. For this value of k, the matrix $\underline{A}^T\underline{A}$ when multiplied by its inverse did not result in a unit matrix. For values of $0.039 \leq k \leq 1.0$, the parameter estimates stabilized and a correct inverse of $\underline{A}^T\underline{A}$ was obtained. Comparing the dispatch results with the load flow

P_D (MW)	λ_p (S/MWh)	P_{G1} (MW)	P_{G13} (MW)	P_L (MW)	F_0 ($/h)
25.9	8.86	7.273 (7.376)	18.679 (18.679)	0.052 (0.141)	573.15
51.8	8.97	19.023 (19.219)	32.971 (32.971)	0.194 (0.384)	801.34
77.7	9.08	31.120 (31.177)	47.366 (47.366)	0.786 (0.839)	1035.08
103.6	9.20	43.265 (43.239)	61.865 (61.865)	1.5630 (1.501)	1271.80
129.5	9.32	55.458 (55.410)	76.471 (76.471)	2.429 (2.382)	1511.57
155.4	9.44	67.701 (67.694)	91.185 (91.185)	3.486 (3.481)	1754.43
181.3	9.56	79.993 (80.050)	106.010 (106.010)	4.703 (4.675)	2000.43
207.2	9.68	92.336 (92.363)	120.948 (120.948)	6.084 (6.090)	2249.65
233.1	9.81	104.730 (104.611)	136.001 (136.001)	7.631 (7.520)	2502.13
259.0	9.94	117.176 (117.167)	151.171 (151.171)	9.347 (9.343)	2757.93

Table 5.7 The Economic Active Dispatch Solutions

of the IEEE 14 Bus Test System

Bus No.	Load=25.9+j7.35MVA		Load=259.0+j73.5MVA	
	Voltage p.u.	Angle Degrees	Voltage p.u.	Angle Degrees
1	1.0300	0.0	1.0600	0.0
2	1.0375	-0.8702	1.0186	-7.7872
3	1.0342	-0.6884	1.0205	-6.4720
4	1.0927	-1.2048	1.0700	-11.8400
5	1.0780	-1.1653	1.0620	-10.8699
6	1.0681	-1.1653	1.0900	-10.8699
7	1.0933	-1.3160	1.0565	-12.4680
8	1.0924	-1.3251	1.0515	-12.6424
9	1.0922	-1.2793	1.0572	-12.3723
10	1.0914	-1.2874	1.0552	-12.6879
11	1.0911	-1.2999	1.0505	-12.7627
12	1.0906	-1.4010	1.0359	-13.5958
13	1.0300	-0.0843	1.0450	-1.7730
14	1.0338	-0.9857	1.0100	-9.8564

Table 5.8 The Voltage Profiles of the IEEE 14 Bus

System Based on the Economic Dispatch Solution

Generator No.	Generator Size (MW)	Source Constraints		Bus No.
		MW	MVARS	
1	400	$10 \leq P_{G1} \leq 400$	$-80 \leq Q_{G1} \leq 60$	1
2	200	$5 \leq P_{G2} \leq 200$	$-80 \leq Q_{G2} \leq 50$	13
3	200	$5 \leq P_{G3} \leq 200$	$-40 \leq Q_{G3} \leq 50$	13

Table 5.9. The IEEE 14 Bus Test System with

Multiple Generators-Unit Sizes - Coal

P_D (MW)	λ_p ($/MWh)	P_{G1} (MW)	P^*_{G2} (MW)	P^*_{G3} (MW)	P_L (MW)	F_0 ($/h)
259.0	9.35	150.999 (151.016)	35.738 (35.738)	82.355 (82.355)	10.092 (10.116)	2953.80
* - Generators feeding bus number 13.						

Table 5.10 The Economic Active Dispatch of the

IEEE 14 Bus Test System - Multiple Generations

Load = 259.0 + j73.5 MVA					
Bus No.	Voltage p.u.	Angle Degrees	Bus No.	Voltage p.u.	Angle Degrees
1	1.0600	0.0	8	1.0515	-13.3677
2	1.0186	-8.5352	9	1.0572	-13.0861
3	1.0205	-7.1532	10	1.0552	-13.3919
4	1.0700	-12.5420	11	1.0505	-13.4687
5	1.0620	-11.6062	12	1.0359	-14.3157
6	1.0900	-11.6062	13	1.0450	-2.7201
7	1.0565	-13.1984	14	1.0100	-10.7001

Table 5.11 The Voltage Profile of the IEEE 14 Bus

Test System Based on the Economic Dispatch

Solution - Multiple Generations

solutions shown in Table 5.7, it is observed that both results agree

very closely for all load levels considered indicating the accuracy

of the estimated parameters and the validity of the dispatch solutions.

The voltage profiles of the load flow solutions based on the economic

dispatch results were within the voltage limits of the feasible operating

region of the system.

5.2   The Active-Reactive Loss Model and the Active-Reactive Dispatch

Results

   The parameter estimates of the active-reactive loss submodel, the

purely reactive submodels and the active-reactive dispatch solutions

of the IEEE 14 bus test system are presented in this section.

5.2.1 The IEEE 14 Bus Test System - Active-Reactive and Purely

Reactive Models

The system configuration is shown in Figure 5.1. On the basis

of equation 2.25, the number of parameters to be evaluated for both

the active and reactive power loss submodels of this system is nine.

Ten load flow solutions were performed for increments of 10 to 100% of

the system nominal load. Using this base data, the parameters of

the active and reactive power loss submodels were evaluated by the ridge

estimator. The parameter estimates obtained are presented in Tables

5.12 and 5.13 for the active and reactive parts respectively.

The purely reactive powers of the IEEE 14 bus system at buses

4, 6 and 14, were modeled in terms of the total reactive load demand of

the network. A third order polynomial was required for each of the

above purely reactive powers as given by the following equation:

$$Q_{GVi} = A_{0i} + A_{1i} \, Q_D + A_{2i} \, Q_D^2 + A_{3i} \, Q_D^3 \tag{5.1}$$

where,

Q_{GVi} - the purely reactive power at bus i in MVARS.

A_i's - the parameters to be evaluated of the model.

Q_D - the total reactive load demand in MVARS.

In the modeling procedure, the reactive power limit constraints were

Parameter	Ridge k = 0.0		Ridge k = 0.0036	
	Estimated Value	Condition Index	Estimated Value	Condition Index
K_{LOP}	0.008012	1	-0.007507	1
E_{PP1}	-0.073204	2	0.011829	2
E_{PP2}	0.023216	3	0.000185	3
E_{PQ1}	-0.107105	8	-0.008589	8
E_{PQ2}	0.077932	42	-0.022917	30
A_{P11}	0.046668	28	0.018480	24
A_{P12}	0.028605	20	0.006619	18
A_{P22}	-0.018060	16	0.018461	15
B_{P12}	0.026518	10	-0.002697	10
Condition Number	42		30	
Mean Square Error	0.7858		0.0049	

Table 5.12 The Active-Reactive Power Loss Model Parameters
of the IEEE 14 Bus Test System in p.u. on 100MVA
Base (Active Part)

Parameter	Ridge k = 0.0		Ridge k = 0.0036	
	Estimated Value	Condition Index	Estimated Value	Condition Index
K_{L0Q}	-0.163923	1	-0.269921	1
E_{QP1}	-0.599327	2	0.014434	2
E_{QP2}	0.167185	3	-0.000945	3
E_{QQ1}	-0.689447	8	0.041474	8
E_{QQ2}	0.746616	42	0.038416	30
A_{Q11}	0.283497	28	0.077715	24
A_{Q12}	0.189502	20	0.030340	18
A_{Q22}	-0.186907	16	0.076610	15
B_{Q12}	0.215005	10	0.003467	10
Condition Number	42		30	
Mean Square Error	4.8089		0.3922	

Table 5.13 The Active-Reactive Power Loss Model Parameters of the IEEE 14 Bus Test System in p.u. on 100MVA Base (Reactive Part)

imposed on equation 5.1 as given below (see Table 5.2):

$$- 6 \leq Q_{GV4} \leq 24 \text{ MVARS} \qquad (5.2)$$

$$- 6 \leq Q_{GV6} \leq 24 \text{ MVARS} \qquad (5.3)$$

$$0 \leq Q_{GV14} \leq 40 \text{ MVARS} \qquad (5.4)$$

The parameters of equation 5.1 for each source model were evaluated by the ridge estimator from the same load flow results used to evaluate the active-reactive loss submodel. The parameter estimates obtained for Q_{GV4}, Q_{GV6} and Q_{GV14} are presented in Tables 5.14, 5.15 and 5.16 respectively.

The shunt reactive power at bus number 7 (Q_{Sh7}) was also modeled in terms of the total reactive load demand as shown in equation 5.1. The parameter estimates obtained for this model are shown in Table 5.17.

5.2.2 The IEEE 14 Bus Test System - Economic Active-Reactive Dispatch

Based on the evaluated active-reactive loss submodels and the purely reactive submodels of this power system, the economic active-reactive dispatch schedules were computed. The results obtained are given in Tables 5.18 and 5.19 for the active and reactive parts respectively. The generator capacities used in the evaluation of the dispatch solutions are shown in Table 5.6.

To verify the accuracy of the evaluated parameters and the validity of the economic active-reactive dispatch solutions, the dispatch results were fed back into the load flow program and the solution obtained for

	Ridge k = 0.0		Ridge k = 0.0048	
Parameter	Estimated Value	Condition Index	Estimated Value	Condition Index
A_0	-2.792907	1	0.631994	1
A_1	-0.038598	3	-0.295159	3
A_2	-0.007088	24	-0.001255	18
A_3	0.000144	340	0.000103	28
Condition Number	340		28	
Mean Square Error	0.0260		0.0257	

Table 5.14 The Parameters of Q_{GV4} of the IEEE

14 Bus System

Parameter	Ridge k = 0.0		Ridge k = 0.0048	
	Estimated Value	Condition Index	Estimated Value	Condition Index
A_0	145.40691	1	-4.93910	1
A_1	-8.870960	5	-0.208065	5
A_2	0.162348	51	0.001396	25
A_3	-0.000887	809	0.000081	28
Condition Number	809		28	
Mean Square Error	0.1650		0.1196	

Table 5.15 The Parameters of Q_{GV6} of the IEEE 14 Bus System

Parameter	Ridge k = 0.0		Ridge k = 0.0012	
	Estimated Value	Condition Index	Estimated Value	Condition Index
A_0	4.398821	1	4.398820	1
A_1	0.647387	3	0.647387	3
A_2	0.011756	8	0.011753	8
A_3	-0.000516	31	-0.000516	27
Condition Number	31		27	
Mean Square Error	19.89		19.88	

Table 5.16 The Parameters of Q_{GV14} of the IEEE

14 Bus System

Parameter	Ridge k = 0.0		Ridge k = 0.0048	
	Estimated Value	Condition Index	Estimated Value	Condition Index
A_0	23.049383	1	22.922212	1
A_1	-0.051008	3	-0.036372	3
A_2	-0.000029	14	-0.000446	12
A_3	0.000005	116	0.000009	27
Condition Number	116		27	
Mean Square Error	0.0002		0.0002	

Table 5.17 The Parameter of Q_{Sh7} of the IEEE
14 Bus System

all load levels. These load flow solutions are shown in brackets in Tables 5.18 and 5.19 for comparison. The load flow voltage profiles obtained for light and heavy loads of the system are presented in Table 5.20.

5.2.3 Discussion of the IEEE 14 Bus Results - Active-Reactive Model

The results of the IEEE 14 bus test system presented in Tables 5.18 and 5.19, show that the load flow solutions (given in brackets) and the economic dispatch results agree very closely with one another for all loads considered. The differences between the two solutions, as measured by the active and reactive powers at the slack bus (bus number 1), and the total active and reactive power losses, are due to errors in the evaluated loss model parameters, variations in the load flow voltages and load flow mismatches. The errors are also due to slight changes in the feedback load flow voltages. For example, at bus 6, the fixed value of the voltage is 1.09 p.u., whereas the load flow solution gave a value of 1.0857 p.u. (Table 5.20). However, these differences are very small which indicate that the parameter estimates obtained for the various system models for the indicated values of ridge k, are satisfactory. This shows that the models provided a good fit to the base load flow data. This data defined the feasible operating region of the power through which the search for the optimal solution was conducted. Examination of the voltage levels of Table 5.20, further verifies that the economic dispatch solutions are satisfactory as all the bus voltage levels are within the operating voltage limits of the power system (i.e., 0.95 - 1.1 p.u.).

P_D (MW)	λ_p ($/MWh)	P_{G1} (MW)	P_{G13} (MW)	P_L (MW)	F_0 ($/h)
25.9	8.85	7.051 (7.368)	19.051 (19.051)	0.202 (0.489)	574.48
51.8	8.96	19.881 (20.063)	32.424 (32.424)	0.505 (0.684)	804.03
77.7	9.08	32.710 (32.827)	45.936 (45.936)	0.946 (1.065)	1036.39
103.6	9.20	45.518 (45.627)	59.608 (59.608)	(1.526) (1.632)	1271.60
129.5	9.32	58.224 (58.385)	73.505 (73.505)	2.229 (2.389)	1509.53
155.4	9.45	70.827 (71.099)	87.663 (87.663)	3.090 (3.400)	1750.54
181.3	9.59	83.485 (83.991)	102.018 (102.018)	4.203 (4.716)	1995.50
207.2	9.72	96.900 (97.456)	116.003 (116.003)	5.704 (6.270)	2245.64
233.1	9.86	110.539 (111.021)	129.991 (129.991)	7.431 (7.951)	2499.59
259.0	10.00	124.426 (124.864)	143.961 (143.961)	9.387 (9.828)	2757.41

Table 5.18 The Economic Active-Reactive

Dispatch of the IEEE 14 Bus Test

System (Active)

Q_D (MVAR)	λ_q ($/MVARh)	Q_{G1} (MVAR)	Q_{G13} (MVAR)	Q_{GV4} (MVAR)	Q_{GV6} (MVAR)	Q_{GV14} (MVAR)	Q_L (MVAR)
7.35	-0.24	-52.111 (-51.688)	8.278 (8.278)	-1.564 (-1.564)	-6.000 (-6.000)	9.587 (9.587)	-26.525 (-25.809)
14.70	-0.23	-45.757 (-45.850)	7.477 (7.477)	-3.651 (-3.651)	-6.000 (-6.000)	14.818 (14.818)	-23.493 (-23.223)
22.05	-0.22	-38.567 (-38.652)	7.509 (7.509)	-5.381 (-5.380)	-6.000 (6.000)	18.861 (18.860)	-23.631 (-23.500)
29.40	-0.20	-30.302 (-30.375)	8.645 (8.540)	-6.000 (-6.000)	-6.000 (-6.000)	20.488 (20.488)	-20.878 (-20.867)
36.75	-0.18	-20.058 (-19.999)	11.815 (11.815)	-6.000 (-6.000)	-6.000 (-6.000)	18.471 (18.470)	-17.103 (-17.256)
44.10	-0.14	-7.624 (-7.433)	17.327 (17.327)	-5.983 (-5.983)	-4.491 (-4.491)	11.581 (11.580)	-12.086 (-12.454)
51.45	-0.09	5.586 (5.057)	23.878 (23.871)	-3.834 (-3.834)	-0.978 (-0.970)	0.0 (0.0)	-5.733 (-6.847)
58.8	-0.08	11.383 (11.503)	23.158 (23.152)	-0.102 (-0.100)	4.029 (4.020)	0.0 (0.0)	0.693 (0.023)
66.15	-0.08	15.712 (15.649)	20.958 (20.958)	5.460 (5.460)	10.722 (10.722)	0.0 (0.0)	7.807 (7.114)
73.5	-0.08	18.374 (18.454)	16.982 (16.980)	13.097 (13.092)	19.293 (19.290)	0.0 (0.0)	15.570 (15.212)

Table 5.19 The Economic Active-Reactive Dispatch of the

IEEE 14 Bus Test System (Reactive)

Bus No.	Load = 25.9+j7.35MVA		Load = 259+j73.5MVA	
	Voltage p.u.	Angle Degrees	Voltage p.u.	Angle Degrees
1	1.0110	0.0	1.0600	0.0
2	1.0399	-1.2167	1.0084	-7.9206
3	1.0344	-1.0040	1.0128	-6.5962
4	1.1008	-1.5530	1.0628	-12.0498
5	1.0820	-1.4905	1.0544	-11.0545
6	1.0722	-1.4905	1.0857	-11.0545
7	1.0980	-1.6300	1.0484	-12.6753
8	1.0978	-1.6424	1.0435	-12.8540
9	1.0989	-1.6100	1.0495	-12.5843
10	1.0993	-1.6339	1.0478	-12.9093
11	1.0987	-1.6409	1.0430	-12.9836
12	1.0966	-1.7251	1.0279	-13.8242
13	1.0309	-0.4347	1.0413	-1.9241
14	1.0440	-1.4755	0.9805	-9.7917

Table 5.20 The Voltage Profiles of the IEEE 14 Bus

Test System Based on the Economic Active-

Reactive Dispatch Solutions

CHAPTER VI

PIECEWISE NETWORK LOSS MODELS AND ECONOMIC DISPATCH

PROCEDURES FOR LARGE POWER SYSTEMS

The problems associated with large power systems may be reduced by evaluating the network loss models in a piecewise manner. The piecewise loss models can then be used in the fuel cost minimization procedure that determines the optimum economic dispatch schedules of a given power system. The network piecewise loss models can be arrived at using diakoptical or network tearing techniques (43-49). In theory, the loss models discussed in Chapter II can be used to represent any power network regardless of its size. The size of the network is dependent upon the number of generation buses of the network (equations 2.3 and 2.25). In the economic dispatch methods that are based on network loss models, it is important to evaluate the coefficients of the loss models of a given network with a high degree of accuracy in order to obtain satisfactory economic dispatch schedules. In practice, however, the evaluation of a large loss model (i.e., containing a large number of parameters), requires a large number of data points to be available for the application of any least squares based estimation technique. The base data points are usually obtained from load flow studies of the power system, and for large systems, this can be a very costly procedure. In addition to the cost, problems of ill-conditioning become more pronounced in the evaluation of a large number of parameters.

Diakoptical techniques are used in the loss model evaluation procedure to eliminate the above two problems. The diakoptical or

piecewise models, can be developed by first tearing the transmission network into a number of subnetworks connected by transmission lines (interconnections), in such a way that each torn subnetwork contains at least one active-reactive generation bus. Each of these subnetworks and the interconnections is represented by a loss submodel. A number of load flow solutions are then carried out for the entire network to obtain the necessary data for the evaluation of all submodel parameters. The number of load flow results required in this case, is the minimum number needed to evaluate the parameters of the largest submodel of the network.

6.1 The Network Total Active and Reactive Power Losses in Terms of Voltages and Admittances

For a given power network, the network total active and reactive power losses can be written as (see Appendix A):

$$P_L = V_p^T \underline{G} \, V_p + V_q^T \underline{G} \, V_q \qquad (6.1)$$

and

$$Q_L = V_p^T \underline{B} \, V_p + V_q^{\perp} \underline{B} \, V_q \qquad (6.2)$$

where,

P_L, Q_L — the network total active and reactive power losses respectively

V — the bus voltage vector which in rectangular form is given by $\underline{V} = V_p + jV_q$.

$\underline{G}$, $\underline{B}$ - the network conductance and sucesptance matrices.

Equations 6.1 and 6.2 may be written in a piecewise manner using the following netowrk tearing criterion.

6.2 The Tearing Criterion

The tearing criterion may be stated as: the tearing branches of a network are chosen such that:

1. their removal result in a network having subnetworks hinged at the datum node. This datum node is usually taken as the ground node.

2. there is no mutual coupling between branches belonging to different subnetworks. The only coupling is a conductive coupling through the torn links.

3. the branches removal result in subnetworks, each containing at least one active-reactive generation bus.

6.3 The Piecewise Active and Reactive Loss Models in Terms of Bus Voltages and Line Admittances

Consider a general large power network which is torn into K subnetworks, each containing a number of generation buses, interconnected by N interconnections, as shown in Figure 6.1. The nodal matrix equation for this network may be written as:

$$\underline{Y}\,\underline{V} = \underline{I} + \underline{I}' \tag{6.3}$$

where,
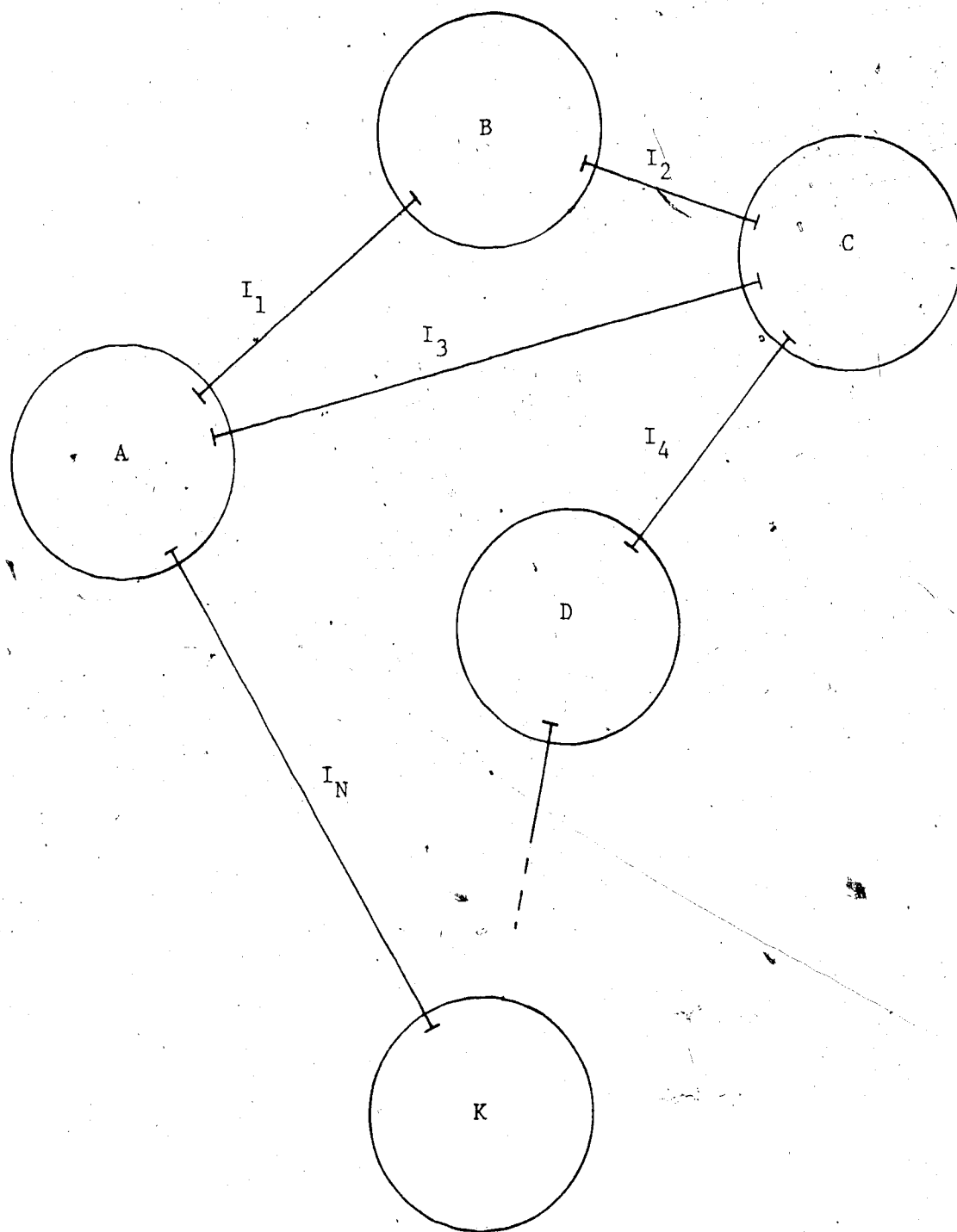
Figure 6.1 A Transmission Network Torn into K

Subnetworks and N Interconnections

$\underline{Y}$ - the entire network bus admittance matrix, where

$\underline{Y} = \underline{G} - j \underline{B}$.

$\underline{V}$ - the network bus voltage vector.

$\underline{I}$ - the network bus current vector.

$\underline{I}'$ - the nodal current vector from interconnections.

Equation 6.3, in terms of the torn subnetwork and interconnection quantities can be written as:

$$
\begin{bmatrix}
\underline{Y}_A & \underline{0} & \cdots & \underline{0} \\
\underline{0} & \underline{Y}_B & & \underline{0} \\
\vdots & & \ddots & \vdots \\
\underline{0} & \cdots & \cdots & \underline{Y}_K
\end{bmatrix}
\begin{bmatrix}
\underline{V}_A \\
\underline{V}_B \\
\vdots \\
\underline{V}_K
\end{bmatrix}
=
\begin{bmatrix}
\underline{I}_A \\
\underline{I}_B \\
\vdots \\
\underline{I}_K
\end{bmatrix}
+
\begin{bmatrix}
\underline{I}'_A \\
\underline{I}'_B \\
\vdots \\
\underline{I}'_K
\end{bmatrix}
\qquad (6.4)
$$

where,

$\underline{Y}_A, \underline{Y}_B, \ldots \underline{Y}_K$ - the bus admittance matrices of subnetworks

A, B, ..., K respectively.

$\underline{V}_A, \underline{V}_B, \ldots \underline{V}_K$ - the nodal voltage vectors of subnetworks

A, B, ..., K respectively.

$\underline{I}_A, \underline{I}_B, \ldots, \underline{I}_K$ - the nodal current vectors of subnetworks A, B,

..., K respectively.

$\underline{I}'_A, \underline{I}'_B, \ldots, \underline{I}'_K$ - the nodal current vectors from interconnections.

The currents are considered positive when flowing into the buses of the network.

Let,

$\underline{I}_I$ — the nodal current vector of interconnections.

$\underline{V}_I$ — the nodal voltage vector of interconnections.

$\underline{Y}_I$ — the bus admittance matrix of interconnections.

Using matrix topology, the current vector $\underline{I}'$, may be written as:

$$\underline{I}' = \begin{bmatrix} \underline{I}'_A \\ \underline{I}'_B \\ \vdots \\ \underline{I}'_K \end{bmatrix} = \underline{C}\ \underline{I}_I \ , \tag{6.5}$$

where,

$\underline{C}$ — the topological or connection matrix whose elements are 0's or 1's.

The nodal voltage vector of interconnections can be written as:

$$\underline{V}_I = -\ \underline{C}^T \underline{V} \ , \tag{6.6}$$

and the current nodal vector of interconnections is given by:

$$\underline{I}_I = \underline{Y}_I\ \underline{V}_I \ . \tag{6.7}$$

Substituting for $\underline{I}_I$ and $\underline{V}_I$ into equation 6.7, gives:

$$\underline{I}'_I = -\ \underline{C}\ \underline{Y}_I\ \underline{C}^T\ \underline{V} \ , \tag{6.8}$$

substituting equation 6.8 into equation 6.4, the following diakoptical

matrix equation is obtained:

$$\left[\begin{bmatrix} \underline{Y}_A & \underline{0} & \underline{0} \\ \underline{0} & \underline{Y}_B & \underline{0} \\ \vdots & & \ddots & \\ \underline{0} & \cdots\cdots & \underline{Y}_K \end{bmatrix} + \underline{C}\ \underline{Y}_I\ \underline{C}^T \right] \begin{bmatrix} \underline{V}_A \\ \underline{V}_B \\ \vdots \\ \underline{V}_K \end{bmatrix} = \begin{bmatrix} \underline{I}_A \\ \underline{I}_B \\ \vdots \\ \underline{I}_K \end{bmatrix} \qquad (6.9)$$

The connection matrix $\underline{C}$ may be partitioned into submatrices $\underline{C}_A$,

$\underline{C}_B$, ..., $\underline{C}_K$, which can be further partitioned into submatrices that

correspond to the interconnections as shown below (see Figure 6.1):

$$\underline{C} = \begin{bmatrix} \underline{C}_A \\ \underline{C}_B \\ \vdots \\ \underline{C}_K \end{bmatrix} = \begin{bmatrix} \underline{C}_{A1} & \underline{C}_{A2} & \cdots\cdots & \underline{C}_{AN} \\ \underline{C}_{B1} & \underline{C}_{B2} & \cdots\cdots & \underline{C}_{BN} \\ \vdots & \vdots & & \vdots \\ \underline{C}_{K1} & \underline{C}_{K2} & \cdots\cdots & \underline{C}_{KN} \end{bmatrix} , \qquad (6.10)$$

if two subnetworks have no common connecting branches, null submatrices

are appropriately substituted in the right hand side of equation 6.10.

The final expression for the diakoptical nodal matrix equation of the

network shown in Figure 6.1, is obtained by substituting equation 6.10

into equation 6.9. For better understanding of the connection matrix

concept, a detailed analysis is given in Appendix D for a nine node

power system which is torn into three subnetworks and two interconnections.

The diakoptical (piecewise) total active power losses of the

network in terms of bus voltages and line admittances for the network

shown in Figure 6.1, can be written as:

$$P_L = \underline{V}_{Ap}^T [\underline{G}_A + \underline{C}_{A1}\, \underline{G}_{I1}\, \underline{C}_{A1}^T + \underline{C}_{A3}\, \underline{G}_{I3}\, \underline{C}_{A3}^T + \underline{C}_{AN}\, \underline{G}_{IN}\, \underline{C}_{AN}^T]\underline{V}_{Ap}$$

$$+ \underline{V}_{Aq}^T [\underline{G}_A + \underline{C}_{A1}\, \underline{G}_{I1}\, \underline{C}_{A1}^T + \underline{C}_{A3}\, \underline{G}_{I3}\, \underline{C}_{A3}^T + \underline{C}_{AN}\, \underline{G}_{IN}\, \underline{C}_{AN}^T]\underline{V}_{Aq}$$

$$+ 2\underline{V}_{Ap}^T [\underline{C}_{A1}\, \underline{G}_{I1}\, \underline{C}_{B1}^T]\underline{V}_{Bp} + 2\underline{V}_{Aq}^T [\underline{C}_{A1}\, \underline{G}_{I1}\, \underline{C}_{B1}^T]\underline{V}_{Bq}$$

$$+ 2\underline{V}_{Ap}^T [\underline{C}_{A3}\, \underline{G}_{I3}\, \underline{C}_{C3}^T]\underline{V}_{Cp} + 2\underline{V}_{Aq}^T [\underline{C}_{A3}\, \underline{G}_{I3}\, \underline{C}_{C3}^T]\underline{V}_{Cq}$$

$$+ \underline{V}_{Bp}^T [\underline{G}_B + \underline{C}_{B1}\, \underline{G}_{I1}\, \underline{C}_{B1}^T + \underline{C}_{R2}\, \underline{G}_{I2}\, \underline{C}_{B2}^T]\underline{V}_{Bp}$$

$$+ \underline{V}_{Bq}^T [\underline{G}_B + \underline{C}_{B1}\, \underline{G}_{I1}\, \underline{C}_{B1}^T + \underline{C}_{B2}\, \underline{G}_{I2}\, \underline{C}_{B2}^T]\underline{V}_{Bq}$$

$$+ 2\underline{V}_{Bp}^T [\underline{C}_{B2}\, \underline{G}_{I2}\, \underline{C}_{B2}^T]\underline{V}_{Cp} + 2\underline{V}_{Bq}^T [\underline{C}_{B2}\, \underline{G}_{I2}\, \underline{C}_{B2}^T]\underline{V}_{Cq}$$

$$+ \underline{V}_{Cp}^T [\underline{G}_C + \underline{C}_{C2}\, \underline{G}_{I2}\, \underline{C}_{C2}^T + \underline{C}_{C3}\, \underline{G}_{I3}\, \underline{C}_{C3}^T]\underline{V}_{Cp}$$

$$+ \underline{V}_{Cq}^T [\underline{G}_C + \underline{C}_{C2}\, \underline{G}_{I2}\, \underline{C}_{C2}^T + \underline{C}_{C3}\, \underline{G}_{I3}\, \underline{C}_{C3}^T]\underline{V}_{Cq}$$

$$\vdots$$

$$+ \underline{V}_{Kp}^T [\underline{G}_K + \underline{C}_{KN}\, \underline{G}_{IN}\, \underline{C}_{KN}^T]\underline{V}_{Kp} + \underline{V}_{Kq}^T [\underline{G}_K + \underline{C}_{KN}\, \underline{G}_{IN}\, \underline{C}_{KN}^T]\underline{V}_{Kq}$$

$$+ 2\underline{V}_{Ap}^T [\underline{C}_{AN}\, \underline{G}_{IN}\, \underline{C}_{AN}^T]\underline{V}_{Kp} + 2\underline{V}_{Aq}^T [\underline{C}_{AN}\, \underline{G}_{IN}\, \underline{C}_{AN}^T]\underline{V}_{Kq} \qquad (6.11)$$

In equation 6.11, it is assumed that subnetwork K has only one common connection with subnetwork A. If, however, it has more than one connection, additional terms will have to be added as was done for subnetworks A, B and C. It should be noted that in equation 6.11, the

following general matrix relation is in order:

$$\underline{C}^T \underline{G} \underline{C} = \underline{C} \underline{G} \underline{C}^T \qquad (6.12)$$

The relation in equation 6.12, is true since the matrix $\underline{Y} = \underline{G} - j\underline{B}$ is a square symmetrix matrix; that is $\underline{Y}^T = \underline{Y}$. Equation 6.11 can be written as:

$$P_L = P_{LA} + P_{LI1A} + P_{LI3A} + P_{LINA} + 2P_{LI1AB}$$

$$+ 2P_{LI3AC} + P_{LB} + P_{LI1B} + P_{LI2B}$$

$$+ 2P_{LI2BC} + P_{LC} + P_{LI2C} + P_{LI3C}$$

$$+$$
$$\vdots$$
$$+ P_{LK} + P_{LINK} + 2P_{LINAK} \qquad (6.13)$$

A similar expression can be easily obtained for Q_L, by replacing $\underline{G}$ by $\underline{B}$ in equation 6.11 leading to:

$$Q_L = Q_{LA} + Q_{LI3A} + Q_{LINA} + 2Q_{LI1AB}$$

$$+ 2Q_{LI3AC} + Q_{LB} + Q_{LI1B} + Q_{LI2B}$$

$$+ 2Q_{LI2BC} + Q_{LC} + Q_{LI2C} + Q_{LI3C}$$

+
.
.
.
$+ Q_{LK} + Q_{LINK} + 2Q_{LINAK}$ $\hspace{4cm}$ (6.14)

The quantities on the right hand side of equations 6.13 and 6.14 in terms of the network active and reactive power generations, have expressions similar to those given by equations 2.23 and 2.24 in Chapter II. From equations 6.13 and 6.14, it is seen that the general network of Figure 6.1, is composed of a number of subnetwork sets. Each of these sets contains two subnetworks interconnected by one interconnection. A detailed analysis of a network torn into two subnetworks with one interconnection is given next.

6.4 The Piecewise Active-Reactive Power Loss Model for a Network Torn into Two Subnetworks

For a power system network torn into two subnetworks A and B with one interconnection I, the active and reactive power losses in terms of voltages and admittances are given by:

$$P_L = P_{LA} + P_{LIA} + P_{LB} + P_{LIB} + 2P_{LIAB} \hspace{2cm} (6.15)$$

where,

$$P_{LA} = V_{AP}^T \, G_A \, V_{Ap} + V_{Aq}^T \, G_A \, V_{Aq} \hspace{2cm} (6.16)$$

$$P_{LIA} = V_{Ap}^T \, C_A \, G_I \, C_A^T \, V_{Ap} + V_{Aq}^T \, C_A \, G_I \, C_A^T \, V_{Aq} \hspace{2cm} (6.17)$$

$$P_{LB} = V_{Bp}^T \; G_B \; V_{Ap} + V_{Bq}^T \; G_B \; V_{Aq} \tag{6.18}$$

$$P_{LIB} = V_{Bp}^T \; C_B \; G_I \; C_B^T \; V_{Bp} + V_{Bq}^T \; C_B \; G_I \; C_B^T \; V_{Bq} \tag{6.19}$$

$$P_{LIAB} = V_{Ap}^T \; C_A \; G_I \; C_B^T \; V_{Bp} + V_{Aq}^T \; C_A \; G_I \; C_B^T \; V_{Bq} \tag{6.20}$$

where,

$$P_{LIBA} = P_{LIAB} \tag{6.21}$$

and,

$$C_A \; G_I \; C_B^T = C_B \; G_I \; C_A^T \tag{6.22}$$

where,

P_{LA}, P_{LB} — the total active power losses of subnetworks A and B respectively.

$P_{LIA} + P_{LIB} + 2P_{LIAB}$ — the total active power losses of interconnections.

Similarly, the reactive power losses of the network may be written as:

$$Q_L = Q_{LA} + Q_{LIA} + Q_{LB} + Q_{LIB} + Q_{LIAB} \tag{6.23}$$

where,

$$Q_{LA} = V_{Ap}^T \underline{B}_A \underline{V}_{Ap} + V_{Aq}^T \underline{B}_A \underline{V}_{Aq} \tag{6.24}$$

$$Q_{LIA} = V_{Ap}^T \underline{C}_A \underline{B}_I \underline{C}_A^T \underline{V}_{Ap} + V_{Aq}^T \underline{C}_A \underline{B}_I \underline{C}_A^T \underline{V}_{Aq} \tag{6.25}$$

$$Q_{LB} = V_{Bp}^T \underline{B}_B \underline{V}_{Bp} + V_{Bq}^T \underline{B}_B \underline{V}_{Bq} \tag{6.26}$$

$$Q_{LIB} = V_{Bp}^T \underline{C}_B \underline{B}_I \underline{C}_B^T \underline{V}_{Bp} + V_{Bq}^T \underline{C}_B \underline{B}_I \underline{C}_B^T \underline{V}_{Bq} \tag{6.27}$$

$$Q_{LIAB} = V_{Ap}^T \underline{C}_A \underline{B}_I \underline{C}_B^T \underline{V}_{Bp} + V_{Aq}^T \underline{C}_A \underline{B}_I \underline{C}_B^T \underline{V}_{Bq} \tag{6.28}$$

where,

$$Q_{LIBA} = Q_{LIAB} \tag{6.29}$$

and,

$$\underline{C}_A \underline{B}_I \underline{C}_B^T = \underline{C}_B \underline{B}_I \underline{C}_A^T \tag{6.30}$$

where,

Q_{LA}, Q_{LB} the total reactive power losses of subnetworks A and B respectively.

$Q_{LIA} + Q_{LIB} + 2Q_{LIAB}$ - the total reactive power losses of interconnections.

The piecewise active and active-reactive power loss models in terms of the power generations of the system are developed in the following sections. Since the active loss model is a special case of the active-reactive power loss model, the latter is formulated first.

6.4.1 The Piecewise Active and Reactive Power Loss Models of a Network Torn into Two Subnetworks in Terms of Active and Reactive Power Generations

Consider the power system shown in Figure 6.2. This system is
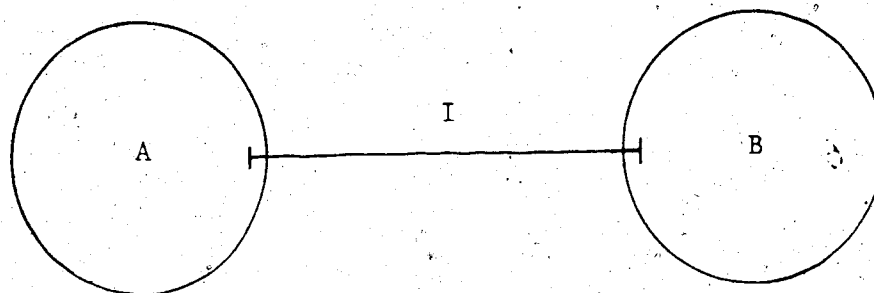
Figure 6.2 A Transmission Network Torn into Two
Subnetworks A and B with One Interconnection I.

torn into two subnetworks A and B, each containing a number of generation buses, interconnected by the torn branches I. Expressions for the diakoptical loss models can be arrived at from first principles as given below:

Let:

$\underline{P}_{GA}$, $\underline{Q}_{GA}$ - the active and reactive power generation vectors of subnetwork A.

$\underline{P}_{GB}$, $\underline{Q}_{GB}$ - the active and reactive power generation vectors of subnetwork B.

Equations 6.16 to 6.19, in terms of the respective active and reactive power generations can be written as (see Appendix A):

$$P_{LA} = K_{LOPA} + [\underline{E}_{PPA}^T \quad \underline{E}_{PQA}^T] \begin{bmatrix} \underline{P}_{GA} \\ \underline{Q}_{GA} \end{bmatrix}$$

$$+ [\underline{P}_{GA}^T \quad \underline{Q}_{GA}^T] \begin{bmatrix} \underline{A}_{PGGA} & -\underline{B}_{PGGA} \\ \underline{B}_{PGGA} & \underline{A}_{PGGA} \end{bmatrix} \begin{bmatrix} \underline{P}_{GA} \\ \underline{Q}_{GA} \end{bmatrix} \qquad (6.31)$$

$$P_{LIA} = K_{LOPIA} + [\underline{E}_{PPIA}^T \quad \underline{E}_{PQIA}^T] \begin{bmatrix} \underline{P}_{GA} \\ \underline{Q}_{GA} \end{bmatrix}$$

$$+ [\underline{P}_{GA}^T \quad \underline{Q}_{GA}^T] \begin{bmatrix} \underline{A}_{PGGIA} & -\underline{B}_{PGGIA} \\ \underline{B}_{PGGIA} & \underline{A}_{PGGIA} \end{bmatrix} \begin{bmatrix} \underline{P}_{GA} \\ \underline{Q}_{GA} \end{bmatrix} \qquad (6.32)$$

and,

$$P_{LB} = K_{LOPB} + [E_{PPB}^T \quad E_{PQB}^T] \begin{bmatrix} P_{GB} \\ \\ Q_{GB} \end{bmatrix}$$

$$+ [P_{GB}^T \quad Q_{GB}^T] \begin{bmatrix} A_{PGGB} & -B_{PGGB} \\ \\ B_{PGGB} & A_{PGGB} \end{bmatrix} \begin{bmatrix} P_{GB} \\ \\ Q_{GB} \end{bmatrix} \qquad (6.33)$$

and,

$$P_{LIB} = K_{LOPIB} + [E_{PPIB}^T \quad E_{PQIB}^T] \begin{bmatrix} P_{GB} \\ \\ Q_{GB} \end{bmatrix}$$

$$+ [P_{GB}^T \quad Q_{GB}^T] \begin{bmatrix} A_{PGGIB} & -B_{PGGIB} \\ \\ B_{PGGIB} & A_{PGGIB} \end{bmatrix} \begin{bmatrix} P_{GB} \\ \\ Q_{GB} \end{bmatrix} \qquad (6.34)$$

where,

$\underline{E}$, $\underline{A}$ and $\underline{B}$ – with appropriate subscripts are the parameters

of the various submodels to be evaluated.

If NGA and NGB are the number of active-reactive generation buses of

subnetworks A and B respectively, then the matrices $\underline{A}_{PGGA}$, $\underline{A}_{PGGIA}$,

$\underline{B}_{PGGA}$ and $\underline{B}_{PGGIA}$ will have the dimension of (NGAxNGA), and the matrices

$\underline{A}_{PGGB}$, $\underline{A}_{PGGIB}$, $\underline{B}_{PGGB}$ and $\underline{B}_{PGGIB}$ will have the dimensions of (NGBxNGB).
Similarly equations 6.24 to 6.27 can be written as:

$$Q_{LA} = K_{LOQA} + [\underline{E}^T_{QPA} \quad \underline{E}^T_{QQA}] \begin{bmatrix} \underline{P}_{GA} \\ \\ \underline{Q}_{GA} \end{bmatrix}$$

$$+ [\underline{P}^T_{GA} \quad \underline{Q}^T_{GA}] \begin{bmatrix} \underline{A}_{QGGA} & -\underline{B}_{QGGA} \\ \\ \underline{B}_{QGGA} & \underline{A}_{QGGA} \end{bmatrix} \begin{bmatrix} \underline{P}_{GA} \\ \\ \underline{Q}_{GA} \end{bmatrix} \tag{6.35}$$

$$Q_{LIA} = K_{LOQIA} + [\underline{E}^T_{QPIA} \quad \underline{E}^T_{QQIA}] \begin{bmatrix} \underline{P}_{GA} \\ \\ \underline{Q}_{GA} \end{bmatrix}$$

$$+ [\underline{P}^T_{GA} \quad \underline{Q}^T_{GA}] \begin{bmatrix} \underline{A}_{QGGIA} & -\underline{B}_{QGGIA} \\ \\ \underline{B}_{QGGIA} & \underline{A}_{QGGIA} \end{bmatrix} \begin{bmatrix} \underline{P}_{GA} \\ \\ \underline{Q}_{GA} \end{bmatrix} \tag{6.36}$$

and,

$$Q_{LB} = K_{LOQIB} + [\underline{E}^T_{QPB} \quad \underline{E}^T_{QQ}] \begin{bmatrix} \underline{P}_{GB} \\ \\ \underline{Q}_{GB} \end{bmatrix}$$

$$+ [\underline{P}^T_{GB} \quad \underline{Q}^T_{GB}] \begin{bmatrix} \underline{A}_{QGGB} & -\underline{B}_{QGGB} \\ \\ \underline{B}_{QGGB} & \underline{A}_{QGGB} \end{bmatrix} \begin{bmatrix} \underline{P}_{GB} \\ \\ \underline{Q}_{GB} \end{bmatrix} \tag{6.37}$$

$$Q_{LIB} = K_{LOQIB} + [E^T_{QPIB} \quad E^T_{QQIB}] \begin{bmatrix} P_{GB} \\ \\ Q_{GB} \end{bmatrix}$$

$$+ [P^T_{GB} \quad Q^T_{GB}] \begin{bmatrix} A_{QGGIB} & -B_{QGGIB} \\ \\ B_{QGGIB} & A_{QGGIB} \end{bmatrix} \begin{bmatrix} P_{GB} \\ \cdot \\ Q_{GB} \end{bmatrix} \qquad (6.38)$$

The coefficient matrices of equations 6.37 and 6.38 have the same
dimensions as in the case of the piecewise active power loss model.
The number of parameters to be evaluated for the above active and
reactive loss models are given by:

$$NCA_P = NCA_Q = NCIA_P = NCIA_Q = (NGA+1)^2 \qquad (6.39)$$

$$NCB_P = NCB_Q = NCIB_P = NCIB_Q = (NGB+1)^2 \qquad (6.40)$$

where,

NCA_P, NCA_Q - the number of parameters of P_{LA} and Q_{LA} respectively.

NCB_P, NCB_Q - the number of parameters of P_{LB} and Q_{LB} respectively.

$NCIA_P$, $NCIA_Q$ -the number of parameters of P_{LIA} and Q_{LIA} respectively.

$NCIB_P$, $NCIB_Q$ - the number of parameters of P_{LIB} and Q_{LIB} respectively.

The submodels P_{LIAB} and Q_{LIAB} can be obtained as follows:

$$\underline{V}_{Ap} = \underline{M}_A \, \underline{P}_A + \underline{N}_A \, \underline{Q}_A \qquad (6.41)$$

$$\underline{V}_{Aq} = \underline{N}_A \, \underline{P}_A - \underline{M}_A \, \underline{Q}_A \qquad (6.42)$$

$$\underline{V}_{Bp} = \underline{M}_B \, \underline{P}_B + \underline{N}_B \, \underline{Q}_B \qquad (6.43)$$

$$\underline{V}_{B_q} = \underline{N}_B \, \underline{P}_B - \underline{M}_B \, \underline{Q}_B \qquad (6.44)$$

where,

$$\underline{M}_A = \text{diag}[\text{Cos } \delta_{Ai}/|I_{Ai}|] \qquad (6.45)$$

$$\underline{N}_A = \text{diag}[\text{Sin } \delta_{Ai}/|I_{Ai}|] \qquad (6.46)$$

$$\underline{M}_B = \text{diag}[\text{Cos } \delta_{Bi}/|I_{Bi}|] \qquad (6.47)$$

$$\underline{N}_B = \text{diag}[\text{Sin } \delta_{Bi}/|I_{Bi}|] \qquad (6.48)$$

Let:

$$\underline{G}_\alpha = \underline{C}_A \, \underline{G}_I \, \underline{C}_B^T \,, \qquad (6.49)$$

hence,

$$P_{LIAB} = \underline{V}_{AP}^T \, \underline{G}_\alpha \, \underline{V}_{BP} + \underline{V}_{Aq}^T \, \underline{G}_\alpha \, \underline{V}_{Bq} \qquad (6.50)$$

substituting for the voltage vectors, then,

$$P_{LIAB} = P_A^T [M_A^T \underline{G}_\alpha \underline{M}_B + \underline{N}_A^T \underline{G}_\alpha \underline{N}_B] \underline{P}_B$$

$$+ \quad \underline{P}_A^T [\underline{M}_A^T \underline{G}_\alpha \underline{M}_B - \underline{N}_A^T \underline{G}_\alpha \underline{M}_B] \underline{Q}_B$$

$$+ \underline{Q}_A^T [\underline{N}_A^T \underline{G}_\alpha \underline{M}_B - \underline{M}_A^T \underline{G}_\alpha \underline{N}_B] \underline{P}_B$$

$$+ \underline{Q}_A^T [\underline{N}_A^T \underline{G}_\alpha \underline{N}_B + \underline{N}_B^T \underline{G}_\alpha \underline{M}_B] \underline{Q}_B \ . \tag{6.51}$$

Grouping similar terms and rearranging, equation 6.51 reduces to:

$$P_{LIAB} = \begin{bmatrix} \underline{P}_A^T & \underline{Q}_A^T \end{bmatrix} \begin{bmatrix} \underline{A}_{PIAB} & -\underline{B}_{PIAB} \\ \underline{B}_{PIAB} & \underline{A}_{PIAB} \end{bmatrix} \begin{bmatrix} \underline{P}_B \\ \underline{Q}_B \end{bmatrix} \tag{6.52}$$

where,

$$\underline{A}_{PIAB} = \underline{M}_A^T \underline{G}_\alpha \underline{M}_B + \underline{N}_A^T \underline{G}_\alpha \underline{N}_B \tag{6.53}$$

and

$$\underline{B}_{PIAB} = \underline{N}_A^T \underline{G}_\alpha \underline{N}_B - \underline{M}_A^T \underline{G}_\alpha \underline{M}_B \ . \tag{6.54}$$

The dimensions of the matrices $\underline{A}_{PIAB}$ and $\underline{B}_{PIAB}$ are of (NGAxNGB). The elements of these matrices are given by:

$$(A_{PIAB})_{ij} = (G_{\alpha ij}) \left[Cos(\delta_{Ai} - \delta_{Bj}) \; |I_{Ai}||I_{Bj}| \right] \qquad (6.55)$$

$$(B_{PIAB})_{ij} = (G_{\alpha ij}) \left[Sin(\delta_{Ai} - \delta_{Bj}) \; |I_{Ai}||I_{Bj}| \right] \qquad (6.56)$$

The net active and reactive powers $\underline{P}_A$, $\underline{Q}_A$, $\underline{P}_B$ and $\underline{Q}_B$ may be partitioned into generation and demand as given below:

$$\underline{P}_A^T = [\underline{P}_{GA}^T \qquad -\underline{P}_{DA}^T] \qquad (6.57)$$

$$\underline{Q}_A^T = [\underline{Q}_{GA}^T \qquad -\underline{Q}_{DA}^T] \qquad (6.58)$$

and

$$\underline{P}_B^T = [\underline{P}_{GB}^T \qquad -\underline{P}_{DB}^T] \qquad (6.59)$$

$$\underline{Q}_B^T = [\underline{Q}_{GB}^T \qquad -\underline{Q}_{DB}^T] \; . \qquad (6.60)$$

The matrices $\underline{A}_{PIAB}$ and $\underline{B}_{PIAB}$ may also be partitioned in terms of generation and demand as:

$$\underline{A}_{PIAB} = \begin{bmatrix} \underline{A}_{PGGIAB} & \underline{A}_{PGDIAB} \\ \\ \underline{A}_{PDGIAB} & \underline{A}_{PDDIAB} \end{bmatrix} \qquad (6.61)$$

and,

$$\underline{B}_{PIAB} = \begin{bmatrix} \underline{B}_{PGGIAB} & \underline{B}_{PGDIAB} \\ \\ \underline{B}_{PDGIAB} & \underline{B}_{PDDIAB} \end{bmatrix} \tag{6.62}$$

Substituting equations 6.57 to 6.62 into equation 6.52, the following equation is obtained:

$$\begin{aligned} P_{LIAB} = {} & \underline{P}_{GA}^{T} \, \underline{A}_{PGGIAB} \, \underline{P}_{GB} - \underline{P}_{GA}^{T} \, \underline{B}_{PGGIAB} \, \underline{Q}_{GB} \\[1em] & + \underline{Q}_{GA}^{T} \, \underline{B}_{PGGIAB} \, \underline{P}_{GB} + \underline{Q}_{GA}^{T} \, \underline{A}_{PGGIAB} \, \underline{Q}_{GB} \\[1em] & + \underline{P}_{DA}^{T} \, \underline{A}_{PDDIAB} \, \underline{P}_{DB} - \underline{P}_{DA}^{T} \, \underline{B}_{PDDIAB} \, \underline{Q}_{DB} \\[1em] & + \underline{Q}_{DA}^{T} \, \underline{B}_{PDDIAB} \, \underline{P}_{DB} + \underline{Q}_{DA}^{T} \, \underline{A}_{PDDIAB} \, \underline{Q}_{DB} \\[1em] & - \underline{P}_{GA}^{T} \, \underline{A}_{PGDIAB} \, \underline{P}_{DB} + \underline{P}_{GA}^{T} \, \underline{B}_{PGDIAB} \, \underline{Q}_{DB} \\[1em] & + \underline{Q}_{GA}^{T} \, \underline{B}_{PGDIAB} \, \underline{P}_{DB} - \underline{Q}_{GA}^{T} \, \underline{A}_{PGDIAB} \, \underline{Q}_{DB} \\[1em] & - \underline{P}_{DA}^{T} \, \underline{A}_{PDGIAB} \, \underline{P}_{GB} + \underline{P}_{DA}^{T} \, \underline{B}_{PDGIAB} \, \underline{Q}_{GB} \\[1em] & - \underline{Q}_{DA}^{T} \, \underline{B}_{PDGIAB} \, \underline{P}_{GB} - \underline{Q}_{DA}^{T} \, \underline{A}_{PDGIAB} \, \underline{Q}_{GB} \end{aligned} \tag{6.63}$$

The final expression for P_{LIAB} is given by:

$$P_{LIAB} = K_{LOPIAB} + [\underline{E}^T_{PPIAB} \quad \underline{E}^T_{PQIAB}] \begin{bmatrix} \underline{P}_{GA} \\ \\ \underline{Q}_{GA} \end{bmatrix}$$

$$+ [\underline{E}^T_{PPIBA} \quad \underline{E}^T_{PQIBA}] \begin{bmatrix} \underline{P}_{GB} \\ \\ \underline{Q}_{GB} \end{bmatrix}$$

$$+ [\underline{P}^T_{GA} \quad \underline{Q}^T_{GA}] \begin{bmatrix} \underline{A}_{PGGIAB} & -\underline{B}_{PGGIAB} \\ \\ \underline{B}_{PGGIAB} & \underline{A}_{PGGIAB} \end{bmatrix} \begin{bmatrix} \underline{\dot{P}}_{GB} \\ \\ \underline{Q}_{GB} \end{bmatrix}$$

$$(6.64)$$

where,

$$K_{LOPIAB} = [\underline{P}^T_{DA} \quad \underline{Q}^T_{DA}] \begin{bmatrix} \underline{A}_{PDDIAB} & -\underline{B}_{PDDIAB} \\ \\ \underline{B}_{PDDIAB} & \underline{A}_{PDDIAB} \end{bmatrix} \begin{bmatrix} \underline{P}_{DB} \\ \\ \underline{Q}_{DB} \end{bmatrix}$$

$$(6.65)$$

and

$$\underline{E}_{PPIAB} = [\underline{B}_{PGDIAB} \, \underline{Q}_{DB} - \underline{A}_{PGDIAB} \, \underline{P}_{DB}]$$

$$(6.66)$$

$$\underline{E}_{PQIAB} = [\underline{B}_{PGDIAB} \, \underline{P}_{DB} - \underline{A}_{PGDIAB} \, \underline{Q}_{DB}]$$

$$(6.67)$$

$$\underline{E}_{PPIBA} = [-\underline{P}_{DA}^T \; \underline{A}_{PDGIAB} - \underline{Q}_{DA}^T \; \underline{B}_{PDGIAB}] \qquad (6.68)$$

$$\underline{E}_{PQIBA} = [\underline{P}_{DA}^T \; \underline{B}_{PDGIAB} - \underline{Q}_{DA}^T \; \underline{A}_{PDGIAB}] \qquad (6.69)$$

In a similar fashion, the piecewise reactive power loss model can be written as:

$$
Q_{LIAB} = K_{LOQIAB} + [\underline{E}_{QPIAB}^T \quad \underline{E}_{QQIAB}^T] \begin{bmatrix} \underline{P}_{GA} \\ \\ \underline{Q}_{GA} \end{bmatrix}
$$

$$
+ [\underline{E}_{QPIBA}^T \quad \underline{E}_{QQIBA}^T] \begin{bmatrix} \underline{P}_{GB} \\ \\ \underline{Q}_{GB} \end{bmatrix}
$$

$$
+ [\underline{P}_{GA}^T \quad \underline{Q}_{GA}^T] \begin{bmatrix} \underline{A}_{QGGIAB} & -\underline{B}_{QGGIAB} \\ \\ \underline{B}_{QGGIAB} & \underline{A}_{QGGIAB} \end{bmatrix} \begin{bmatrix} \underline{P}_{GB} \\ \\ \underline{Q}_{GB} \end{bmatrix} \qquad (6.70)
$$

The number of parameters to be determined of equations 6.64 and 6.70 is given by:

$$NCIAB_P = NCIAB_Q = 2(NGA+1)(NGB+1) - 1 \qquad (6.71)$$

where,

$NCIAB_P$, $NCIAB_Q$ - the number of parameters of P_{LIAB} and Q_{LIAB}

respectively.

The parameters of equations 6.31 to 6.38 and equations 6.64 and 6.70

are functions of voltages, phase angles, admittances and the load

pattern of the network. These parameters are not constant since the

system voltages vary with loads. The piecewise network loss models used

to represent the power system under consideration, are assumed to be

of quadratic form as given by equations 6.31 to 6.38, 6.64 and 6.70.

The parameters of these quadratic functions are evaluated from a set

of "whole system" load flow results covering the feasible operation

range of the power system as before. In the parameter estimation procedure,

the computational time and storage can be minimized by combining

equations 6.31, 6.32 and 6.33, 6.34 into two single equations for the

active part and equations 6.35, 6.36, and 6.37, 6.38 into two single

equations for the reactive part. However, from the computational

experience gained in the preparation of this thesis, it was observed

that in general, it is very difficult to obtain accurate parameter

estimates for P_{LIA}, P_{LIB}, Q_{LIA}, Q_{LIB} (or combined with P_{LA}, P_{LB}, Q_{LA} and

Q_{LB}), P_{LIAB} and Q_{LIAB}. These problems occur as the computed power

losses of P_{LIA}, P_{LIB} and P_{LIAB} (similarly for the reactive components)

do not change by appreciable amounts from one load flow result to

another (i.e., in the matrix equation $\underline{Y} = \underline{A} x + \underline{e}$, the computed

elements of the vector $\underline{Y}$ differ only by a small amount from one another).

The ridge regression algorithm or any other least squares based estimation

method, in such cases will result in a very high value for the mean

square error (e.g., of the order of 10^4 or higher). These problems were encountered in the loss evaluation of the majority of the power systems tested in this work. A detailed study emphasizing these problems is given for the active power loss model of the 5 bus test system in Appendix E.

The above computational difficulties can be overcome by making an approximation to the total active and reactive power losses of interconnections. The approximate models can be evaluated without any numerical difficulties.

6.4.1.1 The Approximate Piecewise Active-Reactive Loss Model

of Interconnections

The total active power losses of interconnections can be written as

$$P_{LIA} + P_{LIB} + 2P_{LIAB} \tag{6.72}$$

An approximation can be made to equation 6.72 by neglecting the quadratic terms in equations 6.32 and 6.34 (these quadratic terms are small compared to the linear terms). Based on this approximation, equation 6.72 reduces to:

$$P_{LI} = K_{OPI} + [E^T_{PPIAA} \quad E^T_{PQIAA}] \begin{bmatrix} P_{GA} \\ \\ Q_{GA} \end{bmatrix}$$

$$+ [E^T_{PPIBB} \quad E^T_{PQIBB}] \begin{bmatrix} P_{GB} \\ \\ Q_{GB} \end{bmatrix}$$

$$+ \begin{bmatrix} P_{GA}^T & Q_{GA}^T \end{bmatrix} \begin{bmatrix} A_{PGGIAB} & -B_{PGGIAB} \\ \\ B_{PGGIAB} & A_{PGGIAB} \end{bmatrix} \begin{bmatrix} P_{GB} \\ \\ Q_{GB} \end{bmatrix} \qquad (6.73)$$

where,

$$K_{LOPI} = K_{LOPIA} + K_{LOPIB} + 2K_{LOPIAB} \qquad (6.74)$$

$$E_{PPIAA} = E_{PPIA} + 2E_{PPIAB} \qquad (6.75)$$

$$E_{PQIAA} = E_{PQIA} + 2E_{PQIAB} \qquad (6.76)$$

$$E_{PQIBB} = E_{PQIB} + 2E_{PQIAB} \qquad (6.77)$$

The above approximation is a good approximation especially when the tearing branches are chosen to have a minimum number of lines.

In a similar fashion, the total reactive power losses of inter-connections can be written as:

$$Q_{LI} = Q_{LIA} + Q_{LIB} + 2Q_{LIAB} \qquad (6.78)$$

The approximate model for the total reactive power losses of inter-connections can be written as:

$$Q_{LI} = K_{LOQI} + [E_{QPIAA}^T \ E_{QQIAA}^T] \begin{bmatrix} P_{GA} \\ \\ Q_{GA} \end{bmatrix}$$

$$+ [E_{QPIBB}^T \ E_{QQIBB}^T] \begin{bmatrix} P_{GB} \\ \\ Q_{GB} \end{bmatrix}$$

$$+ 2[P_{GA}^T \ Q_{GA}^T] \begin{bmatrix} A_{QGGIAB} & -B_{QGGIAB} \\ \\ B_{QGGIAB} & A_{QGGIAB} \end{bmatrix} \begin{bmatrix} P_{GB} \\ \\ Q_{GB} \end{bmatrix} \qquad (6.79)$$

where,

$$K_{LOQI} = K_{LOQIA} + K_{LOQIB} + 2K_{LOQIAB} \qquad (6.80)$$

$$E_{QPIAA} = E_{QPIA} + 2E_{QPIAB} \qquad (6.81)$$

$$E_{QQIAA} = E_{QQIA} + 2E_{QQIAB} \qquad (6.82)$$

$$E_{QPIBB} = E_{QPIB} + 2E_{QPIAB} \qquad (6.83)$$

$$E_{QQIBB} = E_{QQIB} + 2E_{QQIAB} \qquad (6.84)$$

The number of parameters to be evaluated for equations 6.73 and 6.79 are as given by equation 6.71.

The purely reactive source submodels of the network under consideration, are modeled in terms of the entire network total reactive load demand as was discussed in Chapter II (i.e., they remain unchanged).

6.4.2 The Piecewise Active Power Loss Model of a Network Torn into Two Subnetworks in Terms of Active Power Generations

The piecewise active power loss model of the transmission network may be obtained from the piecewise active-reactive loss model by assuming that the Q/P ratio at any source bus remains constant. Based on this assumption, the reactive power generation vector can be written as:

$$\underline{Q}_G = \underline{Q}_{GO} + \underline{F}^T \underline{P}_G \qquad (6.85)$$

or in partitioned form as:

$$\underline{Q}_{GA} = \underline{Q}_{GAO} + \underline{F}_A^T \underline{P}_{GA} \qquad (6.86)$$

and,

$$\underline{Q}_{GB} = \underline{Q}_{GBO} + \underline{F}_B^T \underline{P}_{GB} \qquad (6.87)$$

Substituting equations 6.86 and 6.87 into equations 6.31 to 6.34, the resulting equations are given by:

$$P_{LA} = K_{LOA} + \underline{B}_{OA}^T \underline{P}_{GA} + \underline{P}_{GA}^T \underline{B}_A \underline{P}_{GA} \qquad (6.88)$$

$$P_{LIA} = K_{LOIA} + \underline{B}_{OIA}^T \underline{P}_{GA} + \underline{P}_{GA}^T \underline{B}_{IA} \underline{P}_{GA} \qquad (6.89)$$

$$P_{LB} = K_{LOB} + B_{OB}^T P_{GB} + P_{GB}^T B_B P_{GB} \tag{6.90}$$

$$P_{LIB} = K_{LOIB} + B_{OIB}^T P_{GB} + P_{GB}^T B_{IB} P_{GB} \tag{6.91}$$

where,

$$B_A = A_{PGGA} + F_A^T A_{PGGA} F_A + 2F_A^T B_{PGGA} \tag{6.92}$$

$$B_{OA} = E_{PPA}^T + 2Q_{GAO}^T [A_{PGGA} F_A + B_{PGGA}] + E_{PQA}^T F_A \tag{6.93}$$

$$K_{LOA} = K_{LOPA} + Q_{GAO}^T A_{PGGA} Q_{GAO} + E_{PQA}^T Q_{GAO} \tag{6.94}$$

where,

$$Q_{GAO} = [Q_{GA1O} \quad Q_{GA2O} \quad \cdots\cdots \quad Q_{GAmaO}] \tag{6.95}$$

$$B_{IA} = A_{PGGIA} + F_A^T A_{PGGIA} F_A + 2F_A^T B_{PGGIA} \tag{6.96}$$

$$B_{OIA} = E_{PPIA}^T + 2 Q_{GAO}^T [A_{PGGIA} F_A + B_{PGGIA}] + E_{PQIA}^T F_A \tag{6.97}$$

$$K_{LOIA} = K_{LOPIA} + Q_{GAO}^T A_{PGGIA} Q_{GAO} + E_{PQIA}^T Q_{GAO} \tag{6.98}$$

ma - number of generation buses of subnetwork A.

Similar expressions can easily be obtained for B_B, B_{OB}, B_{IB}, B_{OIB}, K_{LOB}, K_{LOIB} and Q_{GBO} from above. Substituting equations 6.86 and 6.87

into equation 6.64 results in the following equation:

$$P_{LIAB} = K_{LOIAB} + B_{OIAB}^T \; P_{GA}$$

$$+ B_{OIBA}^T \; P_{GB} + P_{GA}^T \; B_{IAB} \; P_{GB} \tag{6.99}$$

where,

$$K_{LOIAB} = K_{LOPIAB} + E_{PQIAB}^T \; Q_{GAO}$$

$$+ E_{PQIBA}^T \; Q_{GBO} + Q_{GAO}^T \; A_{PGGIAB} \; Q_{GBO} \tag{6.100}$$

$$B_{OIAB}^T = E_{PPIAB}^T + E_{PQIAB}^T \; F_A^T$$

$$+ Q_{GBO}^T \; B_{PGGIAB}^T + Q_{GBO}^T \; A_{PGGIAB}^T \; F_A^T \tag{6.101}$$

$$B_{OIBA}^T = E_{PPIBA}^T + E_{PQIBA}^T \; F_B^T$$

$$+ Q_{GAO}^T \; B_{PGGIAB} + Q_{GAO}^T \; A_{PGGIAB} \; F_B^T \tag{6.102}$$

$$B_{IAB} = A_{PGGIAB} + F_A \; B_{PGGIAB}$$

$$+ F_A \; A_{PGGIAB} \; F_B^T + F_B^T \; B_{PGGIAB}^T \tag{6.103}$$

The number of parameters to be evaluated of equations 6.88 to

6.91 and equation 6.99 are given by the following:

$$NCA = NCIA = (NGA+2)(NGA+1)/2 \tag{6.104}$$

$$NCB = NCIB = (NGB+2)(NGB+1)/2 \tag{6.105}$$

and

$$NCIAB = (NGA+1)(NGB+1) \tag{6.106}$$

where,

NCA,NCIA - the number of parameters of submodels P_{LA} and P_{LIA} respectively.

NCB,NCIB - the number of parameters of submodels P_{LB} and P_{LIB} respectively.

NCIAB - the number of parameters of submodel P_{LIAB}.

In a similar fashion to that discussed in Section 6.4.1, the computational time and storage in the parameter estimation procedure can be minimized by combining equations 6.88, 6.89 and 6.90, 6.91 into two single equations. But as mentioned earlier, this poses computational problems. Based on the same reasoning given in Section 6.4.1, an approximation to the total losses in the interconnections can be made without appreciable loss of accuracy.

6.4.2.1 The Approximate Piecewise Active Power Loss Model
of Interconnections

The net active power loss in the interconnections of a given network which is torn into two subnetworks A and B is given by:

$$P_{LI} = P_{LIA} + P_{LIB} + 2P_{LIAB} \qquad (6.107)$$

where,

P_{LI} - the total active power losses of interconnections I.

Substituting for P_{LIA}, P_{LIB} and P_{LIAB}, the total losses of interconnections in terms of active power generations can be written as:

$$P_{LI} = K_{LOI} + \underline{B}^T_{OIAA}\ \underline{P}_{GA} + \underline{B}^T_{OIBB}\ \underline{P}_{GB}$$

$$+ [\underline{P}^T_{GA}\ \underline{P}^T_{GB}] \cdot \begin{bmatrix} \underline{B}_{IAA} & \underline{B}_{IAB} \\ \underline{B}_{IBA} & \underline{B}_{IBB} \end{bmatrix} \cdot \begin{bmatrix} \underline{P}_{GA} \\ \underline{P}_{GB} \end{bmatrix} \qquad (6.108)$$

where,

$$K_{LOI} = K_{LOIA} + K_{LOIB} + 2K_{LOIAB} \qquad (6.109)$$

$$\underline{B}_{OIAA} = \underline{B}_{OIA} + 2\underline{B}_{OIAB} \qquad (6.110)$$

and

$$\underline{B}_{IBA}^{T} = \underline{B}_{IAB} \tag{6.111}$$

The matrices $\underline{B}_{IAA}$ and $\underline{B}_{IBB}$ are square symmetric matrices with dimensions of (NGAxNGA) and (NGBxNGB) respectively. The matrix $\underline{B}_{IAB}$ is of (NGAxNGB) dimensional. Equation (6.108) can be approximated without appreciable loss of accuracy by replacing the submatrices $\underline{B}_{IAA}$ and $\underline{B}_{IBB}$ by null matrices. This is a good approximation particularly when the torn branches are chosen to have a minimum number of lines. The approximate model of the interconnections reduces to:

$$P_{LI} = K_{LOI} + \underline{B}_{OIAA}^{T} \underline{P}_{GA} + \underline{B}_{OIBB}^{T} \underline{P}_{GB}$$

$$+ 2\underline{P}_{GA}^{T} \underline{B}_{IAB} \underline{P}_{GB} \tag{6.112}$$

The number of parameters to be evaluated of this model is given by equation 6.106.

6.5 The Piecewise Active and Active-Reactive Loss Coefficient Evaluation Procedure

The following computational steps are used to evaluate the piecewise active and active-reactive loss model coefficients of a given power network:

1. perform a number of load flow solutions for the entire network at different load and voltage levels spanning the entire operating region of the power system. The

number of load flow runs required, is the minimum number

needed to evaluate the parameters of the largest submodel

of the network.

2.   compute the total active and reactive power losses of each

subnetwork and interconnections from the network line

admittances and complex voltages obtained in 1 above.

3.   set up the computed power losses obtained in 2 above and

the corresponding power generations obtained in 1, in a

format similar to that given by equation 2.6 or equation

2.26 of Chapter II.

4.   apply the ridge regression estimation procedure

(discussed in Chapter III) to evaluate the parameters of

all subnetworks in a piecewise manner (50, 51).

6.6   The Piecewise Active and Active-Reactive Dispatch of Generation

The optimization algorithms used to evaluate the economic active

and active-reactive dispatch schedules of a power system are based on

the piecewise loss models of the transmission network. These methods

are suitable for the evaluation of the economic dispatch conditions of

large power systems.

6.6.1 The Piecewise Economic Active Dispatch Procedure

The cost function representing the generation sources of the

entire network given by equation 2.1 is repeated here for convenience:

$$F_0 = \sum_{i=1}^{m} \alpha_{si} + \beta_{si} \, P_{Gsi} + \gamma_{si} \, P_{Gsi}^2 \, , \qquad\qquad (6.113)$$

This function is minimized subject to:

a.   equality constraints given by:

$$h_p(P_{Gsi}) = 0.0$$

$$= P_D + \sum_{i=A}^{K} P_{Li} + \sum_{i=1}^{N} P_{LIi}$$

$$- \sum_{i=1}^{m} P_{Gsi} \qquad (6.114)$$

where,

A, B, ..., K - represent subnetworks A, B, ... and K.

N - the number of interconnections (interconnecting subnetworks) of the system.

m - the number of generating units of the system.

, b.   inequality constraints given in compact form by:

$$\underline{g}_p(\underline{P}_{Gs}) \leq \underline{0} , \qquad (6.115)$$

equation 6.115, may be written as:

$$\underline{P}_{Gs\ min} - \underline{P}_{Gs} \leq \underline{0} \qquad (6.116)$$

$$\underline{P}_{Gs} - \underline{P}_{Gs\ max} \leq \underline{0}. \qquad (6.117)$$

The optimum economic dispatch conditions of a power system are obtained in one optimization procedure (52-54) by forming the Lagrange-Kuhn-Tucker function as was discussed in Chapter IV.

6.6.2 The Piecewise Economic Active-Reactive Dispatch Procedure

In a similar fashion to the economic active dispatch procedure, the thermal cost function given by equation 6.113, is minimized subject to:

a. equality constraints given by equation 6.114 and:

$$h_q(Q_{Gsi}) = 0.0$$

$$= Q_D + \sum_{i=A}^{K} Q_{Li} + \sum_{i=1}^{N} Q_{Lii}$$

$$- \sum_{i=1}^{m} Q_{Gsi} - \sum_{h=1}^{n} Q_{Gvj}$$

$$- \sum_{k=1}^{r} Q_{Shk} \tag{6.118}$$

where,

n - the number of purely reactive sources of the network.

r - the number of purely shunt reactive powers of the network.

b. inequality constraint given by equation 6.115 and:

$$\underline{g}_q \ (\underline{Q}_{Gs}) \le \underline{0} \qquad\qquad (6.119)$$

where equation 6.119, can be written in alternative compact form as:

$$\underline{Q}_{Gs \ min} - \underline{Q}_{Gs} \le \underline{0} \qquad\qquad (6.120)$$

$$\underline{Q}_{Gs} - \underline{Q}_{Gs \ max} \le \underline{0} \qquad\qquad (6.121)$$

The constrained thermal cost function is minimized in one optimization procedure (55) using a Newton-Raphson based optimization algorithm observing the Kuhn-Tucker optimality conditions as was discussed in Chapter IV.

CHAPTER VII

APPLICATION OF PIECEWISE LOSS MODEL BASED ECONOMIC

DISPATCH METHODS TO MODEL POWER SYSTEMS

In this chapter, the techniques developed in Chapter VI are

applied to sample power test systems. The accuracy of the evaluated

piecewise loss models and the validity of the economic dispatch

solutions are verified by comparison with load flow solutions, as was

done for the entire system loss models. For illustration purposes, the

results obtained for the IEEE 14 bus test system are presented in this

chapter. The methods were also applied to the 5 bus and the 11 bus

(56) test systems which contain 2 and 6 generation buses respectively.

The results obtained for these two systems are given in Appendix E.

The diakoptical methods are expected to produce better dispatch

solutions in comparison to full system methods for large power systems.

A case study comparing the two approaches is given in Chapter VIII

using the 23 bus test system (57). The evaluated piecewise loss co-

efficients of this system are given in Appendix E.

The parameters of the piecewise power loss models of the above

systems were evaluated from load flow studies of the systems which

were carried out for the entire networks for different system load and

voltage levels. The base load flow results obtained for each of the

above systems defined a feasible operating region that covered the

entire load spectrum of the system.

7.1 The Piecewise Active Loss Model and the Active Dispatch Results

The diakoptical active loss model parameter estimates and the

economic ████ patch solutions of the IEEE 14 bus test system are

pr█ented ████ ussed in the following sections.

7.█ The ██ 14 Bus Test System-Piecewise Active Power Loss Model

█ The ██E 14 bus test system is shown in Figure 7.1. The network

is to██ i██ two subnetworks A and B as shown by the dotted line. Each

of the ████bnetworks contain one generation bus (subnetwork A contains

bus nu████ 1, and subnetwork B contains bus number 13). The number of

paramet███ to be evaluated of each subnetwork model and the number of

load fl██ ████esults required for this system are listed in Table 7.1.

Model	P_{LA}	P_{LIA}	P_{LB}	P_{LIB}	P_{LIAB}	P_{LI}
No. of Parameters	3	3	3	3	4	4
No. of Load Flows	4	4	4	4	5	5

Table 7.1 The IEEE 14 Bus Piecewise Active Power

Loss Model Parameter Evaluation Requirements

As shown in Table 7.1, the number of parameters of the largest

submodel is 4. To evaluate the parameters of all submodels of this

power system, a minimum of five load flow results are required, which

were carried out over a wide range of system load and voltage levels.

The nominal system load is 259 + j73.5 MVA. Using the load flow results

obtained, the piecewise active power loss model parameters were
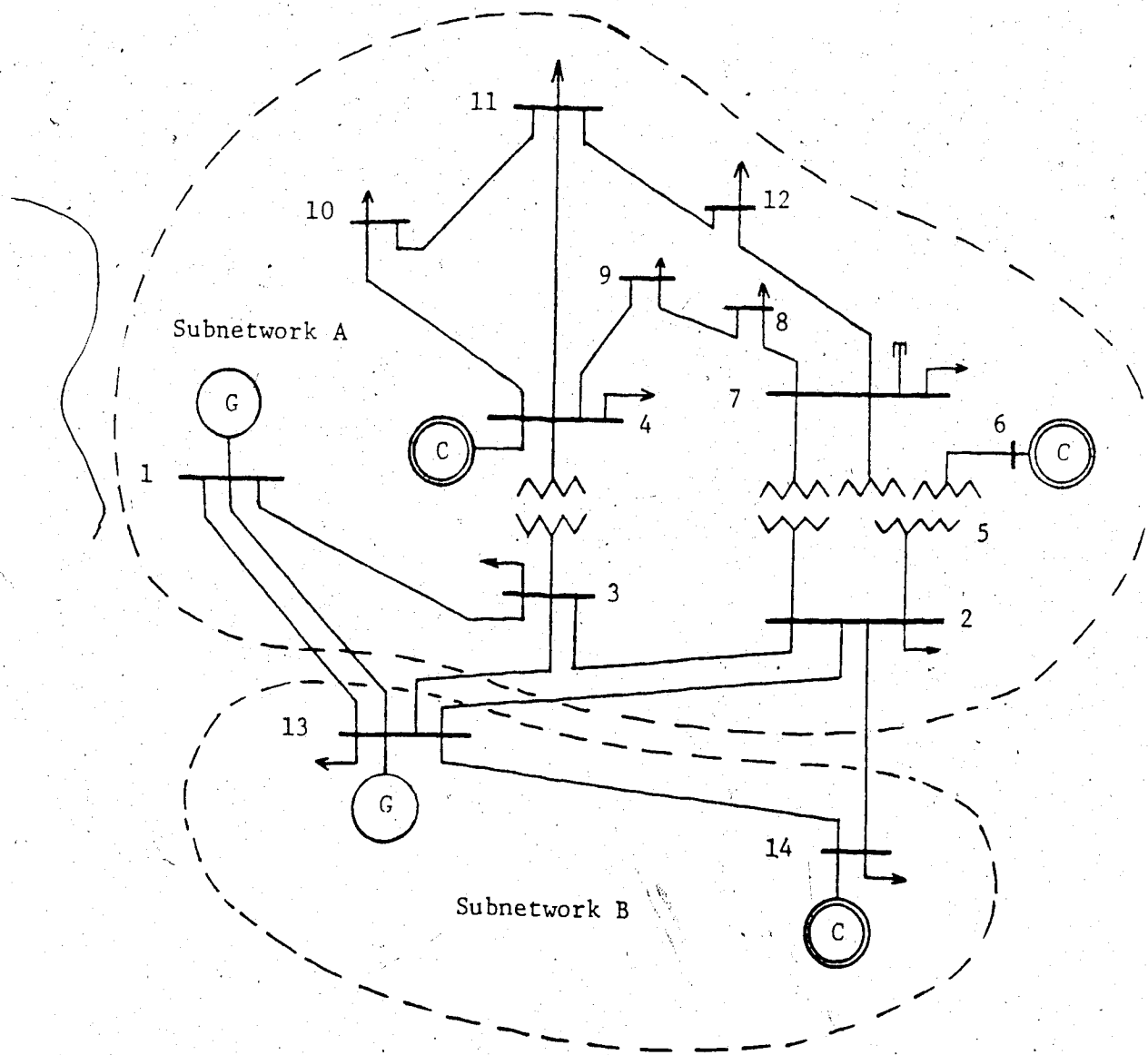
Figure 7.1 The IEEE 14 Bus Test System Torn into two

Subnetworks

evaluated by the ridge estimator. The parameter estimates obtained
for P_{LIA}, P_{LIB} and P_{LIAB} had associated values of mean square error
which were very high (of the order to 10^5), and therefore are not shown
here. The parameter estimates obtained for P_{LA}, P_{LB} and the approximate
model P_{LI} are given in Table 7.2. In Table 7.2, the estimates were
obtained for a value of ridge k = 0.118. For this value of k, the
condition numbers of P_{LA}, P_{LB} and P_{LI} were found to be less than 10.
The mean square error in each case was less than 1.

| | Ridge k = 0.118 | | | |
Parameter	P_{LA}	P_{LB}	Parameter	P_{LI}
K_{LO}	-0.001791	0.002534	K_{LOI}	-0.012097
B_{01}	0.002961	0.019497	B_{OIAA1}	0.028502
B_{11}	0.007269	0.005080	B_{OIBB1}	0.000484
			B_{IAB11}	0.009531

Table 7.2 The Parameters of the Active Power Loss Submodels
P_{LA}, P_{LB} and P_{LI} of the IEEE 14 Bus Test System in
p.u. on 100 MVA Base.

7.1.2 The IEEE 14 Bus Test System-Piecewise Active Loss Model Based Economic Dispatch

Based on the evaluated piecewise active power loss model of this
system, the economic active dispatch schedules of the system were

evaluated. The coal fired generating unit capacities used in the evaluation of the dispatch solutions are given in Table 5.2. The dispatch results obtained for the IEEE 14 bus test system are presented in Table 7.3. The results in this Table were fed back into the load flow program and the solutions obtained for all loads considered. These results are shown in brackets in Table 7.3 for comparison. This procedure was carried out to verify the validity of the economic dispatch solutions. The load flow voltage profiles, based on the economic dispatch results were found to lie within the operating voltage limits of the system. Samples for light and heavy loads voltage profiles are presented in Table 7.4.

7.1.3 Discussion of IEEE 14 Bus Test System - Piecewise Active Results

The piecewise parameter estimates shown in Table 7.2, stabilized for a value of ridge $k = 0.118$, which resulted in a mean square error of less than 1 for each loss submodel. The economic active dispatch results presented in Table 7.3, agree very clearly with the load flow results based on the economic solutions which indicate that the approximation made on the total power losses in the interconnections (P_{LI}) was a good approximation. The voltage profiles that correspond to the economic dispatch solutions were all within acceptable limits as indicated in Table 7.4 for light and heavy load cases.

Comparing the results shown in Table 7.3 with the results obtained for the entire network given in Table 5.3, it is observed that there are some differences between the total fuel costs. These differences are mainly due to the errors in the loss submodel of interconnections of this example system. In the case of the IEEE 14 bus test system which was

P_D MW	λ_p $/MWh	P_{GA1} MW	P_{GB13} MW	P_L MW	F_0 $/h
25.9*	8.97	5.000 (5.692)	20.361 (20.361)	-0.539 (0.140)	568.11
51.8	9.07	14.213 (14.444)	37.792 (37.792)	0.205 (0.379)	801.86
77.7	9.16	26.931 (26.710)	51.839 (51.839)	1.070 (0.833)	1038.00
103.6	9.26	39.676 (39.117)	65.940 (65.940)	2.015 (1.472)	1276.52
129.5	9.35	52.448 (51.760)	80.094 (80.094)	3.041 (2.349)	1517.43
155.4	9.44	65.247 (64.545)	94.302 (94.302)	4.149 (3.444)	1760.76
181.3	9.54	78.075 (77.459)	108.565 (108.565)	5.340 (4.639)	2006.52
207.2	9.63	90.930 (90.395)	122.884 (122.884)	6.614 (6.057)	2254.74
233.1	9.73	103.812 (103.336)	137.260 (137.260)	7.972 (7.501)	2505.43
259.0	9.82	116.723 (116.638)	151.691 (151.691)	9.415 (9.333)	2758.64

* No convergence

Table 7.3 The Diakoptical Economic Active Dispatch of the

IEEE 14 Bus Test System

	Load= 51.8+j14.7MVA		Load= 259+j73.5MVA	
Bus No.	Voltage p.u.	Angle Degrees	Voltage p.u.	Angle Degrees
1	1.0300	0.0	1.0600	0.0
2	1.0321	-1.5257	1.0186	-7.7755
3	1.0293	-1.2301	1.0205	-6.4613
4	1.0827	-2.2704	1.0700	-11.8291
5	1.0689	-2.1302	1.0620	-10.8584
6	1.0590	-2.1302	1.0900	-10.8584
7	1.0824	-2.4403	1.0565	-12.4565
8	1.0810	-2.4678	1.0515	-12.6310
9	1.0812	-2.3968	1.0572	-12.3611
10	1.0802	-2.4359	1.0552	-12.6770
11	1.0794	-2.4557	1.0505	-12.7517
12	1.0777	-2.6348	1.0359	-13.5845
13	1.0300	-0.1664	1.0450	-1.7581
14	1.0300	-1.8777	1.0100	-9.8431

Table 7.4 The Voltage Profiles of the IEEE 14 Bus System

Based on the Diakoptical Economic Active Dispatch

Solutions

torn as shown in Figure 7.1, the total active power losses of inter-
connections were not small compared to the total power losses of sub-
networks A or B. The total fuel costs are expected to agree very closely
in both cases especially when the torn branches are chosen to have a
minimum number of lines. However, it should be remembered that, large
loss models in practice cannot be accurately evaluated for the entire
network due to the problem of ill-conditioning. The piecewise loss
model based methods are expected to produce superior optimal solutions
for large power systems as fewer parameters are estimated at one time.

7.2 The Piecewise Active-Reactive Loss Model and the Active-Reactive Dispatch Results

In this section, the active-reactive power loss model of the
IEEE 14 bus test system is evaluated in a piecewise manner. Based on
the evaluated loss model, the economic active-reactive dispatch
schedules of the system are obtained and discussed.

7.2.1 The IEEE 14 Bus Test System - Piecewise Active-Reactive Loss Model

The single line diagram of this system is shown in Figure 7.1. The
network as a whole has two active-reactive generation buses, 1 and 13,
and three purely reactive sources at buses 4, 6 and 8. The purely
reactive source submodels were evaluated in Chapter V, which remain
unchanged in the piecewise analysis (see Tables 5.14 to 5.17) . The
active-reactive power loss submodel on the other hand, is evaluated
in a piecewise manner by the ridge estimator. The number of parameters
of the piecewise loss submodel and the number of load flow results
required are listed in Table 7.5. From Table 7.5, the number of parameters

of the largest submodel is 7, which requires a minimum of 8 load flow

results to evaluate the parameters of all submodels, which were carried

Model	P_{LA}	Q_{LA}	P_{LB}	Q_{LB}	P_{LI}	Q_{LI}
No. of Parameters	4	4	4	4	7	7
No. of Load Flows	5	5	5	5	8	8

Table 7.5 The IEEE 14 Bus Piecewise Active-Reactive

Power Loss Model Parameter Evaluation Requirements

out for the entire network covering the entire load range of the system.

Using the load flow results obtained, the parameters of the active-

reactive loss submodel were evaluated. The parameter estimates obtained

are presented in Tables 7.6 and 7.7 for the active and reactive parts

respectively.

7.2.2 The IEEE 14 Bus Test System - Piecewise Active-Reactive Loss

Model Based Economic Dispatch

Using the evaluated piecewise active-reactive submodel and the

purely reactive submodels of this system, the economic active-reactive

dispatch solutions were computed using the generator capacities given

in Table 5.6. The dispatch results obtained are presented in Tables

7.8 and 7.9 for the active and reactive parts respectively. The load

flow solutions based on the economic dispatch results are shown in

brackets in Tables 7.8 and 7.9. The load flow voltage profiles that

correspond to light and heavy loads of the system are presented in

k = 5×10^{-5}		k = 0		k = 5×10^{-5}	
Parameter	P_{LA}	Parameter	P_{LB}	Parameter	P_{LI}
K_{LOPA}	0.001526	K_{LOPB}	-0.000065	K_{LOPI}	-0.011654
E_{PPA1}	0.004149	E_{PPB1}	0.020309	E_{PPAA1}	0.024895
E_{PQA1}	0.017191	E_{PQB1}	0.012706	E_{PQAA1}	-0.010761
A_{PA11}	0.006346	A_{PB11}	0.007207	E_{PPBB1}	-0.015052
				E_{PQBB1}	-0.048165
				A_{PIAB11}	0.018446
				B_{PIAB11}	-0.032053

Table 7.6 The IEEE 14 bus Piecewise Active–Reactive Power Loss Model

Parameters in p.u. on 100 MVA Base (Active Part)

$k = 5\times10^{-5}$		$k = 0$		$k = 5\times10^{-5}$	
Parameter	Q_{LA}	Parameter	Q_{LB}	Parameter	Q_{LI}
K_{LOQA}	-0.045514	K_{LOQB}	-0.044626	K_{LOQI}	-0.170283
E_{QPA1}	0.193240	E_{QPB1}	0.082434	E_{QPAA1}	0.048298
E_{QQA1}	0.110568	E_{QQB1}	0.047199	E_{QQAA1}	0.005868
A_{QA11}	0.039891	A_{QB11}	0.033781	E_{QPBB1}	-0.057856
				E_{QQBB1}	-0.049940
				A_{QIAB11}	0.063829
				B_{QIAB11}	-0.080902

Table 7.7 The IEEE 14 Bus Piecewise Active-Reactive Power Loss Model

Parameters in p.u. on 100 MVA Base (Reactive Part)

Table 7.10.

7.2.3 Discussion of IEEE 14 Bus Test System - Piecewise Active-Reactive Results

As seen from Tables 7.6 and 7.7, the parameter estimates of P_{LA}, P_{LI}, Q_{LA} and Q_{LI} of this system stabilized at $k = 5 \times 10^{-5}$, while the parameters of P_{LB} and Q_{LB} were stable for $k = 0.0$. The economic dispatch results and the load flow solutions, shown in Tables 7.8 and 7.9 agree very closely with one another, indicating the accuracy of the loss model parameters and the validity of the dispatch solutions. The differences between the two solutions in the active and reactive power generations at the slack bus (bus number 1), are picked up by the system total active and reactive power losses. The total fuel costs obtained are lower for some loads than those obtained using the diakoptical active power loss model. The total fuel cost at the 100% load level (259+j73.5 MVA) is slightly higher than that based on the diakoptical active loss model. This is due to the fact that the voltage levels at this loading are in general lower than their active loss model based counterparts. The voltage profiles obtained using the diakoptical active-reactive loss model were all within the limits of the system operating voltage levels.

P_D MW	λ_p' $/MWh	P_{G1} MW	P_{G13} MW	P_L MW	F_0 $/h
25.9	–	–	–	–	–
51.8	8.95	13.314 (12.780)	39.566 (39.566)	1.080 (0.516)	809.70
77.7	9.03	24.257 (23.810)	54.905 (54.905)	1.462 (0.986)	1041.85
103.6	9.11	34.661 (34.500)	70.785 (70.785)	1.846 (1.686)	1275.73
129.5	9.32	43.737 (43.864)	88.003 (88.003)	2.240 (2.344)	1511.62
155.4	9.53	50.813 (51.237)	107.665 (107.665)	3.078 (3.509)	1753.83
181.3	9.60	58.112 (58.786)	127.139 (127.139)	3.951 (4.628)	1998.29
207.2	9.69	70.664 (71.210)	141.970 (141.970)	5.434 (5.980)	2248.60
233.1	9.79	84.394 (84.686)	155.869 (155.869)	7.163 (7.536)	2502.56
259.0	9.89	99.438 (99.491)	168.764 (168.764)	9.201 (9.320)	2760.78

Table 7.8 The Diakoptical Economic Active-Reactive Dispatch

of the IEEE 14 Bus Test System (Active Part)

Q_D MVAR	λ_q $/MVARh	Q_{G1} MVAR	Q_{G13} MVAR	Q_{GV4} MVAR	Q_{GV6} MVAR	Q_{GV14} MVAR	Q_L MVAR
7.35	—	—	—	—	—	—	—
14.70	-0.12	5.999 (4.837)	-40.000 (-40.000)	-3.651 (-3.651)	-6.000 (-6.000)	14.818 (14.812)	-22.647 (-23.771)
22.05	-0.16	13.225 (11.898)	-40.000 (-40.000)	-5.381 (-5.381)	-6.000 (-6.000)	18.861 (18.860)	-20.400 (-21.979)
29.40	0.20	22.141 (22.215)	-40.000 (-40.000)	-6.000 (-6.000)	-6.000 (-6.000)	20.488 (20.489)	-17.752 (-18.634)
36.75	-0.22	-8.657 (-8.355)	2.450 (2.450)	-6.000 (-6.000)	-6.000 (-6.000)	18.471 (18.470)	-15.379 (-16.037)
44.10	-0.23	-38.751 (-38.751)	50.000 (50.000)	-5.983 (-5.983)	-4.491 (-4.490)	11.581 (11.581)	-10.534 (-11.535)
51.45	-0.27	-20.230 (-20.257)	50.000 (50.000)	-3.834 (-3.830)	-0.978 (-0.978)	0.0 (0.0)	-5.163 (-6.505)
58.80	-0.32	-16.664 (-16.364)	50.000 (50.000)	-0.102 (-0.102)	4.029 (4.030)	0.0 (0.0)	0.561 (-0.979)
66.15	-0.36	-14.835 (-14.953)	50.000 (50.000)	5.460 (5.460)	10.722 (10.720)	0.0 (0.0)	6.819 (5.512)
73.50	-0.40	-16.936 (-16.724)	50.000 (50.000)	13.097 (13.100)	19.293 (19.290)	0.0 (0.0)	13.751 (13.232)

Table 7.9 The Diakoptical Economic Active-Reactive Dispatch

of the IEEE 14 Bus Test System (Reactive Part)

	Load=51.8+j14.7 MVA		Load=259+j73.5 MVA	
Bus No.	Voltage p.u.	Angle Degrees	Voltage p.u.	Angle Degrees
1	1.0000	0.0	1.0480	0.0
2	1.0003	-1.5386	1.0125	-7.5905
3	0.9971	-1.2305	1.0155	-6.3054
4	1.0516	-2.3490	1.0663	-11.7061
5	1.0358	-2.1735	1.0586	-10.7058
6	1.0255	-2.1735	1.0898	-10.7058
7	1.0492	-2.4990	1.0526	-12.3172
8	1.0481	-2.5320	1.0476	-12.4942
9	1.0491	-2.4688	1.0534	-12.2324
10	1.0487	-2.5236	1.0514	-12.5587
11	1.0477	-2.5405	1.0467	-12.6323
12	1.0450	-2.7164	1.0320	-13.4614
13	0.9929	0.0051	1.0491	-1.5779
14	1.0057	-2.0370	0.9868	-9.3999

Table 7.10 The Voltage Profiles of the IEEE 14 Bus

Test System Based on the Diakoptical

Economic Active-Reactive Dispatch Solution

CHAPTER VIII

DISCUSSIONS, CONCLUSIONS AND SUGGESTIONS

FOR FUTURE RESEARCH

Discussions of the loss model based economic dispatch methods proposed in this thesis are presented in this chapter. The chapter also includes the conclusions and suggestions for future research work in optimum economic dispatch of electric power systems.

8.1 Discussions of the Proposed Methods

The proposed methods, are based on the ridge regression estimation algorithm which is used to evaluate the various network models of the power system. The performance of the proposed methods largly depend on the performance of the ridge regression algorithm.

8.1.1 The Ridge Regression Estimation Routine

The problem of ill-conditioning is often encountered in the evaluation of power system network loss models. This problem gives rise to unstable parameter estimates when ordinary least squares or similar methods are used to evaluate the network loss model parameters. The method of ordinary least squares is sensitive to slight variations in the observed data. The ridge regression on the other hand is not affected by small changes in the observation data and produces stable parameter estimates. The performance of the ridge estimator was evaluated by comparing it to the Powell regression algorithm (58, 59). The active power loss model of the IEEE 30 bus test system ▮▮▮▮ the above two estimation routines, using the same ▮▮▮ults of the system. It was observed that for a ▮▮▮al to zero (ridge estimator reduces to ordinary

least squares when k = 0), the parameter estimates obtained by the

ridge estimator resulted in erroneous economic dispatch solutions.

Feeding these parameter estimates as initial guesses into Powell

regression algorithm, the latter routine gave no improvement on the

results. For small positive values of k, the ridge estimates stabilized

and resulted in accurate dispatch solutions. Using these new parameter

estimates as initial guesses in Powell regression gave no improvement

over the ridge estimator results. Powell algorithm requires good initial

guesses to converge into a solution. The ridge regression can treat

ill-conditioned situations and requires no initial guesses.

8.1.2 The Proposed Methods Versus the Optimal Load Flow Methods

The performance of the proposed dispatch methods were evaluated

by comparing their dispatch solutions to the dispatch solutions obtained

by the optimal load flow method reported in Reference 60. The sample

test system used for this comparison is the 5 bus test system reported

in Reference 4. The proposed active power loss model based dispatch

method is compared to the optimal load flow method with fixed generator

voltages while the proposed active-reactive dispatch method is compared

to the optimal load flow method with variable generator voltages.

The single line diagram of the test system in question is shown

in Figure 8.1, which contains two active-reactive generation buses,

1 and 2. The active power loss model of this system was evaluated from

load flow studies of the system. The parameter estimates obtained by

the ridge estimator for k = 0.031 are given in Table 8.1. Based on the

loss model parameters and the cost coefficients shown in Table 8.2,
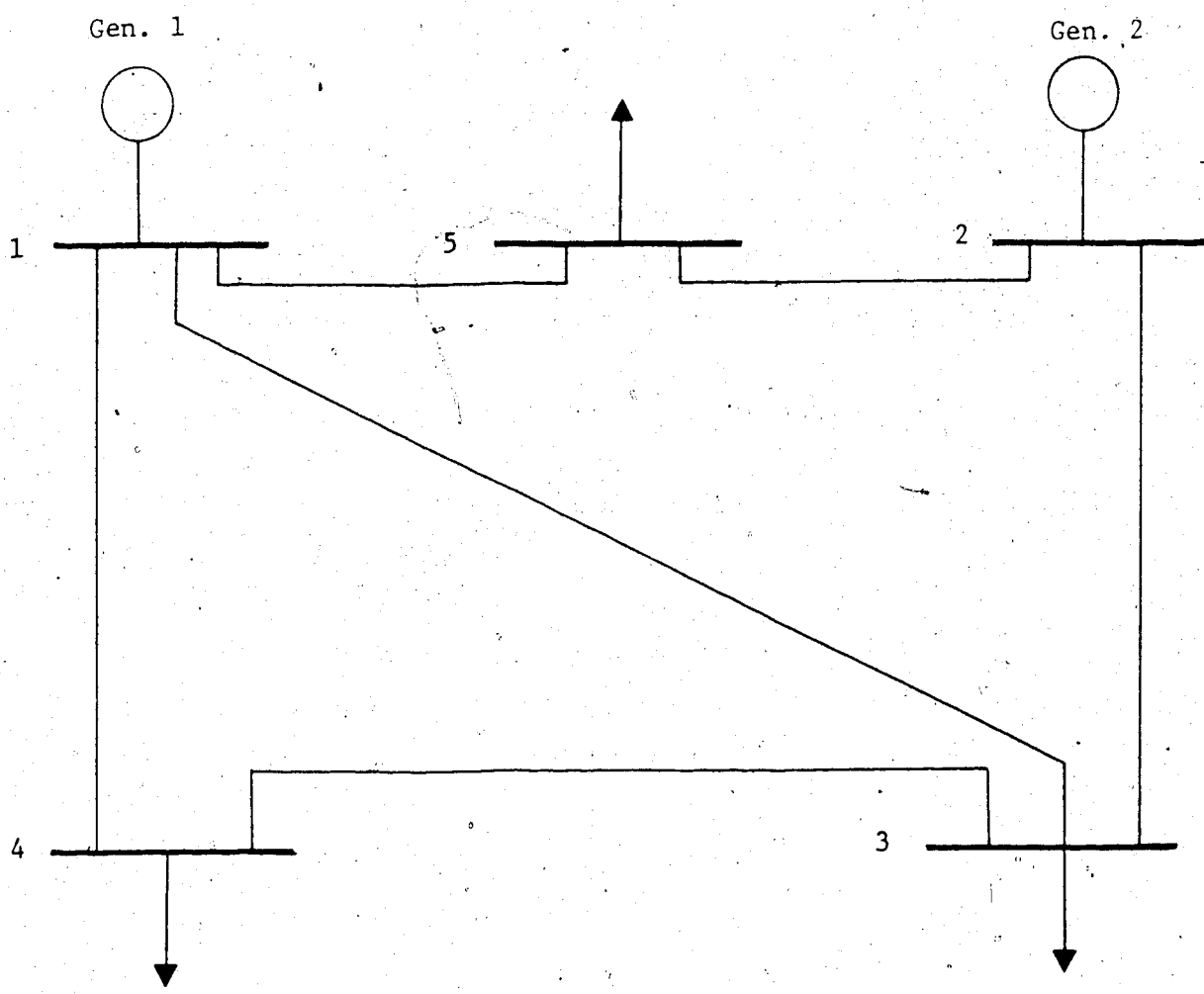
Figure 8.1 The 5 Bus Test System (4)

Ridge k = 0.031			
Parameter	Estimated Value	Parameter	Estimated Value
K_{LO}	0.000920	B_{11}	0.026717
B_{01}	0.000929	B_{12}	0.013661
B_{02}	-0.006847	B_{22}	0.024140

Table 8.1 The 5 Bus System of Reference 4. The

Parameters of the Active Loss Model in p.u.

on 100 MVA Base.

Gen. No.	α $/h	β $/MWh	γ $h/(MWh)^2
1	44.4	3.510	0.005
2	40.6	3.890	0.005

Table 8.2 The 5 Bus Generator Cost Coefficients of

Reference 60.

the economic active dispatch solution of the power system under

consideration, was obtained as shown in Table 8.3. Table 8.3 also

contains the results obtained by the optimal load flow method of

Reference 60, for comparison.

Bus No.	Proposed Active Dispatch Method				Optimal Load Flow Method With Fixed Generator Voltages of Reference 60			
	Voltage p.u.	Angle Degrees	P MW	Q MVAR	Voltage p.u.	Angle Degrees	P MW	Q MVAR
1	1.0200	0.0	97.052	27.561	1.0200	0.0	97.000	27.600
2	1.0400	-2.191	68.123	53.141	1.0400	-2.189	68.100	53.100
3	0.9552	-6.443	-60.000	-30.000	0.900	-6.442	-60.000	-30.000
4	0.9227	-9.479	-40.000	-10.000	0.9000	-9.478	-40.000	-10.000
5	0.9931	-4.189	-60.000	-20.000	0.9000	-4.188	-60.000	-20.000
	Total cost = 760.87 $/h				Total cost = 760.61 $/h			

Table 8.3 The Optimum Economic Active Dispatch of

the 5 Bus System (Proposed Method Versus

Optimal Load Flow Method)

As seen from Table 8.3, the solutions agree very closely with

one another. If the active powers obtained by the proposed method

are rounded off, it will give a value for the total fuel cost of

760.61 $/h . which is identical to the value obtained by the optimal

load flow method.

The active-reactive power loss model of the 5 bus system shown

in Figure 8.1, was evaluated from a series of load flow studies of the

system. The parameter estimates obtained for ridge $k = 7.5 \times 10^{-4}$ are

shown in Table 8.4. Using these parameters and the cost coefficients

Ridge k = 7.5×10^{-4}			
Parameter	Estimated Value	Parameter	Estimated Value
K_{LOP}	-0.000745	K_{LOQ}	-0.002980
E_{PP1}	0.000142	E_{QP1}	0.000556
E_{PP2}	-0.001043	E_{QP2}	-0.004137
E_{PQ1}	-0.000949	E_{QQ1}	-0.003808
E_{PQ2}	0.008182	E_{QQ2}	0.032725
A_{P11}	0.020504	A_{Q11}	0.082035
A_{P12}	0.006891	A_{Q12}	0.027569
A_{P22}	0.016544	A_{Q22}	0.066129
B_{P12}	0.001131	B_{Q12}	0.004501

Table 8.4 The 5 Bus System of Reference 4. The Parameters

of the Active-Reactive Loss Model in p.u. on

100 MVA Base.

of Table 8.2, the economic active-reactive dispatch schedules of the

system were obtained as shown in Table 8.5. This Table also includes

the optimal load flow solution of the system with variable generator

voltages reported in Reference 60. From Table 8.5, it is observed

that the two solutions agree very closely in the active power generations.

There are however, small differences in the reactive power generations.

These differences are as a result of the different voltage profiles

obtained in each case. The proposed method gave slightly lower bus

	Proposed Active-Reactive Dispatch Method				Optimal Load Flow Method With Variable Generator Voltages of Reference 60			
Bus No.	Voltage p.u.	Angle Degrees	P MW	Q MVAR	Voltage p.u.	Angle Degrees	P MW	Q MVAR
1	1.0900	0.0	97.834	44.110	1.0900	0.0	98.000	41.200
2	1.0733	-1.4534	66.689	33.976	1.0790	-1.571	66.400	36.800
3	1.0085	-5.4879	-60.000	-30.000	1.0120	-5.528	-60.000	-30.000
4	0.9873	-8.2186	-40.000	-10.000	0.9900	-8.222	-40.000	-10.000
5	1.0468	-3.5056	-60.000	-20.000	1.0500	-3.550	-60.000	-20.000
Total cost = 757.75 $/h					Total cost = 757.34 $/h			

Table 8.5 The Optimum Economic Active-Reactive Dispatch

of the 5 Bus System (Proposed Method Versus

Optimal Load Flow Method)

voltage levels in general which resulted in a slightly higher value

for the total cost (i.e., 757.75 $/h as compared to 757.34 $/h).

The sum of the reactive power generations is the same in both cases.

The differences in the reactive power generations are expected to

diminish when the base load flow solutions used to evaluate the active-

reactive power loss model of the system are obtained at higher voltage

levels.

8.1.3 The Proposed Economic Active and Active-Reactive Dispatch Methods

In general, the divided active-reactive power loss model (i.e.,

the active-reactive sources are separated from the purely reactive

sources was found to give superior economic dispatch solutions to the active power loss model based dispatch method (32, 61). The active-reactive dispatch method, can handle voltage variations and variations of Q/P ratios of the power system. If the purely reactive sources are included in the active-reactive loss model, the number of parameters to be evaluated will increase drastically, increasing the number of data points required for the parameter estimation procedure. For example, in the case of the IEEE 14 bus test system, the number of parameters will increase from 9 to 30. The inclusion of the purely reactive sources in the active-reactive loss model is also likely to cause ill-conditioning which will result in unstable solutions. If the function of a purely reactive source is to maintain voltage levels, the separation of the purely reactive sources from the active-reactive sources is satisfactory. If however, it is to control power losses, then it can be included in the active-reactive model as an active-reactive source which is always at its lower active power limit (i.e., zero).

Although the active-reactive loss model based method gives improved dispatch results over the active dispatch method, the latter has advantages with respect to computational time and storage as fewer parameters are associated with the active power loss model, and fewer variables are evaluated in the optimization algorithm.

8.1.4 The Proposed Diakoptical Active and Active-Reactive Dispatch Methods

The advantages gained by using the diakoptical active and active-reactive dispatch methods proposed in this thesis, as opposed to analyzing the power network as a whole are twofold:

1. significant savings in the computational time and
   storage

2. minimized possibility of obtaining unstable parameter
   estimates

The savings realized for the example systems tested in this thesis,
which were torn as described, are summarized in Tables 8.6 and 8.7 for
the diakoptical active and active-reactive power loss models respectively.

Power System	Torn Network		Entire Network	
	Maximum No. of Parameters	Minimum No. of Load Flows	Maximum No. of Parameters	Minimum No. of Load Flows
5 Bus	4	5	6	7
14 Bus	4	5	6	7
11 Bus	15	16	28	29
23 Bus	15	16	28	29

Table 8.6 The Number of Load Flow Results Required to
Evaluate the Parameters of the Diakoptical Active
Loss Model and the Entire Network Loss Model

Power System	Torn Network		Entire Network	
	Maximum No. of Parameters	Minimum No. of Load Flows	Maximum No. of Parameters	Minimum No. of Load Flows
5 Bus	7	8	9	10
14 Bus	7	8	9	10
11 Bus	29	30	49	50

Table 8.7 The Number of Load Flow Results Required to Evaluate
the Parameters of the Diakoptical Active-Reactive
Loss Model and the Entire Network Loss Model

The diakoptical based economic dispatch solutions are expected
to agree with the entire network based dispatch solutions in the
total cost. Variations in power generation schedules are expected,
since the total cost function has a wide and almost flat minimum.
Because of this phenomenon, any errors in the evaluated loss model can
cause shifts in generations (62-64). The shift in power generations
can also be caused by variations in bus voltage levels of the base
load flow results used in the evaluation of the loss models.

In large power systems, the diakoptical based economic dispatch
solutions are expected to be far superior to the solutions based on the
entire network loss models. To show the effectiveness of the diakoptical
based economic dispatch methods, the 23 bus test system shown in
Figure 8.2, was analyzed by the diakoptical active dispatch method and
by the entire network loss model based method. The generator capacities
used are given in Table 8.8. The cost coefficients of these thermal
generators are given in Table 2.1. The economic dispatch and the
feedback load flow solutions obtained for this system are shown in
Table 8.9. The load flow voltage profiles based on the economic dispatch
solutions are given in Table 8.10. As seen from Table 8.9, the
diakoptical method posed no problems and produced the dispatch solution
in three iterations (the piecewise active power loss model parameters
are given in Appendix E). However, in analyzing the entire network
loss model, it was observed that the system matrix D had three small
eigenvalues which is an indication of ill-conditioning. Depending on
the severity of ill-conditioning, the parameter estimates obtained may
or may not result in accurate dispatch solutions. Based on the parameter
estimates obtained, the dispatch algorithm converged to a solution after
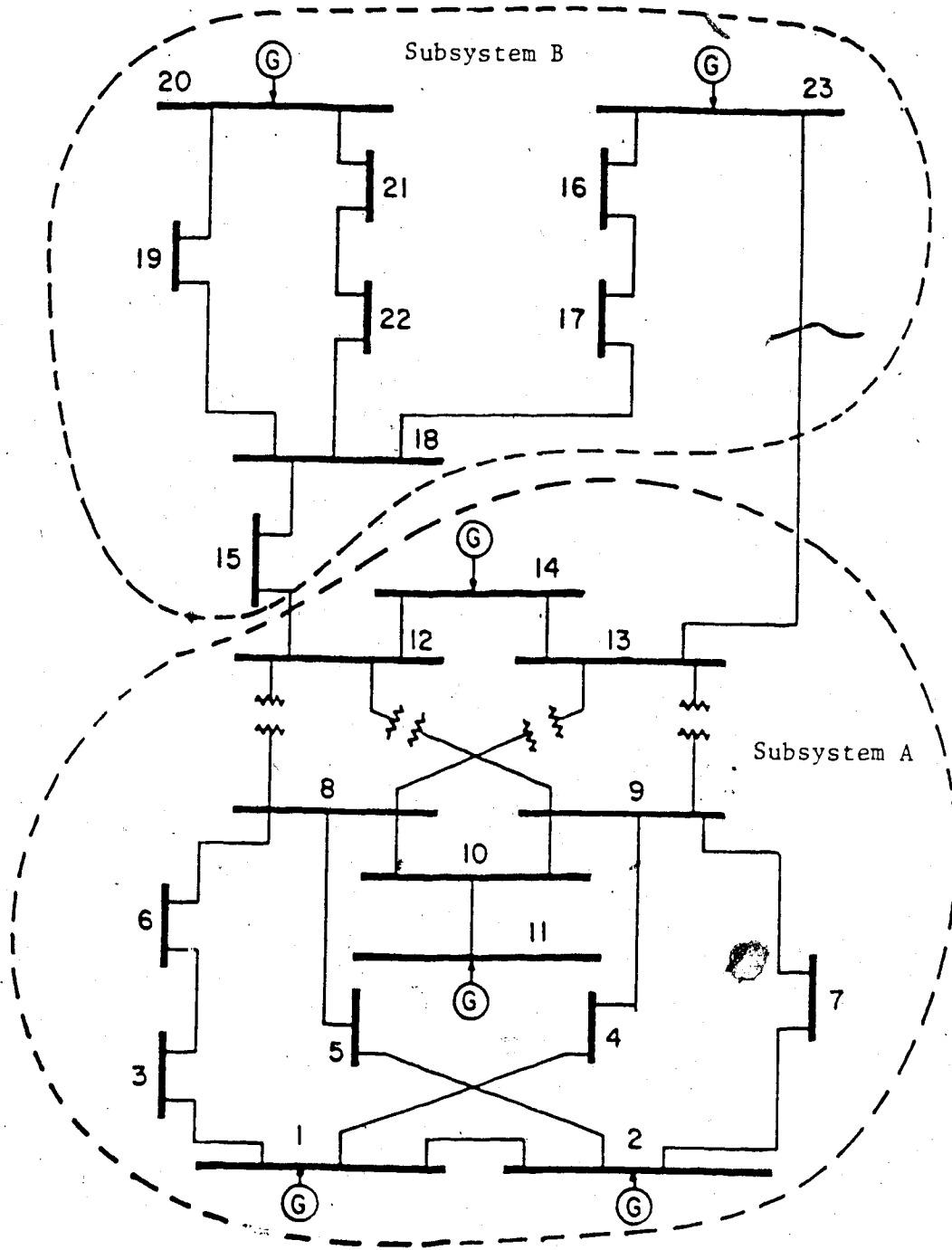
Figure 8.2   The 23 Bus Test System

Generator Number	Generator Size (MW)	Source Constraints		Bus Number
		MW	MVAR	
1	400	$5 \le P_{G1} \le 400$	$-100 \le Q_{G1} \le 200$	1
2	200	$5 \le P_{G2} \le 200$	$-30 \le Q_{G2} \le 194.65$	2
3	400	$5 \le P_{G3} \le 400$	$-30 \le Q_{G3} \le 40.0$	11
4	800	$10 \le P_{G4} \le 800$	$-120 \le Q_{G4} \le 430.00$	14
5	800	$10 \le P_{G5} \le 800$	$-155 \le Q_{G5} \le 514.13$	20
6	1200	$50 \le P_{G6} \le 1200$	$-205 \le Q_{G6} \le 774.96$	23

Table 8.8 The 23 Bus Test System Generator Capacities - Coal

Variable	System Load = 2643 + j660 MVA			
	Torn Network		Entire Network	
	Economic Solution	Load Flow Solution	Economic Solution	Load Flow Solution
P_{G1} MW	200.929	200.449	220.870	213.968
P_{G2} MW	26.926	26.926	28.867	28.867
P_{G11} MW	202.978	202.978	220.891	220.891
P_{G14} MW	666.182	666.182	668.016	668.016
P_{G20} MW	627.257	627.257	492.711	492.711
P_{G23} MW	955.878	955.878	1055.308	1055.308
P_L MW	37.150	36.684	43.665	36.817
F_0 $/h	25310.540		25397.052	
No. of Iter.	3		50	

Table 8.9 The Diakoptical and Full Network Economic

Active Dispatch of the 23 Bus Test System

| Bus Number | System Load = 2643 + j660 MVA | | | |
| | Torn Network | | Entire Network | |
	Voltage p.u.	Angle Degrees	Voltage p.u.	Angle Degrees
1	1.0500	0.0	1.0500	0.0
2	1.0220	-5.2950	1.0220	-5.6420
3	1.0210	-0.0050	1.0210	-0.1300
4	1.0020	-1.7300	1.0020	-2.0270
5	1.0030	-3.6590	1.0028	-4.1970
6	1.0030	-1.6160	1.0027	-2.0790
7	1.0018	-4.2970	1.0011	-4.8130
8	1.0136	-0.4710	1.0124	-1.1600
9	1.0109	-2.6800	1.0099	-3.2460
10	0.9960	-6.0060	0.9960	-5.8540
11	1.0350	-4.5180	1.0350	-3.7570
12	1.0459	2.3110	1.0462	0.9390
13	1.0434	4.4780	1.0432	3.6590
14	1.0500	5.0860	1.0500	4.0060
15	1.0307	2.1230	1.0311	0.0700
16	1.0267	8.1230	1.0251	6.6860
17	1.0203	6.1390	1.0189	4.2880
18	1.0267	5.0630	1.0268	2.3590
19	1.0214	4.7080	1.0219	1.5520
20	1.0500	10.8570	1.0500	6.4350
21	1.0350	7.6000	1.0355	3.7610
22	1.0385	7.4330	1.0390	4.0090
23	1.0500	13.2150	1.0500	12.6020

Table 8.10 The Voltage Profiles of the 23 Bus Test System Based on the
Economic Dispatch of the Diakoptical and the Entire Network
Solutions

50 iterations to the same accuracy of the diakoptical solution (i.e.,
an accuracy of $\leq 10^{-12}$ on the Newton-Raphson function vector $\underline{f}$) as
shown in Table 8.9. However, the dispatch solution when fed back into
the load flow program, the solution obtained did not agree with the
dispatch result. While both voltage profiles of Table 8.10, are
within the base load flow voltage limits, the total cost in the case of
the entire network is much higher than the diakoptical case. In the
diakoptical case, the dispatch and the feedback load flow solutions
are in close agreement.

In the diakoptical analysis, the approximation made on the total
power losses of interconnections is a good approximation as is evident
from the results obtained for the various power systems tested. This
is particularly true, when the interconnections of the torn network are
chosen to have a minimum number of lines. If the torn subnetworks have
much higher total power losses than interconnections, the quadratic
terms in the approximate models of interconnections can be neglected, and
if the losses in interconnections are very small compared to the losses
of the torn subnetworks, these losses can be neglected altogether.
This is expected to give satisfactory solutions, since small variations
in the total losses will only cause shifts in generations in the flat
minimum portion of the total fuel cost function. This approximation will
significantly reduce the computational cost in the parameter estimation
procedure.

8.2 Conclusions

In this thesis, two new approaches to the economic dispatch problem

in electric power systems, were proposed and rigorously tested. The first method is suitable for small power systems with a small number of generation buses. The second method, uses diakoptical techniques to handle large power systems. The proposed methods retain the simplicity of the classical dispatch methods and produce better accuracy for different system load levels. The presented methods are also superior to the classical dispatch methods that update the loss model coefficients iteratively from load flow results based on previous dispatch solutions.

The proposed methods produce economic dispatch solutions that agree very closely with optimal load flow methods with fixed and variable generator voltages in less computational time and storage. The methods do not provide the flexibility given by optimal load flow methods, for example, transformer tap changing. In practice, however, given well known problems with convergence and sensitivity to load flow mismatches of optimal load flow methods, the proposed methods can be superior to optimal load flow methods, particularly where the dispatch solutions for many system load levels are required.

The proposed methods can handle ill-conditioned situations (i.e., when small eigenvalues are encountered in the parameter estimation procedure), and well-conditioned cases, as they are based on the ridge regression algorithm, which has proven to treat multicolinearities. If the ill-conditioning is severe, the network may be evaluated in a piecewise manner. The methods are simple to implement and can be used

for on-line economic dispatch schedules of power systems as the bulk of the computational effort is done off-line.

8.3 Suggestions for Future Work

It would be worthwhile to explore the following areas:

1. apply the proposed methods to mixed hydro-thermal power systems,

2. solve the optimization problem in a piecewise manner and compute the total optimum fuel cost. This will result in area or subnetwork incremental cost of generation,

3. evaluate a form of tearing where the interconnection power losses are included in the subnetworks, i.e., tear at the connection points. This requires extra fictitious buses, but should pose no problems,

4. evaluate the loss model coefficients using the decoupled load flow program.

The thrust in alternatives 3 and 4 is to minimize the computational effort in the loss model evaluation procedure.

REFERENCES

1. Kirchmayer, L.K., "Economic Operation of Power Systems",

    John Wiley and Sons, New York, N.Y., 1958.

2. Savulescu, S.C., "Computerized Operation of Power Systems",

    Elsevier Scientific Publishing Company, New York,

    N.Y., 1976.

3. Stagg, G.W., El-Abiad, A.H., "Computer Methods in Power

    System Analysis", McGraw-Hill Book Company, New York,

    N.Y., 1968.

4. Stevenson, W.D., "Elements of Power System Analysis", McGraw-

    Hill Book Company, New York, N.Y., 1962.

5. Elgerd, O.I., "Electric Energy Systems Theory: An Introduction",

    McGraw Hill Book Company, New York, N.Y., 1971.

6. Brown, H.E., "Solution of Large Networks by Matrix Methods",

    Wiley-Interscience Publication, John Wiley and Sons,

    Inc., New York, N.Y., 1975.

7. Sullivan, R.L., "Power System Planning", McGraw-Hill Book

    Company, New York, N.Y., 1977.

8. Stott, B., "Review of Load Flow Calculation Methods", Proc.

    IEEE, Vol. 62, No. 7, July, 1974.

9. El-Hawary, M.E., "Electric Network Models in Optimum Economic

    Dispatch in Electric Power Systems", Proc. 2nd

    International Symposium on Large Engineering Systems,

    University of Waterloo, Ontario, May, 1978.

10. Blasznski, G.M., "Sensitivity Study of Economic Dispatch", Proc. PICA Conf. 1975.

11. El-Hawary, M.E., Christensen, G.S., "Optimal Active-Reactive Dispatch in Power Systems: Realistic Hydro Model", Proc. IFAC Multivariable Technologies System Symposium, Fredricton, N.B., 1977.

12. Dopazo, J.F., Klittin, D.A., Stagg, G.W., Watson, M., "An Optimization Technique for Real and Reactive Power Allocations", IEEE Trans. Vol. PAS-86, pp. 1877-1885, 1967.

13. Happ, H.H., "Optimal Power Dispatch", IEEE Trans. Vol. PAS-93, pp. 820-830, 1974.

14. Nicholson, H., Sterling, M.J.M., "Optimum Dispatch of Active and Reactive Generation by Quadratic Programming", IEEE Trans. Vol. PAS-92, No. 1, 1973.

15. Billinton, R., Sachdeva, S.S., "Real and Reactive Optimization by Suboptimal Techniques", IEEE PES Summer Meeting, Portland, Oregon, June, 1971.

16. Sasson, A.M., Merrill, H.M., "Some Applications of Optimization Techniques to Power System Problems", Proc. IEEE Vol. 62, 1974.

17. Dommel, H.W., Tinney, W.F., "Optimal Power Flow Solutions", IEEE Trans. Vol. PAS-87, No. 10, pp. 1866-1876, 1968.

18. Sasson, A.M., Viloria, F., Aboytes, F., "Optimal Load Flow Solutions Using the Hessian Matrix", IEEE Trans. Vol. PAS-92, No. 1, pp. 31-41, 1973.

19. Rashed, A.M.H., Kelly, D.H., "Optimal Load Flow Solution Using the Lagrangian Multipliers and the Hessian Matrix, IEEE Trans. Vol. PAS-93, No. 5, pp. 1292-1297, 1974.

20. Mukherijee, P.K., Dhar, R.N., "Optimal Load Flow Solution by Reduced Gradient Method", Proc. IEE Vol. 121, No. 6, June 1974.

21. Alsac, O., Stott, B., "Optimal Load Flow with Steady State Security", IEEE PES Summer Meeting, Vancouver, B.C., 1973.

22. El-Hawary, M.E., Mansour, S.Y., "Parameter Estimation for Optimal Control of Electric Power Systems", Proc. Canadian Conference on Automatic Control, CCAC, McGill University, Montreal, Quebec, May, 1979.

23. El-Hawary, M.E., Mansour, S.Y., "Optimal Parameter Estimation for Basic Problems in Electric Power Systems", Optimal Control Application and Methods, Vol. 2, pp. 269-287, 1981.

24. El-Hawary, M.E., Mansour, S.Y., "Performance Evaluation of Parameter Estimation Algorithms for Economic Operation of Power Systems", IEEE Trans. Vol. PAS-101, 1982.

25. Brameller, A., Allan, R.N., Hamam, Y.M., "Sparsity", Pitman Publishing Corporation, New York, N.Y., 1976.

26. Mikhail, E.M., "Observations and Least Squares", IEP-A Dun-
    Donnelly Publisher, New York, N.Y., 1976.

27. Rust, B.W., Burrus, W.R., "Mathematical Programming and the
    Numerical Solution of Linear Equations", American
    Elsevier Publishing Company Inc., New York, N.Y., 1972.

28. Bard, Y., "A Functional Maximization Method with Application
    to Parameter Estimation", Scientific Centre Report
    322.0902, IBM, New York, N.Y., 1967.

29. Marquardt, D.W., "An Algorithm for Least Squares Estimation of
    Non-Linear Parameters", SIAM, J.11, pp. 431-441, 1963.

30. Powell, M.J.D., "A Method for Minimizing a Sum of Squares of
    Non-Linear Functions Without Calculating Derivatives",
    Computer J.7, pp. 155-162, 1965.

31. El-Hawary, M.E., Christensen, G.S., "Optimal Economic Operation
    of Power Systems", Academic Press, New York, N.Y., 1979.

32. Mansour, S.Y., Koval, D.O., Kelly, D.H., "Performance Evaluation
    of Optimum Power System Models", Proc. Optimization Days'
    82, University of Montreal, Montreal, Quebec, May, 1982.

33. Kelly, D.H., Mansour, S.Y., Koval, D.O., "Power Systems Generation
    Scheduling by a Divided Active-Reactive Power Loss Model",
    Proc. Midwest Power Symposium, University of Wisconsin,
    Madison, Wisconsin, November, 1982.

34. Mansour, S.Y., Kelly, D.H., Koval, D.O., "Power Systems Economic
    Dispatch by a Rearranged Active-Reactive Power Loss Model",
    Canadian Electrical Engineering Journal, CEEJ, Vol. 8, No. 4,
    pp. 142-146, October, 1983.

35. Mansour, S.Y., Koval, D.O., Kelly, D.H., "Graphical Method

    for the Optimal Economic Dispatch in Electric Power Systems",

    Proc. Midwest Power Symposium, University of Illinois,

    Urbana, Illinois, October, 1981.

36. Mansour, S.Y., Kelly, D.H., Koval, D.O., "Minimum Fuel Cost

    Dispatch through Least Squares Estimation", Proc. 4th

    International Symposium on Large Engineering Systems,

    University of Calgary, Calgary, Alberta, June, 1982.

37. Horel, A.E., Kennard, R.W., "Ridge Regression Biased Estimation

    for Non-Orthogonal Problems", Technometrics 12, 1970.

38. Freund, R.J., Minton, P.D., "Regression Methods", Marcel

    Dekker Inc., New York, N.Y., 1979.

39. Mansour, S.Y., Koval, D.O., Kelly, D.H., "Application of Ridge

    Regression to Ill-Conditioned Power System Parameter

    Estimation Problems", Proc. Midwest Power Symposium,

    University of Wisconsin, Madison, Wisconsin, November, 1982.

40. Belsley, D.A., Kuh, E., Welsch, R.E., "Regression Diagnostics",

    John Wiley and Sons Inc., New York, N.Y., 1980.

41. Laithwaite, E.R., Freris, L.L., "Electric Energy: Its

    Generation, Transmission and Use", McGraw Hill Book

    Company Limited, Maidenhead, Berkshire, England, 1980.

42. Freris, L.L., Sasson, A.M., "Investigation of the Load Flow

    Problems", Proc. IEE Vol. 115, No. 10, October, 1968.

43. Kron, G., "Diakoptics: The Piecewise Solution of Large Scale Systems", McDonald, London, 1963.

44. Happ, H.H., "Diakoptics and Networks", Academic Press, New York, N.Y., 1971.

45. Happ, H.H., "Piecewise Methods and Applications to Power Systems", John Wiley and Sons Inc., New York, N.Y., 1980.

46. Kevorkian, A.K., "Structural Aspects of Large Dynamic Systems", 6th IFAC World Congress, Boston, Paper No. 19.3, 1975.

47. Barameller, A., Scott, M.R., "Practical Diakoptics for Electrical Networks", Chapman and Hall Ltd., London, U.K., 1969.

48. Nicholson, H., "Structure of Interconnected Systems", Peter Peregrinus Ltd., Southgate House, Stevenage, Herts, U.K., 1978.

49. Wu, F.F., "Diakoptic Network Analysis", Proc. PICA Conference, New Orleans, Louisiana, June, 1975.

50. Mansour, S.Y., Kelly, D.H., Koval, D.O., "Diakoptical Loss Model Parameter Estimation for Optimum Economic Dispatch of Large Power Systems", Proc. Optimization Days 83, Ecole Polytechnique, Montreal, Quebec, May, 1983.

51. Mansour, S.Y., Koval, D.O., Kelly, D.H., "Transmission Line Loss Modeling for Optimum Economic Dispatch in Large Power Systems", Proc. Optimization Days '84, Concordia University, Montreal, Quebec, May, 1984.

52. Mansour, S.Y., Koval, D.O., Kelly, D.H., "Large Power System Generation Scheduling by a Diakoptical Network Loss Model", Proc. IEEE International, Electrical Electronics and Exposition, Toronto, Ontario, September, 1983.

53. Mansour, S.Y., Kelly, D.H., Koval, D.O., "Economic Dispatch of Large Power Systems Using a Piecewise Network Loss Model", Proc. Midwest Power Symposium, Iowa State University, Ames, Iowa, October, 1983.

54. Mansour, S.Y., Koval, D.O., Kelly, D.H., "Piecewise Loss Co-efficient Simulation for Large Power Systems Economic Generation Scheduling", Proc. IASTED (International Association of Science and Technology for Development), Symposium on Simulation and Modelling, Orlando, Florida, November, 1983.

55. Mansour, S.Y., Kelly, D.H., Koval, D.O., "Diakoptical Active-Reactive Dispatch of Generation", Proc. IEEE International Symposium on Circuits and Systems, Montreal, Quebec, May, 1984.

56. Hill, E.F., Stevenson, W.D., "An Improved Method of Determining Incremental Loss Factors from Power System Admittances and Voltages", IEEE Trans. Vol. PAS-87, No. 6, June, 1968.

57. Aboytes, F., Cory, B.J., "An Alternative Formulation of the Stochastic Load Flow Method", Proc. PICA, pp. 209-215, 1975.

58. Mansour, S.Y., Koval, D.O. Kelly, D.H., "Power System Economic Dispatch by Ridge and Powell Regression", Proc. Optimization Days '83, Ecole Polytechnique, Montreal, Quebec, May, 1983.

59. Mansour, S.Y., Kelly, D.H., Koval, D.O., "Network Parameter
        Estimation for Power Systems Economic Dispatch", Proc.
        Midwest Power Symposium, Iowa State University, Ames,
        Iowa, October, 1983.

60. Bala, J.L., Thanikachalam, A., "An Improved Second Order
        Method for Optimal Load Flow", IEEE Trans. Vol. PAS-97,
        No. 4, July/August, 1978.

61. Kelly, D.H., Mansour, S.Y., Koval, D.O., "Comparison of Loss
        Model Based Power System Optimization Algorithms", Proc.
        Midwest Power Symposium, University of Wisconsin,
        Wisconsin, November, 1982.

62. Mansour, S.Y., Koval, D.O., Kelly, D.H., "Sensitivity of Power
        Systems Optimum Economic Dispatch Solutions to Reactive
        Loss Coefficients", Proc. Optimization Days '83,
        Concordia University, Montreal, Quebec, May, 1984.

63. Mansour, S.Y., Kelly, D.H., Koval, D.O., "Impact of Reactive
        Power Flow on the Optimum Economic Operation of Power
        Systems", Proc. Canadian Society for Electrical Engineering
        Conference CSEE, Halifax, Nova Scotia, May, 1984.

64. Mansour, S.Y., Koval, D.O., Kelly, D.H., "Problems Associated
        with Evaluation of Large Power Systems Active-Reactive Loss
        Models", Proc. 27th Midwest Symposium on Circuits and
        Systems (MSCS), West Virginia University, West Virginia,
        June, 1984.

APPENDIX A

THE ACTIVE AND ACTIVE-REACTIVE POWER LOSS MODELS AS

FUNCTIONS OF POWER GENERATIONS

The active power loss model of a transmission network, is a simplified version of the active-reactive power loss model. This simplified model is obtained by making certain assumptions on the network operation. The active-reactive loss model is given first followed by the active power loss model.

A.1   The Active-Reactive Power Loss Model

This model can be arrived at by considering the complex power balance equation of a transmission network which can be written as:

$$S_D + S_L - \sum_{i=1}^{m} S_{Gi} = 0.0 \qquad\qquad (A.1)$$

where,

S_D , S_L - the system total complex load demand and the system total complex power losses respectively

S_{Gi} - the complex power generation of the ith unit

m - the number of generation sources feeding the power network

Equation A.1, may be written in terms of the real and imaginary quantities as given below:

160

$$P_L + jQ_L = \sum_{i=1}^{m} (P_{Gi} + jQ_{Gi}) - (P_D + jQ_D) \qquad (A.2)$$

where,

    P, Q - the active and reactive powers respectively

    D, L, G - represent demand, losses and generation respectively

The network bus voltage and current vectors in rectangular form are given by:

$$\underline{V} = \underline{V}_p + j\, \underline{V}_q \qquad (A.3)$$

$$\underline{I} = \underline{I}_p + j\, \underline{I}_q \qquad (A.4)$$

where,

    p,q - represent the real and imaginary parts respectively

The complex power losses can be written as:

$$S_L = \underline{V}^T\, \underline{I}^* \qquad (A.5)$$

where,

    * - represent complex conjugate

The nodal equation of the power network in compact form is written as:

$$\underline{I} = \underline{Y} \; \underline{V} \tag{A.6}$$

where,

$\underline{Y}$ - the bus admittance matrix of the network

and,

$$\underline{Y} = \underline{G} - j \; \underline{B} \tag{A.7}$$

where,

$\underline{G}$, $\underline{B}$ - the conductance and the susceptance matrices of the
network

Substituting equations A.3, A.4 and A.7 into equation A.5 gives the
following equation:

$$P_L + j \; Q_L = [\underline{V}_p^T + j \; \underline{V}_q^T][\underline{G} + j \; \underline{B}][\underline{I}_p - j \; \underline{I}_q] \tag{A.8}$$

Simplifying equation A.8, and equating the real and imaginary parts,
the active and reactive power losses are obtained as given below:

$$P_L = V_p^T \ \underline{G} \ V_p + V_q^T \ \underline{G} \ V_q \qquad \text{(A.9)}$$

$$Q_L = V_p^T \ \underline{B} \ V_p + V_q^T \ \underline{B} \ V_q \qquad \text{(A.10)}$$

The complex power at the ith node of the network is given by:

$$P_i + j \ Q_i = V_i \ I_i^* \qquad \text{(A.11)}$$

and,

$$I_i = |I_i| \ [\text{Cos} \ \delta_i + j \ \text{Sin} \ \delta_i] \qquad \text{(A.12)}$$

The voltage at the ith node is given by:

$$V_i = V_{pi} + j \ V_{qi} \qquad \text{(A.13)}$$

Substituting equations A.12 and A.13, into equation A.11, gives:

$$P_i + j \ Q_i = [V_{pi} + j \ V_{qi}] \ |I_i| [\text{Cos} \ \delta_i - j \ \text{Sin} \ \delta_i] \qquad \text{(A.14)}$$

equating the real and imaginary parts, then,

$$P_i = |I_i| \ [V_{pi} \ \text{Cos} \ \delta_i + V_{qi} \ \text{Sin} \ \delta_i] \qquad \text{(A.15)}$$

and,

$$Q_i = |I_i| \, [V_{qi} \, \text{Cos} \, \delta_i - V_{pi} \, \text{Sin} \, \delta_i] \qquad (A.16)$$

The active and reactive components of the voltage at node i, can be easily obtained from equations A.15 and A.16 as given below:

$$V_{pi} = \frac{1}{|I_i|} \, [P_i \, \text{Cos} \, \delta_i - Q_i \, \text{Sin} \, \delta_i] \qquad (A.17)$$

and,

$$V_{qi} = \frac{1}{|I_i|} \, [P_i \, \text{Sin} \, \delta_i + Q_i \, \text{Cos} \, \delta_i] \qquad (A.18)$$

Let:

$$\underline{M} = \text{diag}[\text{Cos} \, \delta_i / |I_i|] \qquad (A.19)$$

and

$$\underline{N} = \text{diag}[\text{Sin} \, \delta_i / |I_i|] \qquad (A.20)$$

for i = 1, 2, ..., n, where n is the number of buses in the network. The active and reactive parts of the bus voltage vector in compact form are then given by:

$$\underline{V}_p = \underline{M} \, \underline{P} - \underline{N} \, \underline{Q} \, , \qquad (A.21)$$

$$\underline{V}_q = \underline{N}\,\underline{P} + \underline{M}\,\underline{Q}\,. \tag{A.22}$$

Substituting for $\underline{V}_p$ and $\underline{V}_q$ into equation A.9, gives:

$$P_L = [\underline{M}\,\underline{P} - \underline{N}\,\underline{Q}]^T \cdot \underline{G}\,[\underline{M}\,\underline{P} - \underline{N}\,\underline{Q}]$$

$$+ [\underline{N}\,\underline{P} + \underline{M}\,\underline{Q}]^T\,\underline{G}\,[\underline{N}\,\underline{P} + \underline{M}\,\underline{Q}]\,, \tag{A.23}$$

multiplying through and rearranging, gives:

$$P_L = [\underline{P}^T\,\underline{M}^T - \underline{Q}^T\,\underline{N}^T]\,\underline{G}\,[\underline{M}\,\underline{P} - \underline{N}\,\underline{Q}]$$

$$+ [\underline{P}^T\,\underline{N}^T + \underline{Q}^T\,\underline{M}^T]\,\underline{G}\,[\underline{N}\,\underline{P} + \underline{M}\,\underline{Q}] \tag{A.24}$$

Equation A.24, in a more compact form may be written as:

$$P_L = [\underline{P}^T\,\underline{Q}^T] \begin{bmatrix} (\underline{M}^T\,\underline{G}\,\underline{M} + \underline{N}^T\,\underline{G}\,\underline{N}) & -(\underline{M}^T\,\underline{G}\,\underline{N} - \underline{N}^T\,\underline{G}\,\underline{M}) \\ (\underline{M}^T\,\underline{G}\,\underline{N} - \underline{N}^T\,\underline{G}\,\underline{M}) & (\underline{M}^T\,\underline{G}\,\underline{M} + \underline{N}^T\,\underline{G}\,\underline{N}) \end{bmatrix} \begin{bmatrix} \underline{P} \\ \underline{Q} \end{bmatrix} \tag{A.25}$$

Let:

$$\underline{A}_p = \underline{M}^T\,\underline{G}\,\underline{M} + \underline{N}^T\,\underline{G}\,\underline{N} \tag{A.26}$$

and,.

$$\underline{B}_p = \underline{M}^T \underline{G} \underline{N} - \underline{N}^T \underline{G} \underline{M} \tag{A.27}$$

then equation A.25, may be written as:

$$P_L = [\underline{P}^T \ \underline{Q}^T] \begin{bmatrix} \underline{A}_p & -\underline{B}_p \\ \underline{B}_p & \underline{A}_p \end{bmatrix} \begin{bmatrix} \underline{P} \\ \underline{Q} \end{bmatrix} \tag{A.28}$$

where,

$$A_{pij} = G_{ij} \ \text{Cos}(\delta_i - \delta_j) \ |I_i| \ |I_j| \tag{A.29}$$

and,

$$B_{pij} = G_{ij} \ \text{Sin}(\delta_i - \delta_j) \ |I_i| \ |I_j| \tag{A.30}$$

The net active and reactive powers $\underline{P}$ and $\underline{Q}$, may be partitioned into generation and demand as given below:

$$\underline{P}^T = [\underline{P}_G^T \quad -\underline{P}_D^T] , \tag{A.31}$$

$$\underline{Q}^T = [\underline{Q}_G^T \quad -\underline{Q}_D^T] . \tag{A.32}$$

The matrices $\underline{A}_p$ and $\underline{B}_p$, may also be partitioned accordingly as given below:

$$\underline{A}_P = \begin{bmatrix} \underline{A}_{PGG} & \underline{A}_{PGD} \\ \\ \underline{A}_{PDG} & \underline{A}_{PDD} \end{bmatrix} \tag{A.33}$$

and,

$$\underline{B}_P = \begin{bmatrix} \underline{B}_{PGG} & \underline{B}_{PGD} \\ \\ \underline{B}_{PDG} & \underline{B}_{PDD} \end{bmatrix} \tag{A.34}$$

The matrix $\underline{A}_P$ is a square symmetric matrix with $\underline{A}_P^T = \underline{A}_P$, and the matrix $\underline{B}_P$ is a skew symmetric matrix with $\underline{B}_P^T = -\underline{B}_P$. Substituting equations A.31, A.32 and A.33, A.34, into equation A.28, the network total active power losses can be written as:

$$P_L = K_{LOP} + [\underline{E}_{PP}^T \quad \underline{E}_{PQ}^T] \begin{bmatrix} \underline{P}_G \\ \\ \underline{Q}_G \end{bmatrix}$$

$$+ [\underline{P}_G^T \quad \underline{Q}_G^T] \begin{bmatrix} \underline{A}_{PGG} & -B_{PGG} \\ \\ \underline{B}_{PGG} & \underline{A}_{PGG} \end{bmatrix} \begin{bmatrix} \underline{P}_G \\ \\ \underline{Q}_G \end{bmatrix} \tag{A.35}$$

where,

$$\underline{E}_{PP} = 2[\underline{B}_{PGD} \, \underline{Q}_D - \underline{A}_{PGD} \, \underline{P}_D] \tag{A.36}$$

$$E_{PQ} = [B_{PDG} \ P_D - A_{PDG} \ Q_D] \tag{A.37}$$

and,

$$K_{LOP} = [P_D^T \ Q_D^T] \begin{bmatrix} A_{PDD} & -B_{PDD} \\ B_{PDD} & A_{PDD} \end{bmatrix} \begin{bmatrix} P_D \\ Q_D \end{bmatrix} \tag{A.38}$$

where,

G, D - stand for generation and demand respectively.

Similarly, an expression for the total reactive power losses in terms of the active and reactive power generations of the network may be written as:

$$Q_L = K_{LOQ} + [E_{QP}^T \ E_{QQ}^T] \begin{bmatrix} P_G \\ Q_G \end{bmatrix}$$

$$+ [P_G^T \ Q_G^T] \begin{bmatrix} A_{QGG} & -B_{QGG} \\ B_{QGG} & A_{QGG} \end{bmatrix} \begin{bmatrix} P_G \\ Q_G \end{bmatrix} \tag{A.39}$$

The coefficeints K_{LOQ}, E_{QP} and E_{QQ}, are similar to the expressions of the active power loss model P_L.

At this point, the expressions given by equations A.35 and A.39 are general expressions. The coefficients of these expressions are functions of the system voltages and loads and hence are not constant. In this thesis, quadratic expressions for the active and reactive power losses of the system under consideration are assumed as given by equations A.35 and A.39. The coefficients of these expressions are evaluated by the Ridge regression estimator from a set of load flow results of the system, which are obtained for different system load and voltage levels. This set of load flow results, define a feasible operating region of the power system under consideration. The evaluated quadratic functions, are functions that best fit the system power losses over the entire range of system loads considered.

A.2 The Active Power Loss Model

In the classical method of evaluation of the economic dispatch schedules of a power system, the active power loss model is formulated from the active-reactive power loss model by assuming that the ratio of reactive to active powers at any node remains constant. This assumption implies that the reactive power generation at node i, can be written as a linear function of the active power generation of that node as given by the following equation:

$$Q_{Gi} = Q_{Gi0} + f_i \, P_{Gi} , \qquad (A.40)$$

Equation A.40 in compact form can be written as:

$$\underline{Q}_G = \underline{Q}_{GO} + \underline{F}^T \underline{P}_G \tag{A.41}$$

where,

$$\underline{F} = \text{diag}\left[f_i\right] \tag{A.42}$$

Substituting equation A.41 into equation A.35, the new model coefficients are given by:

$$\underline{B} = \underline{A}_{PGG} + \underline{F}^T_{PGG} \underline{F} + 2\underline{F}^T \underline{B}_{PGG} \tag{A.43}$$

and,

$$\underline{B}_0 = \underline{E}^T_{PP} + 2\underline{Q}^T_{GO} \left[\underline{A}_{PGG} \underline{F} + \underline{B}_{PGG}\right] + \underline{E}^T_{PQ} \underline{F} \tag{A.44}$$

and,

$$K_{LO} = K_{LOP} + \underline{Q}^T_{GO} \underline{A}_{PGG} \underline{Q}_{GO} + \underline{E}^T_{PQ} \underline{Q}_{GO} \tag{A.45}$$

where,

$$\underline{Q}_{GO} = \left[Q_{G10}\ Q_{G20}\ \cdots\ Q_{GmO}\right] \tag{A.46}$$

where, m is the number of generation buses of the network. Collecting terms, the active power loss model may be written as:

$$P_L = K_{LO} + \underline{B}_0^T \underline{P}_G + \underline{P}_G^T \underline{B} \underline{P}_G \qquad (A.47)$$

The matrix $\underline{B}$ is a square symmetric matrix. Equation A.47, can be written in a summation form as:

$$P_L = K_{LO} + \sum_{i=1}^{m} B_{io} P_{Gi} + \sum_{i=1}^{m} \sum_{j=1}^{m} P_{Gi} B_{ij} P_{Gj} \qquad (A.48)$$

As in the case of the active-reactive power loss model, the co-efficients of equation A.47 or A.48, are functions of voltages and loads and hence are not constant. In the classical method, these coefficients are assumed to remain constant. In this thesis, a quadratic function as that given by equation A.47, is assumed. The parameters of this quadratic function for a given power system, are evaluated in a similar fashion to that discussed for the active-reactive loss model.

APPENDIX B

MATRIX SCALING

In general, scaling of a matrix minimizes the round off errors in the matrix inversion procedure. Matrix scaling can be obtained using the following schemes (40):

1. row scaling

2. column scaling

3. column scaling to unit column lengths

Row and column scaling are obtained by dividing each element in each row or column by the largest absolute value in that row or column. The most effective scaling scheme is the third scheme. In the third scheme, the matrix is scaled such that each column of the matrix has a unit length. This scaling technique is used to examine the condition of a given matrix. A matrix with small singular values suggests near dependices between the matrix columns. To scale a matrix to unit column lengths, consider the following equation:

$$\underline{Y} = \underline{A} \, \underline{x} \; . \tag{B.1}$$

The vector $\underline{Y}$ is of (nx1), $\underline{A}$ is of dimension (nxp) and the vector $\underline{x}$ is of dimension (px1). To scale the matrix $\underline{A}$ and the vector $\underline{Y}$ to unit column lengths, divide each element in the column of $\underline{A}$ by:

$$\left[\sum_{i=1}^{n} (a_{ij})^2 \right]^{\frac{1}{2}} = \frac{1}{d_j} \qquad (B.2)$$

where,

$$j = 1,2,\ldots,p,$$

and divide each element of the vector $\underline{Y}$ by:

$$\left[\sum_{i=1}^{n} (Y_i)^2 \right]^{\frac{1}{2}} = \frac{1}{d_{p+1}} \quad , \qquad (B.3)$$

where the length of any vector $\underline{C}$ (say) is given by:

$$||\underline{C}|| = [\underline{C}^T\underline{C}]^{\frac{1}{2}} = \left[\sum_{i=1}^{n} C_i^2 \right]^{\frac{1}{2}} \qquad (B.4)$$

where,

$$||.|| - \text{the norm of the vector.}$$

Let $\underline{D}$ be a diagonal matrix given by:

$$\underline{D} = \text{diag} \left[d_1 \; d_2 \; \ldots d_p \right] \qquad (B.5)$$

then

$$\underline{A} \text{ (scaled)} = \underline{A} \; \underline{D} \quad . \qquad (B.6)$$

Column scaling the matrix equation B.1 to unit column lengths gives

the following equation:

$$d_{p+1} \, \underline{Y} = [\underline{A} \ \underline{D}] \cdot \underline{Z} \ , \tag{B.7}$$

where the vector $\underline{Z}$ is given by:

$$\underline{Z} = d_{p+1} [(\underline{A} \ \underline{D})^T \cdot (\underline{A} \ \underline{D})]^{-1} \, (\underline{A}^T \ \underline{D}) \, \underline{Y} \ . \tag{B.8}$$

The solution vector $\underline{x}$ is found as follows:

$$\underline{A}^T \, \underline{Y} = \underline{A}^T \, \underline{A} \, \underline{x}, \tag{B.9}$$

hence,

$$\underline{Z} = d_{p+1} \, [(\underline{A} \ \underline{D})^T \cdot (\underline{A} \ \underline{D})]^{-1} \, \underline{D}^T \, \underline{A}^T \, \underline{A} \, \underline{x} \ , \tag{B.10}$$

this gives:

$$\underline{x} = \frac{1}{d_{p+1}} \, [\underline{D}] \, \underline{Z} \ , \tag{B.11}$$

since,

$$[\underline{D}^T]^{-1} \, \underline{D}^T = \underline{I} \ , \tag{B.12}$$

and

$$[\underline{A}^T \underline{A}]^{-1} \underline{A}^T \underline{A} = \underline{I},$$

where,

$\underline{I}$ - a unit matrix.

APPLICATION OF LOSS MODEL BASED ECONOMIC DISPATCH

METHODS TO EXAMPLE TEST SYSTEMS

This appendix presents the results obtained for the 5 bus and

the IEEE 30 bus test systems. These results include, the active and

active-reactive power loss model parameter estimates and the economic

dispatch schedules of the above power systems. The 5 and 30 bus test

system operating conditions, impedances and line charging data are

tabulated in Appendix F.

The data used to evaluate the power loss model parameters

(including the purely reactive source model parameters), of the above

power systems, were obtained from series of load flow studies of the

power systems. The load flow solutions of each system were carried out

for different load and voltage levels to create a feasible operating

region that covers the entire load spectrum of the power system. Based

on the load flow results, the parameters of the network loss models were

evaluated by the iterative ridge regression procedure. Using the

evaluated model (or models) of the system under consideration, the search

for the optimal solution was conducted through the feasible operating

region of the system.

C.1 The Active Loss Models and the Economic Dispatch Schedules of

Model Power Systems

In this section, the active power loss models and the economic

active dispatch results are presented for the 5 and 30 bus test systems.

C.1.1 The 5 Bus Test System – Active Power Loss Model

The single line diagram of the 5 bus test system is shown in Figure C.1. The system has two generation buses, 1 and 4. On the basis of equation 2.3, the number of parameters to be evaluated is 6. A minimum of 7 load flow solutions were carried out to obtain sufficient data for the parameter estimation procedure. Using these results, the active power loss model parameters were evaluated. The parameter estimates obtained are presented in Table C.1.

Ridge k = 0.0		
Parameter	Estimated Value	Condition Index
K_{LO}	0.000984	1
B_{01}	-0.001919	3
B_{02}	-0.000270	5
B_{11}	0.022088	37
B_{12}	0.008350	39
B_{22}	0.011034	41
Condition Number	41	
Mean Square Error	0.0003	

Table C.1 The Active Power Loss Model Parameters of the
5 Bus Test System in p.u. on 100 MVA Base
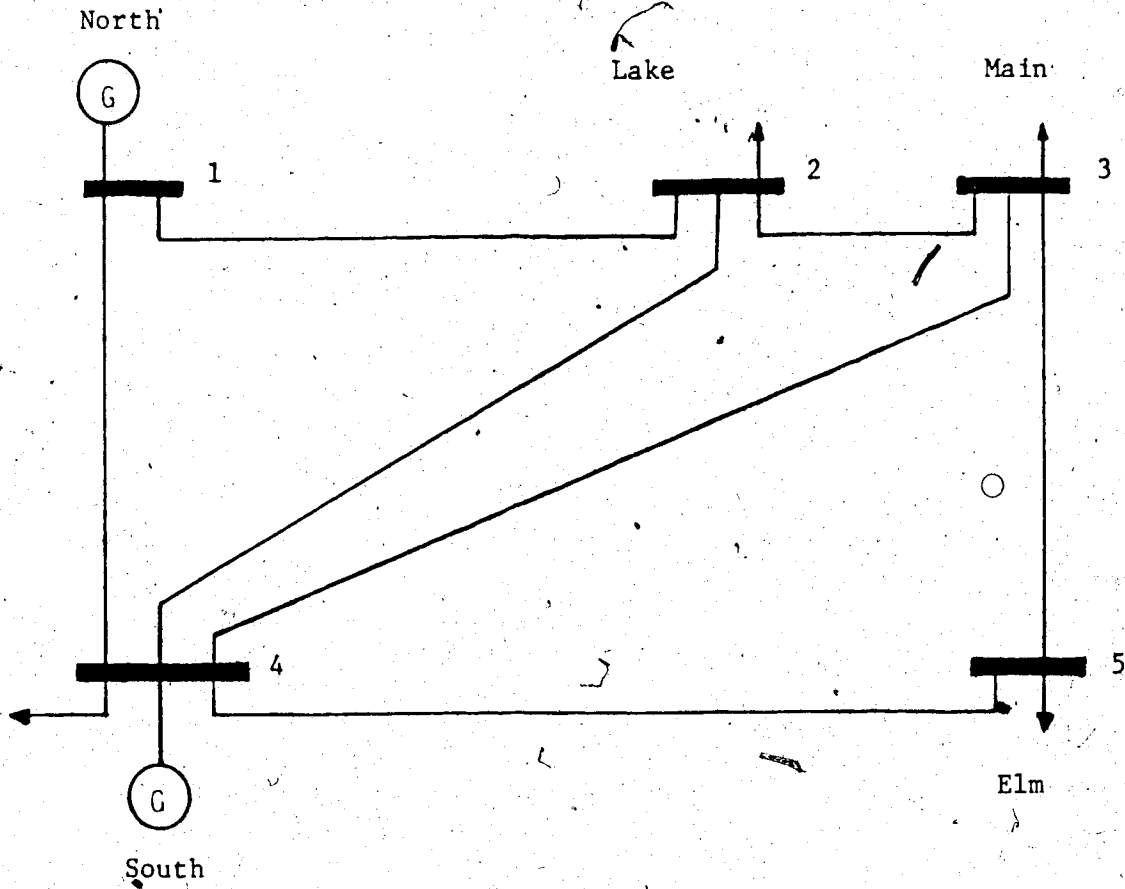
Figure C.1 The 5 Bus Test System

C.1.2 The 5 Bus Test System - Economic Active Dispatch

The thermal generation unit capacities used in the evaluation of the economic active dispatch conditions of this system are shown in Table C.2. Based on the evaluated active power loss model parameters for ridge k = 0.0 (Table C.1), the economic active dispatch solutions

Generator No.	Generator Size (MW)	Source Constraints		Bus No.
		MW	MVAR	
1	200	$5 \leq P_{G1} \leq 200$	$-50 \leq Q_{G1} \leq 50$	1
2	200	$5 \leq P_{G4} \leq 200$	$-40 \leq Q_{G4} \leq 50$	4

Table C.2 The 5 Bus Test System Generator Capacities

- Coal

of the 5 bus system were evaluated for different system loads. The results obtained are shown in Table C.3. The solutions in Table C.3, were fed back into the load flow program and the solution obtained for all loads considered, to validate the economic dispatch solutions. The load flow results are shown in brackets in Table C.3.

The load flow solutions based on the economic dispatch results gave acceptable voltage profiles that were within the voltage limits of the system feasible operating region. Samples of these voltage profiles are shown in Table C.4 for light and heavy loads of the system.

C.1.3 Discussion of the 5 Bus System Results - Active Model

As shown in Table C.1, the parameter estimates were stable at k = 0.0 . At this value of ridge k, a correct inverse of the matrix

P_D (MW)	λ_P ($/MWh)	P_{G1} (MW)	P_{G4} (MW)	P_L (MW)	F_0 ($/h)
16.50	8.73	8.172 (8.160)	8.443 (8.443)	0.115 (0.104)	491.59
33.00	8.81	15.127 (15.125)	18.069 (18.069)	0.197 (0.192)	636.31
49.50	8.88	22.092 (22.096)	27.751 (27.751)	0.344 (0.345)	782.26
66.00	8.96	29.068 (29.099)	37.489 (37.489)	0.556 (0.567)	929.44
82.50	9.03	36.053 (36.059)	47.282 (47.282)	0.835 (0.840)	1077.87
99.00	9.11	43.048 (43.052)	57.132 (57.132)	1.181 (1.181)	1227.56
115.50	9.19	50.053 (50.056)	67.041 (67.041)	1.594 (1.593)	1378.52
132.00	9.27	57.069 (57.073)	77.007 (77.007)	2.076 (2.077)	1530.79
148.50	9.35	64.094 (64.104)	87.033 (87.033)	2.627 (2.634)	1684.36
165.00	9.43	71.129 (71.151)	97.119 (97.119)	3.248 (3.266)	1839.26

Table C.3 The Economic Active Dispatch of the 5 Bus

Test System

Bus No	Load=16.5 + j1.0MVA		Load = 165.0 + j10.0 MVA	
	Voltage p.u.	Angle Degrees	Voltage p.u.	Angle Degrees
1	1.0600	0.0	1.0600	0.0
2	1.0570	-0.3945	1.0241	-3.7451
3	1.0568	-0.4175	1.0234	-3.9897
4	1.0506	0.0039	1.0470	-1.1193
5	1.0538	-0.4324	1.0175	-4.5794

Table C.4 The Voltage Profiles of the 5 Bus System

Based on the Economic Dispatch Solutions

$\underline{A}^T\underline{A}$ was obtained. Comparing the results shown in Table C.3, it is observed that the load flow solutions agree very closely with the economic dispatch solutions for all system loads considered which indicate the accuracy of the estimated network loss model parameters. The load flow solutions based on the economic dispatch results, gave voltage levels that all fell within the feasible operating region of the system as indicated by the example cases of light and heavy loads shown in Table C.4.

C.1.4 The IEEE 30 Bus Test System - Active Power Loss Model

The single line diagram of the IEEE 30 bus test system is shown in Figure C.2. The network has three generation buses, 1, 2 and 13, and three purely reactive sources at buses 5, 8 and 11. From equation 2.3, the number of parameters to be evaluated for the active power loss model of this system is 9. 10 load flow solutions of the system were performed to provide the necessary data for the parameter estimation procedure. Applying the ridge estimator, the parameters of the active power loss model were evaluated. The results obtained are presented in Table C.5.

C.1.5 The IEEE 30 Bus Test System - Economic Active Dispatch

The capacity of the coal fired generating units which were used to obtain the economic active dispatch schedules of this system are given in Table C.6. Based on the active power loss model with parameters shown in Table C.5 for k = 0.003, the economic dispatch solutions of the power system were obtained for different load levels as shown in Table C.7. The dispatch solutions in Table C.7, were fed back into the
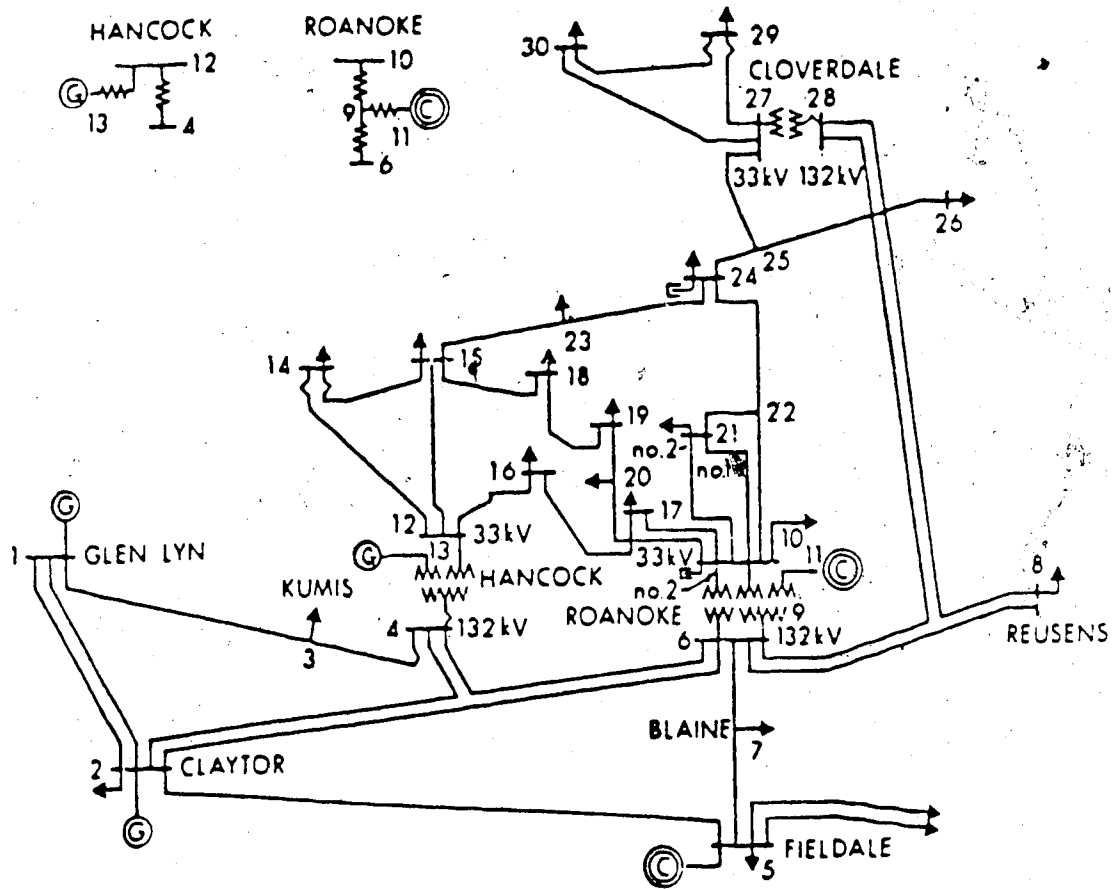
Figure C.2 The IEEE 30 Bus Test System

Parameter	Ridge k = 0.0		Ridge k = 0.003	
	Estimated Value	Condition Index	Estimated Value	Condition Index
K_{LO}	-0.003247	1	0.000245	1
B_{01}	0.013804	3	0.004815	3
B_{02}	0.042220	5	-0.006300	5
B_{03}	-0.031464	26	0.004096	23
B_{11}	0.014574	28	0.014178	25
B_{12}	-0.030566	33	0.010089	28
B_{13}	0.029642	87	0.012560	45
B_{22}	0.168133	40	0.013673	32
B_{23}	-0.144970	68	0.004313	42
B_{33}	0.152370	23	0.019669	21
Condition Number	87		45	
Mean Square Error	25.6225		12.4846	

Table C.5 The Active Power Loss Model Parameters of
the IEEE 30 Bus Test System in p.u. on
100 MVA Base

Generator No.	Generator Size (MW)	Source Constraints		Bus No.
		MW	MVAR	
1	200	$0 \leq P_{G1} \leq 200$	$-50 \leq Q_{G1} \leq 50$	1
2	200	$5 \leq P_{G2} \leq 200$	$-40 \leq Q_{G2} \leq 50$	2
3	200	$5 \leq P_{G13} \leq 200$	$-6 \leq Q_{G13} \leq 24$	13

Table C.6 The IEEE 30 Bus Test System Generator

Capacities - Coal

load flow program and the solution obtained for all loads considered. The load flow solutions obtained are shown in brackets in Table C.7 for comparison. Sample of the load flow voltage profiles (corresponding to the economic dispatch solutions) are shown in Table C.8 for light and heavy loads of the system.

C.1.6 Discussion of the IEEE 30 Bus Results - Active Model

From Table C.5, the parameter estimates for this system stabilized for a value of ridge k of 0.003 which resulted in a correct inverse of $\underline{A}^T \underline{A}$. As observed from Table C.7, the dispatch solutions agree very closely with the load flow results obtained for all loads considered which indicate the accuracy of the estimated parameters and the validity of the dispatch method. The errors between the two solutions in the

P_D (MW)	λ_P ($/MWh)	P_{G1} (MW)	P_{G2} (MW)	P_{G13} (MW)	P_L (MW)	F_0 ($/h)
28.34	8.77	1.162 (1.313)	21.421 (21.421)	5.762 (5.762)	0.005 (0.148)	767.72
56.68	8.87	9.538 (9.661)	32.657 (32.657)	14.752 (14.752)	0.266 (0.385)	1017.72
85.02	8.97	17.942 (18.056)	43.994 (43.994)	23.794 (23.794)	0.710 (0.820)	1270.60
113.36	9.08	26.375 (26.467)	55.435 (55.435)	32.890 (32.890)	1.339 (1.429)	1526.42
141.70	9.19	34.836 (34.941)	66.981 (66.981)	42.040 (42.040)	2.157 (2.260)	1785.25
170.04	9.29	43.326 (43.397)	78.636 (78.636)	51.247 (51.247)	3.169 (3.238)	2047.13
198.38	9.41	51.845 (51.935)	90.402 (90.402)	60.510 (60.510)	4.377 (4.468)	2312.13
226.72	9.52	60.393 (60.354	102.281 (102.281)	69.832 (69.832)	5.785 (5.746)	2580.32
255.06	9.64	68.969 (68.842	114.276 (114.276)	79.213 (79.213)	7.399 (7.273)	2851.76
283.40	9.75	77.574 (77.372)	126.391 (126.391)	88.656 (88.656)	9.221 (9.024)	3126.51

Table C.7 The Economic Active Dispatch of the IEEE

30 Bus Test System

Bus No.	Load=28.34 + j12.62 MVA		Load=283.4 + j126.2 MVA	
	Voltage p.u.	Angle Degrees	Voltage p.u.	Angle Degrees
1	1.0200	0.0	1.0600	0.0
2	1.0200	0.0638	1.0450	-1.1427
3	1.0232	-0.3796	1.0296	-3.1103
4	1.0228	-0.4398	1.0223	-3.6937
5	1.0200	-0.8284	1.0100	-9.0607
6	1.0250	-0.6083	1.0154	-5.1622
7	1.0230	-0.7704	1.0054	-7.2850
8	1.0214	-0.6190	1.0100	-5.7970
9	1.0660	-0.8056	1.0498	-6.3928
10	1.0819	-0.9067	1.0390	-7.0431
11	1.0541	-0.8056	1.0820	-6.3928
12	1.0826	-0.5498	1.0645	-2.2047
13	1.0748	-0.1526	1.0710	4.0451
14	1.0816	-0.6783	1.0491	-3.6097
15	1.0812	-0.7386	1.0402	-4.2104
16	1.0815	-0.7270	1.0446	-4.4851
17	1.0812	-0.8719	1.0348	-6.4751
18	1.0803	-0.8613	1.0270	-5.8947
19	1.0800	-0.9165	1.0226	-6.7138
20	1.0804	-0.9195	1.0258	-6.8560
21	1.0812	-0.9621	1.0269	-7.4022
22	1.0814	-0.9657	1.0276	-7.3594
23	1.0813	-0.8964	1.0268	-5.6928
24	1.0822	-1.0748	1.0183	-7.3589
25	1.0729	-0.9503	1.0127	-8.1391
26	1.0713	-0.9875	0.9949	-8.5627
27	1.0679	-0.8596	1.0183	-8.3631
28	1.0263	-0.6719	1.0106	-5.6094
29	1.0661	-0.9708	0.9984	-9.6054
30	1.0651	-1.0481	0.9868	-10.4972

Table C.8 The Voltage Profiles of the IEEE 30 Bus Test

System Based on the Economic Dispatch Solution

active power generations at the slack bus (bus number 1) are picked up by the total active power losses. These errors are small for all loads considered. For example at 100% load level, the error in the active power generation is 0.202 MW which if added to the total system losses, the two solutions will agree very closely with each other.

C.2 The Active-Reactive Loss Submodels/Purely Reactive Submodels and the Economic Dispatch Schedules of Model Power Systems

In this section, the active-reactive power loss submodels, the purely reactive submodels and the economic active-reactive dispatch results are presented for the 5 and 30 bus test systems.

C.2.1 The 5 Bus Test System - Active-Reactive and Purely Reactive Submodels

The single line diagram of this system is given in Figure C.1. The network contains two active-reactive generation buses at buses 1 and 4 and has no purely reactive sources. According to equation 2.25, the number of parameters to be evaluated for both the active and reactive submodels is 9. This requires a minimum of ten load flow results which were carried out for different system load levels. Using the data base obtained, the parameters of the active and reactive loss submodels were evaluated by the ridge estimator. The parameter estimates obtained are shown in Table C.9 for the active and reactive parts.

C.2.2 The 5 Bus Test System - Economic Active-Reactive Dispatch

Based on the evaluated active-reactive loss model of this system and using the generating units given in Table C.2, the economic active-reactive dispatch solutions of the system were evaluated for different system load levels. The results obtained are shown in Tables C.10 and

	Active Part k = 0.0		Reactive Part k = 0.0		
Parameter	Estimated Value	Parameter	Estimated Value	Condition Index	
K_{LOP}	0.312527	K_{LOQ}	0.600941	1	
E_{PP1}	-0.072205	E_{QP1}	-0.202811	3	
E_{PP2}	0.061686	E_{QP2}	-0.178671	3	
E_{PQ1}	0.934509	E_{QQ1}	2.793037	41	
E_{PQ2}	0.954526	E_{QQ2}	2.831435	41	
A_{P11}	-0.035429	A_{Q11}	-0.104821	35	
A_{P12}	-0.015374	A_{Q12}	-0.045213	32	
A_{P22}	-0.021236	A_{Q22}	-0.062532	33	
B_{P12}	0.003705	B_{Q12}	0.010975	19	
Condition Number	41	Condition Number	41		
Mean Square Error	0.0002	Mean Square Error	0.0001		

Table C.9 The Active-Reactive Power Loss Model Parameters

of the 5 Bus Test System in p.u. on 100 MVA Base

P_D (MW)	λ_P ($/MWh)	P_{G1} (MW)	P_{G4} (MW)	P_L (MW)	F_o ($/h)
16.5	9.02	6.736 (6.714)	9.841 (9.841)	0.077 (0.058)	491.27
33.0	9.10	13.982 (13.958)	19.187 (19.187)	0.169 (0.142)	636.09
49.5	9.17	21.233 (21.205)	28.591 (28.591)	0.324 (0.294)	782.11
66.0	9.25	28.489 (28.461)	38.054 (38.054)	0.543 (0.513)	929.35
82.5	9.33	35.249 (35.726)	47.578 (47.578)	0.827 (0.803)	1077.81
99.0	9.41	43.014 (43.004)	57.163 (57.163)	1.177 (1.164)	1227.53
115.5	9.49	50.282 (50.263)	66.812 (66.812)	1.594 (1.599)	1378.51
132.0	9.59	57.553 (57.586)	76.526 (76.526)	2.079 (2.111)	1530.77
148.5	9.65	64.826 (64.895	86.307 (86.307)	2.634 (2.700)	1684.35
165.0	9.74	72.101 (72.215)	96.158 (96.158)	3.259 (3.371)	1839.25

Table C.10 The Economic Active-Reactive Dispatch of the 5

Bus Test System (Active)

Q_D (MVAR)	λ_q ($/MVARh)	Q_{G1} (MVAR)	Q_{G4} (MVAR)	Q_L (MVAR)
1.0	-4.67	-4.139 (-4.208)	-27.208 (-27.208)	-32.347 (-32.406)
2.0	-4.71	-1.490 (-1.573)	-28.403 (-28.403)	-31.892 (-31.973)
3.0	-4.75	1.208 (1.109)	-29.455 (-29.455)	-31.247 (-31.341)
4.0	-4.80	3.955 (3.859)	-30.364 (-30.364)	-30.409 (-30.501)
5.0	-4.84	6.752 (6.669)	-31.127 (-31.127)	-29.375 (-29.451)
6.0	-4.88	9.599 (9.558)	-31.741 (-31.740)	-28.142 (-28.182)
7.0	-4.93	12.498 (12.511)	-32.204 (-32.200)	-26.064 (-26.693)
8.0	-4.97	15.450 (15.545)	-32.514 (-32.514)	-25.064 (-24.968)
9.0	-5.02	18.455 (18.648)	-32.668 (+32.668)	-23.213 (-23.009)
10.0	-5.07	21.514 (21.856)	-32.663 (-32.663)	-21.149 (-20.805)

Table C.11 The Economic Active-Reactive Dispatch of

the 5 Bus Test System (Reactive)

C.11 for the active and reactive parts respectively. The load flow

solutions based on the economic dispatch solutions are shown in brackets

in Tables C.10 and C.11. These load flow solutions were carried out to

verify the accuracy of the active-reactive submodels and the economic

dispatch solutions. The load flow voltage profiles obtained for light

and heavy loads of the 5 bus system are shown in Table C.12.

C.2.3 Discussion of the 5 Bus Results - Active-Reactive Model

As seen from Table C.9, the parameters were stable for k = 0.0.

Any other value of k resulted in very high mean square errors. The

economic active-reactive dispatch solutions obtained agree very closely

with the load flow solutions shown in Tables C.10 and C.11 which

indicates the accuracy of the loss model parameters. The load flow

solutions gave acceptable voltage profiles which fell within the volt-

age limits of the feasible operating region of the system. Comparing

the total fuel costs obtained in Table C.10 to the total costs obtained

using the active power loss model shows that lower fuel costs can be

obtained by using the active-reactive loss model. The voltage levels

in the case of the active-reactive model are slightly higher than those

of Table C.4 which resulted in lower fuel costs in general.

C.2.4 The IEEE 30 Bus Test System - Active-Reactive and Purely Reactive

Submodels

The single line diagram of this system is shown in Figure C.2.

The network has three active-reactive generation buses, 1, 2 and 13,

and three purely reactive generation buses, 5, 8 and 11. The power

system also has two shunt capacitors at buses 10 and 24. The number of

parameters to be evaluated for both the active and reactive power loss

	Load = 16.5 + j1.0 MVA		Load = 165. + j10 MVA	
Bus No.	Voltage p.u.	Angle Degrees	Voltage p.u.	Angle Degrees
1	1.0600	0.0	1.0600	0.0
2	1.0619	-0.4498	1.0197	-3.7161
3	1.0621	-0.4760	1.0187	-3.9599
4	1.0571	-0.0730	1.0413	-1.0491
5	1.0599	-0.5004	1.0120	-4.5494

Table C.12 The Voltage Profiles of the 5 Bus Test

System Based on the Economic Active-Reactive

Dispatch Solutions

submodels is 16 (on the basis of equation 2.25). A minimum of 17 load

flow solutions were carried out for different system load and voltage

levels. Based on these results, the parameters of the active and

reactive power loss submodels were evaluated by the ridge estimator.

The parameter estimates obtained are presented in Table C.13 for the

active and the reactive parts.

The purely reactive submodels of this system were evaluated by

plotting the reactive powers at buses 5, 8 and 11 and the shunt

reactive powers at buses 10 and 24 as functions of the total reactive

load demand of the system using the base load flow data obtained above.

The graph obtained is shown in Figure C.3. From this graph it is seen

that the purely reactive powers, Q_{GV5}, Q_{GV8}, Q_{GV11}, Q_{Sh10} and Q_{Sh24} can

be modeled as linear functions of the network total reactive load

	Active Part		Reactive Part	
Parameter	k = 0.0	Parameter	k = 0.0	Condition Index
K_{LOP}	-0.003013	K_{LOQ}	-0.340099	1
E_{PP1}	-0.002748	E_{QP1}	0.037692	2
E_{PP2}	0.000618	E_{QP2}	0.066143	2
E_{PP3}	-0.000284	E_{QP3}	-0.085877	17
E_{PQ1}	-0.002735	E_{QQ1}	0.006646	11
E_{PQ2}	-0.005746	E_{QQ2}	-0.044228	20
E_{PQ3}	-0.018013	E_{QQ3}	0.143928	14
A_{P11}	0.021143	A_{Q11}	0.045753	22
A_{P12}	0.013560	A_{Q12}	0.008094	11
A_{P13}	-0.002796	A_{Q13}	0.032388	19
A_{P22}	0.041411	A_{Q22}	0.242443	9
A_{P23}	-0.032094	A_{Q23}	-0.234596	13
A_{P33}	0.072948	A_{Q33}	0.504533	11
B_{P12}	0.002011	B_{Q12}	0.019930	11
B_{P13}	-0.001519	B_{Q13}	-0.051330	9
B_{P23}	0.008637	B_{Q23}	0.023718	18
Condition Number	22	Condition Number	22	
Mean Square Error	0.0010	Mean Square Error	15.0459	

Table C.13 The Active-Reactive Power Loss Model Parameters

of the IEEE 30 Bus Test System in p.u. on 100 MVA Base

demand Q_D. In the modeling process, the reactive power limit constraints
at buses 5, 8 and 11 were taken into consideration. These constraints
are given below:

$$- 40 \leq Q_{GV5} \leq 40 \text{ MVARS} \tag{C.1}$$

$$- 10 \leq Q_{GV8} \leq 40 \text{ MVARS} \tag{C.2}$$

$$- 6 \leq Q_{GV11} \leq 24 \text{ MVARS} \tag{C.3}$$

The parameter estimates of Q_{GV5}, Q_{GV8} and Q_{GV11} which were computed from
the graph of Figure C.3, are given in Tables C.14, C.15 and C.16
respectively. Similarly, the purely reactive power models at buses 10
and 24 were evaluated from the graph of Figure C.3. The parameter
estimates obtained for these models are presented in Table C.17. In
Tables C.14 to C.17, the reactive powers and the total reactive load
demand are in MVARS.

Parameter	$0 \leq Q_D \leq 92$	$92 \leq Q_D \leq 95.5$	$95.5 \leq Q_D \leq 101$	$101 \leq Q_D \leq 126.20$
A_0	-8.000	40.000	401.181	-41.000
A_1	0.520	0.000	-3.782	0.600

Table C.14 The Parameters of Q_{GV5} of the IEEE 30

Bus Test System. Q_D is in MVARS
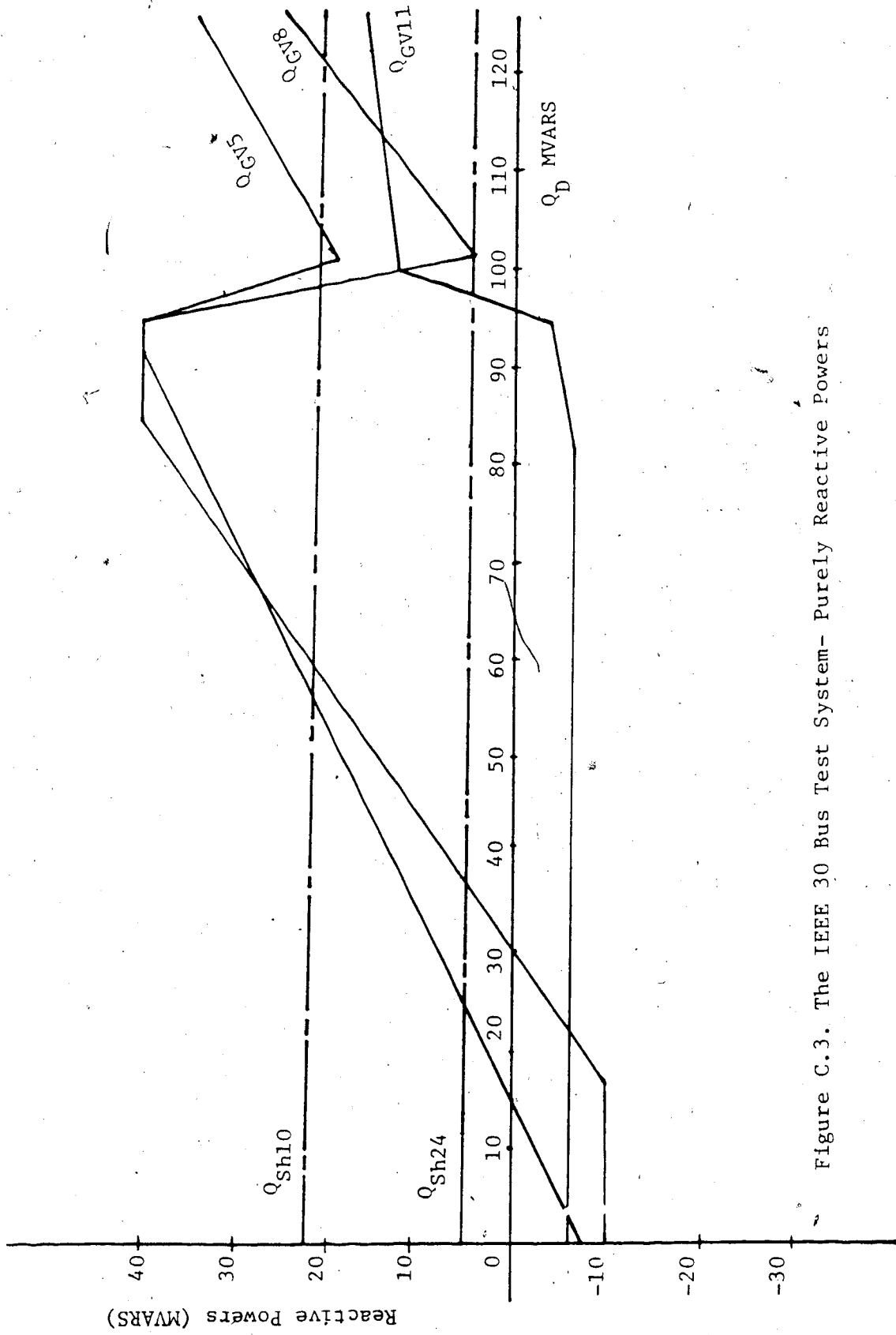
Figure C.3. The IEEE 30 Bus Test System- Purely Reactive Powers

Parameter	$0 \leq Q_D \leq 17$	$17 \leq Q_D < 84.9$	$84.9 \leq Q_D < 94.5$	$94.5 < Q_D < 101$	$101 \leq Q_D < 126.20$
A_0	-10.000	-22.000	40.000	528.830	-76.000
A_1	0.000	0.833	0.000	-5.167	0.800

Table C.15 The Parameters of Q_{GV8} of the IEEE 30

Bus Test System. Q_D is in MVARS

Parameter	$0 \leq Q_D < 82$	$82 \leq Q_D < 95$	$95 \leq Q_D \leq 101$	$101 \leq Q_D \leq 126.2$
A_0	-6.000	-21.769	-264.750	3.001
A_1	0.000	0.192	2.750	0.099

Table C.16 The Parameters of Q_{GV11} of the IEEE 30

Bus Test System. Q_D is in MVARS

Parameter	Q_{Sh10}	Q_{Sh24}
A_0	22.500	5.000
A_1	-0.0212	-0.004

Table C.17 The Parameters of Q_{Sh10} and Q_{Sh24} of the

IEEE 30 Bus Test System

C.2.5 The IEEE 30 Bus Test System - Economic Active-Reactive Dispatch

The economic active-reactive dispatch solutions obtained for the IEEE 30 bus test system are presented in Tables C.18 and C.19 for the active and reactive parts respectively. These solutions were based on the evaluated active-reactive and the purely reactive submodels of the system with the generator capacities given in Table C.6. The load flow solutions based on the economic dispatch solutions are shown in brackets in Tables C.18 and C.19. The load flow solutions were carried out to validate the accuracy of the estimated parameters and of the economic solution. The load flow voltage profile obtained for light and heavy loads are presented in Table C.20.

C.2.6 Discussion of the IEEE 30 Bus Results - Active-Reactive Model

The active-reactive parameter estimates were obtained for ridge $k = 0.0$ as shown in Table C.13. Any other value of k gave higher mean square error as compared to the values indicated in the Table. The reactive parameters resulted in a higher mean square error than the active parameters. This is expected since the load flow total reactive power losses usually are more scattered than the active power losses. The dispatch solutions and the load flow solutions shown in Tables C.18 and C.19 agree very closely with one another for all system loads which indicate the accuracy of the evaluated parameters. The difference between the two solutions in the active and reactive powers at the slack bus (bus number 1) are small and are picked up by the total system active and reactive power losses. The voltage profiles obtained for all system loads were within the bus voltage levels of the feasible operating region of the system.

P_D (MW)	λ_P ($/MWh)	P_{G1} (MW)	P_{G2} (MW)	P_{G13} (MW)	P_L (MW)	F_0 ($/h)
28.34	8.77	5.626 (5.850)	13.220 (13.220)	9.552 (9.552)	0.059 (0.275)	767.73
56.68	8.86	13.989 (14.174)	24.075 (24.075)	18.962 (18.962)	0.346 (0.535)	1017.86
85.02	8.96	22.378 (22.565)	34.998 (34.998)	28.464 (28.464)	0.819 (1.000)	1270.89
113.36	9.05	30.796 (31.024)	46.016 (46.016)	38.005 (38.005)	1.457 (1.669)	1526.67
141.70	9.15	39.247 (39.547)	57.134 (57.134)	47.580 (47.580)	2.262 (2.552)	1785.23
170.04	9.25	47.744 (48.174)	68.377 (68.377)	57.136 (57.136)	3.217 (3.638)	2046.47
198.38	9.36	56.371 (57.018)	79.909 (79.909)	66.313 (66.313)	4.212 (4.853)	2309.41
226.72	9.49	66.040 (66.953)	91.844 (91.844)	73.966 (73.966)	5.130 (6.038)	2572.98
255.06	9.61	74.970 (75.923)	103.228 (103.228)	83.549 (83.549)	6.687 (7.594)	2843.67
283.40	9.73	83.882 (84.743)	114.740 (114.740)	93.223 (93.223)	8.444 (9.296	3117.57

Table C.18 The Economic Active-Reactive Dispatch of the

IEEE 30 Bus Test System (Active)

Q_D (MVAR)	λ_q ($/MVARh)	Q_{G1} (MVAR)	Q_{G2} (MVAR)	Q_{G13} (MVAR)	Q_{GV5} (MVAR)	Q_{GV8} (MVAR)	Q_{GV11} (MVAR)	Q_L (MVAR)
12.62	-0.14	-30.570 (-30.578)	-2.695 (-2.695)	3.535 (3.530)	-1.444 (-1.440)	-10.000 (-10.000)	-6.000 (-6.000)	-32.339 (-32.333)
25.24	-0.14	-30.541 (-31.053)	-4.283 (-4.283)	4.022 (4.020)	5.112 (5.110)	-0.967 (-0.967)	-6.000 (-6.000)	-30.686 (-31.314)
37.86	-0.15	-30.663 (-31.362)	-6.233 (-6.230)	4.270 (4.270)	11.668 (11.660)	9.550 (9.550)	-6.000 (-6.000)	-28.304 (-29.310)
50.48	-0.15	-30.639 (-31.393)	-7.829 (-7.829)	4.785 (4.785)	18.223 (18.220)	20.067 (20.060)	-6.000 (-6.000)	-25.153 (-26.385)
63.10	-0.15	-30.463 (-30.595)	-9.064 (-9.064)	5.565 (5.560)	24.780 (24.780)	30.583 (30.580)	-6.000 (-6.000)	-21.223 (-22.295)
75.72	-0.15	-29.903 (-29.773)	-9.406 (-9.406)	6.969 (6.960)	21.335 (1.335)	40.000 (40.000)	-6.000 (-6.000)	-16.495 (-17.375)
88.34	-0.13	-27.330 (-26.853)	-5.253 (-5.250)	11.421 (11.420)	37.891 (37.891)	40.000 (40.000)	-5.225 (-5.220)	-10.851 (-11.694)
100.96	-0.01	-7.323 (-8.096)	15.045 (15.040)	24.000 (24.000)	19.478 (19.478)	7.203 (7.203)	12.734 (12.730)	-4.082 (-5.852)
113.58	0.01	-3.824 (-4.568)	14.139 (14.138)	24.000 (24.000)	27.038 (27.030)	14.864 (14.862)	14.325 (14.320)	2.459 (0.769)
126.20	0.02	-1.509 (-2.787)	12.825 (12.825)	24.000 (24.000)	34.498 (34.591)	24.960 (24.960)	15.917 (15.920)	9.842 (8.037)

Table C.19 The Economic Active-Reactive Dispatch of the IEEE 30 Bus Test System (Reactive)

Bus No.	Load=28.34+j12.62MVA		Load=283.4+j126.2MVA	
	Voltage p.u.	Angle Degrees	Voltage p.u.	Angle Degrees
1	1.0050	0.0	1.0350	0.0
2	1.0146	-0.2709	1.0268	-1.5582
3	1.0188	-0.5550	1.0153	-3.4406
4	1.0206	-0.6625	1.0102	-4.0979
5	1.0163	-1.1115	0.9957	-9.6826
6	1.0232	-0.8426	1.0037	-5.6124
7	1.0204	-1.0263	0.9926	-7.8181
8	1.0197	-0.8516	0.9991	-6.2716
9	1.0678	-0.9303	1.0415	-6.7144
10	1.0854	-0.9750	1.0333	-7.2931
11	1.0559	-0.9303	1.0724	-6.7144
12	1.0948	-0.5704	1.0713	-2.4033
13	1.0992	0.0663	1.0953	3.9827
14	1.0927	-0.7136	1.0543	-3.8182
15	1.0911	-0.7671	1.0436	-4.4043
16	1.0900	-0.7610	1.0461	-4.6826
17	1.0863	-0.9273	1.0312	+6.7036
18	1.0880	-0.9016	1.0272	-6.1014
19	1.0864	-0.9639	1.0210	-6.9325
20	1.0860	-0.9709	1.0231	-7.0808
21	1.0849	-1.0305	1.0215	-7.6569
22	1.0852	-1.0342	1.0222	-7.6140
23	1.0889	-0.9439	1.0269	-5.9111
24	1.0868	-1.1498	1.0141	-7.6255
25	1.0750	-1.0553	1.0053	-8.4678
26	1.0733	-1.0923	0.9874	-8.8977
27	1.0684	-0.9864	1.0090	-8.7329
28	1.0248	-0.8974	0.9994	-6.0600
29	1.0666	-1.0974	0.9889	-9.9987
30	1.0655	-1.1747	0.9772	-10.9079

Table 5.20 The Voltage Profiles of the IEEE 30

Bus Test System Based on the Economic

Active-Reactive Dispatch Solutions

APPENDIX D

DIAKOPTICAL ACTIVE AND REACTIVE POWER LOSS MODELS

OF A NETWORK TORN INTO THREE SUBNETWORKS

AND TWO INTERCONNECTIONS

In this Appendix, the active and reactive power losses of a

network torn into three subnetworks and two interconnections are

expressed as functions of bus voltages and line admittances. Consider

the network shown in Figure D.1. The lines connecting the various
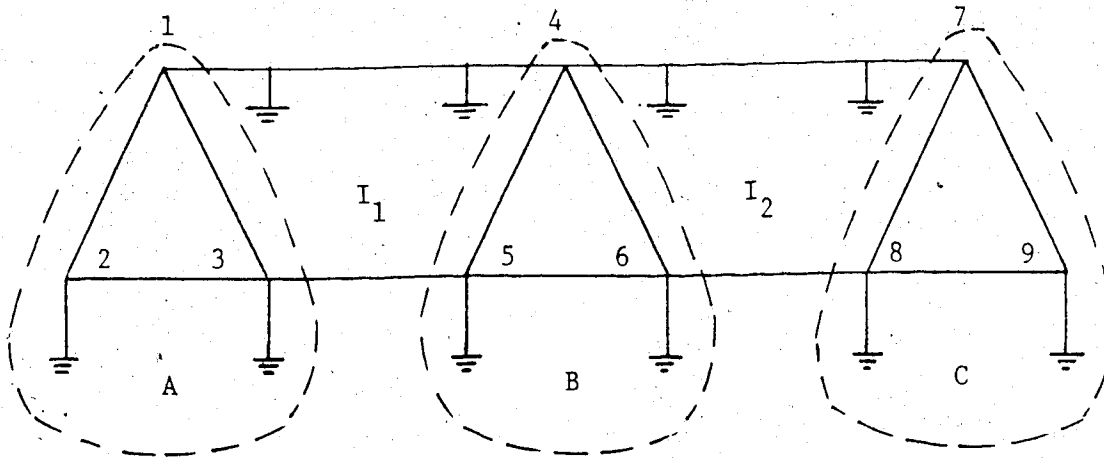
Figure D.1 A Nine Node Network Torn into Three

Subnetworks and Two Interconnections

buses are assumed to have finite impedances. The netowrk is torn as

shown by the dotted line into subnetworks A, B and C, interconnected

by the interconnections I_1 and I_2. The subnetworks and interconnections may be separated as shown in Figure D.2 to show the various nodal currents of the assembly. The nodal matrix equation of the torn network is given by:

$$\underline{Y}\,\underline{V} = \underline{I} + \underline{I}' \tag{D.1}$$

Equation D.1 in terms of the subnetwork quantities may be written as:

$$
\begin{bmatrix}
\underline{Y}_A & \underline{0} & \underline{0} \\
\underline{0} & \underline{Y}_B & \underline{0} \\
\underline{0} & \underline{0} & \underline{Y}_C
\end{bmatrix}
\begin{bmatrix}
\underline{V}_A \\
\underline{V}_B \\
\underline{V}_C
\end{bmatrix}
=
\begin{bmatrix}
\underline{I}_A \\
\underline{I}_B \\
\underline{I}_C
\end{bmatrix}
+
\begin{bmatrix}
\underline{I}_A' \\
\underline{I}_B' \\
\underline{I}_C'
\end{bmatrix}
\tag{D.2}
$$

where,

A, B, C - represent the subnetworks A, B and C respectively.

If,

$\underline{I}_{I1}$ - nodal current vector of interconnections I_1.

$\underline{I}_{I2}$ - nodal current vector of interconnections I_2.

$\underline{V}_{I1}$ - nodal voltage vector of interconnections I_1.

$\underline{V}_{I2}$ - nodal voltage vector of interconnections I_2.

Using matrix topology, the current vector $\underline{I}'$ is given by:
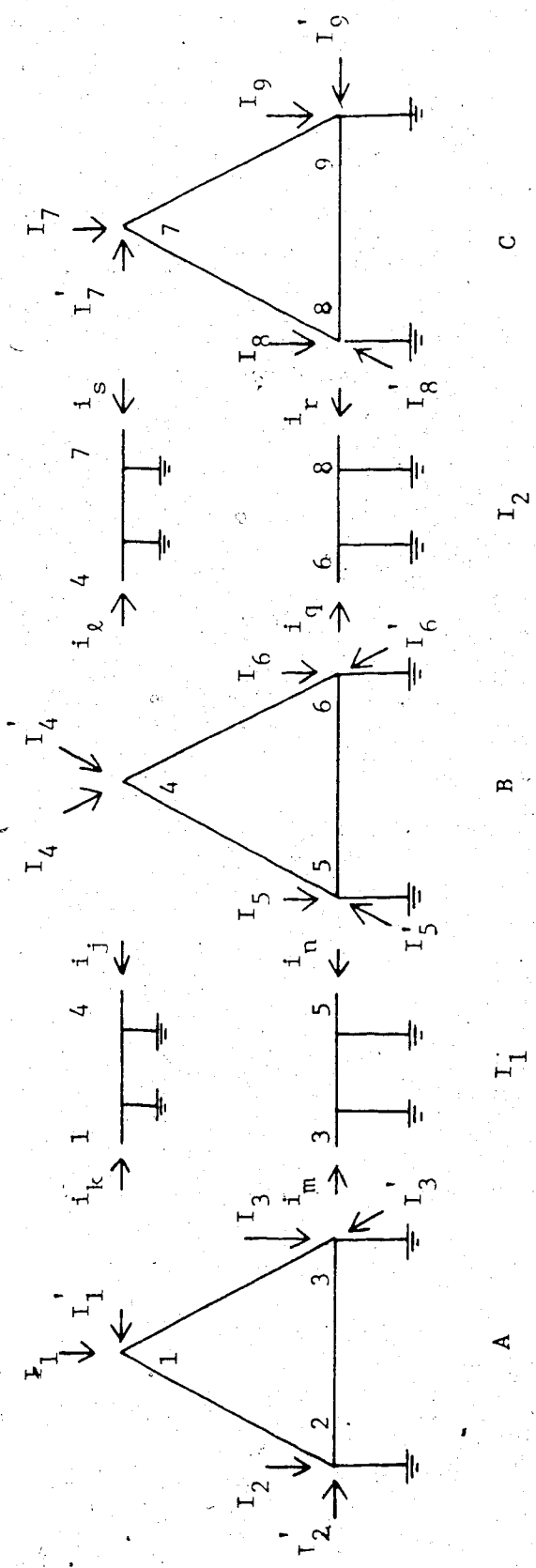
Figure D.2 A Nine Node Network Torn into Three Subnetworks A, B and C and

Two Interconnections I_1 and I_2

$$\underline{I}' = \begin{bmatrix} \underline{I}'_A \\ \\ I'_B \\ \\ I'_C \end{bmatrix} = \underline{C} \ \underline{I}_I \tag{D.3}$$

where,

$$\underline{I}_I = \begin{bmatrix} \underline{I}_{I_1} \\ ---- \\ \underline{I}_{I2} \end{bmatrix} = \begin{bmatrix} i_k \\ i_j \\ i_m \\ i_n \\ --- \\ i_\ell \\ i_s \\ i_q \\ i_r \end{bmatrix} \tag{D.4}$$

and the ~~ion~~ matrix $\underline{C}$ is given by:

	i_k	i_j	i_m	i_n	i_ℓ	i_s	i_q	i_r	
1	-1	0	0	0	0	0	0	0	$\underline{C}_A$
2	0	0	0	0	0	0	0	0	
3	0	0	0	0	0	0	0	0	
4	0	-1	0	0	-1	0	0	0	
5	0	0	0	-1	0	0	0	0	$\underline{C}_B$
6	0	0	0	0	0	0	-1	0	
7	0	0	0	0	0	-1	0	0	
8	0	0	0	0	0	0	0	0	$\underline{C}_C$
9	0	0	0	0	0	0	0	-1	

$$\underline{C} = \quad \underbrace{\qquad}_{\underline{Y}_{I1}} \quad \underbrace{\qquad}_{\underline{Y}_{I2}} \tag{D.5}$$

The vector $\underline{I}'$ is then given by:

$$\underline{I}' = \begin{bmatrix} \underline{I}'_A \\ \underline{I}'_B \\ \underline{I}'_C \end{bmatrix} = \begin{bmatrix} \underline{C}_A \\ \underline{C}_B \\ \underline{C}_C \end{bmatrix} \begin{bmatrix} \underline{I}_{I1} \\ \underline{I}_{I2} \end{bmatrix} \tag{D.6}$$

and

$$\underline{V}_I = \begin{bmatrix} \underline{V}_{I1} \\ \underline{V}_{I2} \end{bmatrix} = - [\underline{C}_A^T \ \underline{C}_B^T \ \underline{C}_C^T] \begin{bmatrix} \underline{V}_A \\ \underline{V}_B \\ \underline{V}_C \end{bmatrix} \tag{D.7}$$

The nodal matrix equation of interconnections may be written as:

$$\underline{I}_I = \begin{bmatrix} \underline{I}_{I1} \\ \underline{I}_{I2} \end{bmatrix} = - \begin{bmatrix} \underline{Y}_{I1} & \underline{0} \\ \underline{0} & \underline{Y}_{I2} \end{bmatrix} [\underline{C}_A^T \ \underline{C}_B^T \ \underline{C}_C^T] \begin{bmatrix} \underline{V}_A \\ \underline{V}_B \\ \underline{V}_C \end{bmatrix} \tag{D.8}$$

but:

$$\underline{I}' = - \underline{C} \ \underline{Y}_I \ \underline{C}^T \ \underline{V}, \tag{D.9}$$

then,

$$\begin{bmatrix} \underline{I}'_A \\ \underline{I}'_B \\ \underline{I}'_C \end{bmatrix} = - \begin{bmatrix} \underline{C}_A \\ \underline{C}_B \\ \underline{C}_C \end{bmatrix} \begin{bmatrix} \underline{Y}_{I1} & \underline{0} \\ \underline{0} & \underline{Y}_{I2} \end{bmatrix} [\underline{C}_A^T \ \underline{C}_B^T \ \underline{C}_C^T] \begin{bmatrix} \underline{V}_A \\ \underline{V}_B \\ \underline{V}_C \end{bmatrix} \tag{D.10}$$

Substituting equation D.10 into equation D.2, results in the diakoptical matrix equation given by:

$$\left[\begin{bmatrix} \underline{Y}_A & \underline{0} & \underline{0} \\ \underline{0} & \underline{Y}_B & \underline{0} \\ \underline{0} & \underline{0} & \underline{Y}_C \end{bmatrix} + \begin{bmatrix} \underline{C}_A \\ \underline{C}_B \\ \underline{C}_C \end{bmatrix} \begin{bmatrix} \underline{Y}_{I1} & \underline{0} \\ & \\ \underline{0} & \underline{Y}_{I2} \end{bmatrix} [\underline{C}_A^T \ \underline{C}_B^T \ \underline{C}_C^T] \right] \begin{bmatrix} \underline{V}_A \\ \underline{V}_B \\ \underline{V}_C \end{bmatrix} = \begin{bmatrix} \underline{I}_A \\ \underline{I}_B \\ \underline{I}_C \end{bmatrix}$$

$$(D.11)$$

The active and reactive power losses for the network shown in Figure D.2 can be obtained by further partitioning the matrices $\underline{C}_A$, $\underline{C}_B$ and $\underline{C}_C$ into the following equation to correspond with interconnections I_1 and I_2:

$$\begin{bmatrix} \underline{C}_A \\ \underline{C}_B \\ \underline{C}_C \end{bmatrix} = \begin{bmatrix} \underline{C}_{A1} & \underline{C}_{A2} \\ \underline{C}_{B1} & \underline{C}_{B2} \\ \underline{C}_{C1} & \underline{C}_{C2} \end{bmatrix}$$

$$(D.12)$$

For the example system under consideration, there is no branches between A and C, hence equation D.12 reduces to:

$$\begin{bmatrix} \underline{C}_A \\ \underline{C}_B \\ \underline{C}_C \end{bmatrix} = \begin{bmatrix} \underline{C}_{A1} & \underline{0} \\ \underline{C}_{B1} & \underline{C}_{B2} \\ \underline{0} & \underline{C}_{C2} \end{bmatrix}$$

$$(D.13)$$

Substituting equation D.13 into equation D.11, the following matrix

equation is obtained:

$$
\begin{bmatrix} \underline{Y}_A & \underline{0} & \underline{0} \\ \underline{0} & \underline{Y}_B & \underline{0} \\ \underline{0} & \underline{0} & \underline{Y}_C \end{bmatrix}
+
\begin{bmatrix} \underline{C}_{A1}\,\underline{Y}_{I1}\,\underline{C}_{A1}^{T} & \underline{C}_{A1}\,\underline{Y}_{I1}\,\underline{C}_{B1}^{T} & \underline{0} \\ \underline{C}_{B1}\,\underline{Y}_{I1}\,\underline{C}_{A1}^{T} & \underline{D} & \underline{C}_{B2}\,\underline{Y}_{I2}\,\underline{C}_{C2}^{T} \\ \underline{0} & \underline{C}_{C2}\,\underline{Y}_{I2}\,\underline{C}_{B2}^{T} & \underline{C}_{C2}\,\underline{Y}_{I2}\,\underline{C}_{C2}^{T} \end{bmatrix}
\begin{bmatrix} \underline{V}_A \\ \underline{V}_B \\ \underline{V}_C \end{bmatrix}
$$

$$
= \begin{bmatrix} \underline{I}_A \\ \underline{I}_B \\ \underline{I}_C \end{bmatrix}
\tag{D.14}
$$

where,

$$
\underline{D} = \underline{C}_{B1}\,\underline{Y}_{I1}\,\underline{C}_{B1}^{T} + \underline{C}_{B2}\,\underline{Y}_{I2}\,\underline{C}_{B2}^{T}
\tag{D.15}
$$

The bus admittance matrices can be written in rectangular form in terms

of the real and imaginary parts as:

$$
\underline{Y} = \underline{G} - j\underline{B}
\tag{D.16}
$$

where,

$\underline{G}$, $\underline{B}$ - the conductance and susceptance matrices.

Based on equation D.14 and equation D.16, the diakoptical active and
reactive power losses for the network shown in Figure D.1 in terms of
the network bus voltages and line admittances may be written as:

$$P_L = \underline{V}_{AP}^T [\underline{G}_A + \underline{C}_{A1} \underline{G}_{I1} \underline{C}_{A1}^T] \underline{V}_{AP}$$

$$+ \underline{V}_{Aq}^T [\underline{G}_A + \underline{C}_{A1} \underline{G}_{I1} \underline{C}_{A1}^T] \underline{V}_{Aq}$$

$$+ \underline{V}_{AP}^T [\underline{C}_{A1} \underline{G}_{I1} \underline{C}_{B1}^T] \underline{V}_{BP} + \underline{V}_{Aq}^T [\underline{C}_{A1} \underline{G}_{I1} \underline{C}_{B1}^T] \underline{V}_{Bq}$$

$$+ \underline{V}_{BP}^T [\underline{C}_{B1} \underline{G}_{I1} \underline{C}_{A1}^T] \underline{V}_{AP} + \underline{V}_{Bq}^T [\underline{C}_{B1} \underline{G}_{I1} \underline{C}_{A1}^T] \underline{V}_{Aq}$$

$$+ \underline{V}_{BP}^T [\underline{G}_B + \underline{C}_{B1} \underline{G}_{I1} \underline{C}_{B1}^T + \underline{C}_{B2} \underline{G}_{I2} \underline{C}_{B2}^T] \underline{V}_{BP}$$

$$+ \underline{V}_{Bq}^T [\underline{G}_B + \underline{C}_{B1} \underline{G}_{I1} \underline{C}_{B1}^T + \underline{C}_{B2} \underline{G}_{I2} \underline{C}_{B2}^T] \underline{V}_{Bq}$$

$$+ \underline{V}_{BP}^T [\underline{C}_{B2} \underline{G}_{I2} \underline{C}_{C2}^T] \underline{V}_{CP} + \underline{V}_{Bq}^T [\underline{C}_{B2} \underline{G}_{I2} \underline{C}_{C2}^T] \underline{V}_{Cq}$$

$$+ \underline{V}_{CP}^T [\underline{C}_{C2} \underline{G}_{I2} \underline{C}_{B2}^T] \underline{V}_{BP} + \underline{V}_{Cq}^T [\underline{C}_{C2} \underline{G}_{I2} \underline{C}_{B2}^T] \underline{V}_{Bq}$$

$$+ \underline{V}_{CP}^T [\underline{G}_C + \underline{C}_{C2} \underline{G}_{I2} \underline{C}_{C2}^T] \underline{V}_{CP}$$

$$+ \underline{V}_{Cq}^T [\underline{G}_C + \underline{C}_{C2} \underline{G}_{I2} \underline{C}_{C2}^T] \underline{V}_{Cq} \qquad (D.17)$$

A similar expression for Q_L can easily be obtained by replacing $\underline{G}$

by $\underline{B}$ in equation D.17. Expressions for the diakoptical active and active-reactive power losses in terms of the power generations for this system can easily be generated.

APPENDIX E

APPLICATION OF PIECEWISE LOSS MODEL BASED ECONOMIC

DISPATCH METHODS TO EXAMPLE TEST SYSTEMS

This Appendix presents the piecewise active and active-reactive

power loss models and the economic dispatch solutions of the 5 and 11

bus test systems. Also in this Appendix, the piecewise active power

loss model parameters are obtained for the 23·bus test system. The

economic active dispatch solution of this system is given in Chapter

VIII where it is compared to the dispatch solution based on the full

system active power loss model. In the piecewise loss model evaluation

of each of the above power systems, the data used is obtained from a

series of load flow studies of the system which are carried out for

different load and voltage levels that cover the entire operating

range of the power system. The above power systems operating conditions

and line data are given in Appendix F.

E.1   Piecewise Active Loss Models and Economic Dispatch Schedules of

      Model Power Systems

      In this Section, the piecewise active loss models and the economic

active dispatch solutions are presented for the above test systems.

E.1.1 The 5 Bus Test System - Piecewise Active Power Loss Model

      The power system condiguration is shown in Figure E.1. The

network is torn into two subnetworks A and B, interconnected by the

interconnections I as shown by the dotted line. Each of the subnetworks

A and B, contains one generation bus, 1 and 4 respectively. The number

of parameters to be evaluated of each subnetwork model, and the number

of load flow results required are given in Table E.1.

Model	P_{LA}	P_{LIA}	P_{LB}	P_{LIB}	P_{LIAB}	P_{LI}
No. of Parameters	3	3	3	3	4	4
No. of Load Flows	4	4	4	4	5	5

Table E.1 The 5 Bus Piecewise Active Power Loss

Model Parameter Evaluation Requirements

From Table E.1, the number of parameters to be evaluated of
the largest submodel is 4. A minimum of five load flow results
are required, which were carried out for different system loads
(nominal system load is 165 + j10 MVA). From the load flow results
obtained, the piecewise active power loss models (i.e., P_{LA}, P_{LIA},
P_{LB}, P_{LIB}, P_{LIAB} and the approximate model P_{LI}) were evaluated by the
ridge estimator. The results obtained are presented in Tables E.2,
E.3 and E.4 respectively.

As seen from Tables E.2, E.3 and E.4, the evaluated loss models
P_{LIA}, P_{LIB} and P_{LIAB} are in error as the mean square error in each case
is very high (of the order of 10^4 and higher). Other values of ridge
k were also used but without any improvement. These models, therefore
cannot be used in the evaluation of the dispatch schedules of the system.
The approximate model P_{LI}, on the other hand was evaluated without any
difficulties and as seen resulted in a very small value for the mean
square error. This phenomenon was observed in most of the systems tested.
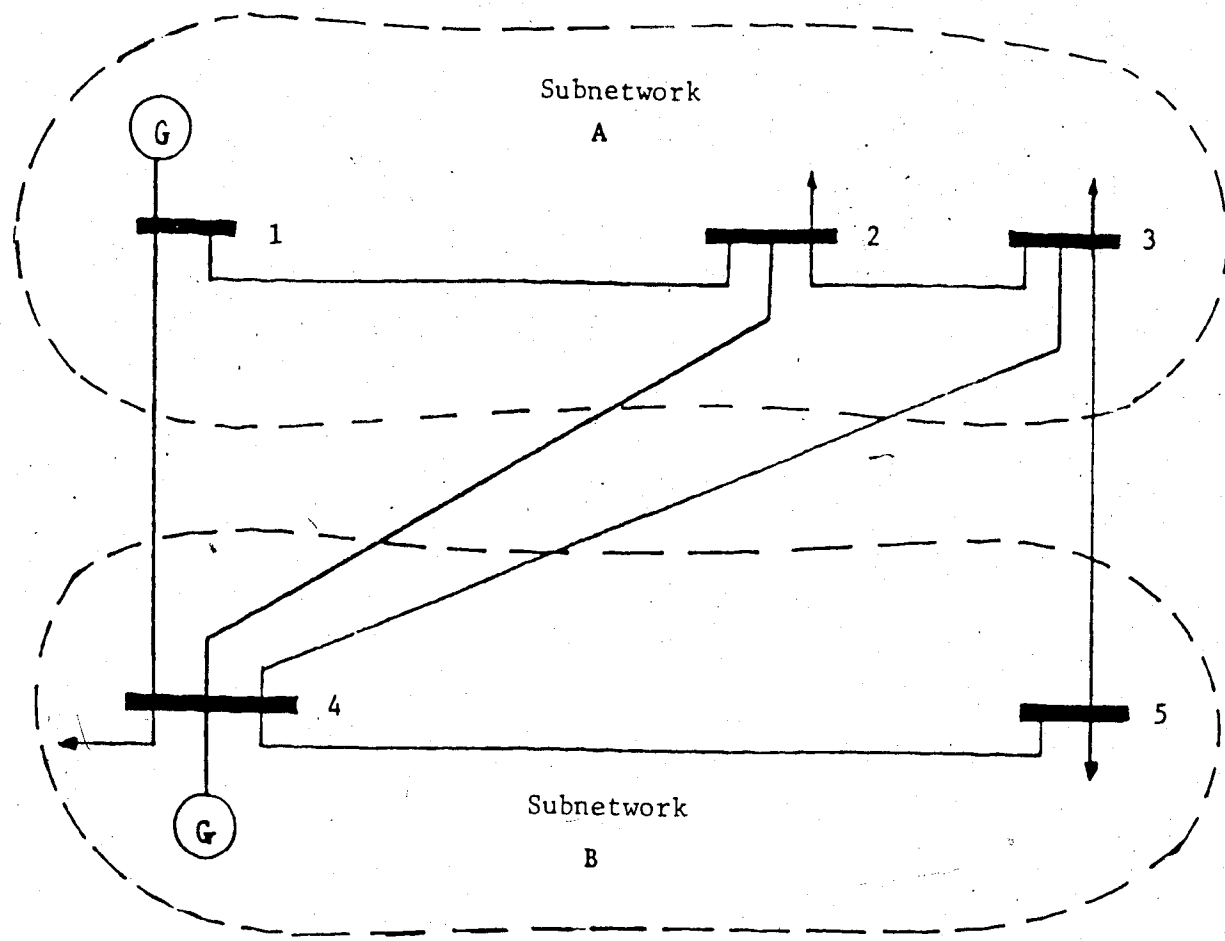
Figure E.1 The 5 Bus Test System Torn into Two

Subnetworks

Parameter	k = 0.0 P_{LA}	k = 0.0 P_{LIA}	η	k = 0.365 P_{LA}	k = 0.365 P_{LIA}	η
K_{L0}	-0.001194	10.799041	1	0.000096	8.664032	1
B_{01}	0.007075	-0.588002	3	0.003602	3.787407	2
B_{11}	0.002755	0.225776	19	0.004601	-1.470644	3
Condition Number	19	19		3	3	
Mean Square Error	0.5617	1.231×10^3		0.0455	4.6235×10^4	

Table E.2 The Parameters of the Active Submodels P_{LA} and P_{LIA}
of the 5 Bus Test System in p.u. on 100 MVA Base

Parameter	k = 0.0 P_{LB}	k = 0.0 P_{LIB}	n	k = 0.365 P_{LB}	k = 0.365 P_{LIB}	n
K_{LO}	-0.005596	10.839720	1	0.001412	8.272727	1
B_{01}	0.051192	-0.505018	3	0.006305	5.056620	2
B_{11}	-0.047694	0.452593	23	-0.000562	-1.891581	3
Condition Number	23	23		3	3	
Mean Square Error	42.8614	3.4562×10^3		2.8963	8.2850×10^4	

Table E.3 The Parameters of the Active Submodels P_{LB} and P_{LIB} of the 5 Bus Test System in p.u. on 100 MVA Base

215

Parameter	k = 0.0 P_{LIAB}	k = 0.0 P_{LI}	n	k = 0.365 P_{LIAB}	k = 0.365 P_{LI}	n
K_{L0}	-21.381523	0.001526	1	-15.534273	-0.000807	1
B_{01A}	0.460028	0.004595	4	-4.810968	0.009428	3
B_{01B}	0.487100	-0.016214	5	-8.262364	-0.002555	3
B_{11}	-0.420124	0.037369	33	5.608871	0.015811	3
Condition Number	33	33		3	3	
Mean Square Error	2.5699×10^2	5.0880		1.2458×10^6	6.3493	

Table E.4 The Parameters of the Active Submodels P_{LIAB} and P_{LI} of the 5 Bus Test System in p.u. on 100 MVA Base

in this thesis. The approximate model (P_{LI}) is expected to result in satisfactory dispatch solutions especially when the interconnections are chosen to have a minimum number of lines. This is also true, when the power losses of subnetworks A and B are much higher than the losses in the interconnections.

E.1.2 The 5 Bus Test System – Piecewise Active Power Dispatch

Based on the piecewise loss model (i.e., P_{LA}, P_{LB} and P_{LI}), the economic active dispatch solutions of the 5 bus test system were obtained for different load levels as shown in Table E.5. The load flow solutions based on the economic dispatch results are shown in brackets in Table E.5. The voltage profiles obtained for light and heavy load levels are presented in Table E.6.

As seen from Table E.5, the two solutions agree very closely with each other for all system loads considered. At a load of 16.5 MW, the slack bus active power limit of 5 MW was violated (bus number 1). The differences in the active power generations between the two solutions at the slack bus are very small and are picked up by the system total active power losses, which indicate the accuracy of the evaluated piece-wise loss models P_{LA}, P_{LB} and the approximate model P_{LI} The bus voltage levels that correspond to the optimal solutions were all within the allowable limits of the feasible operation range of the power system.

E.1.3 The 11 Bus Test System – Picewise Active Power Loss Model

The 11 bus test system is shown in Figure E.2. The network is torn as shown by the dotted line into two subnetworks A and B. Subnetwork A contains four generation buses, 1 2, 6 and 7, while subnetwork B contains two generation buses, numbers 10 and 11. The number of parameters

P_D MW	λ_P $/MWh	P_{GA1} MW	P_{GB4} MW	P_L MW	F_0 $/h
16.5	8.77	5.000* (4.908)	11.694 (11.694)	0.196 (0.100)	492.33
33.0	8.86	6.715 (6.568)	26.608 (26.608)	0.324 (0.175)	637.87
49.5	8.92	15.098 (14.865)	34.956 (34.956)	0.554 (0.320)	784.52
66.0	8.98	23.500 (23.217)	43.321 (43.321)	0.821 (0.536)	932.14
82.5	9.03	31.921 (31.556)	51.703 (51.703)	1.124 (0.826)	1080.73
99.0	9.09 -	40.361 (40.060)	60.103 (60.103)	1.464 (1.162)	1230.30
115.5	9.15	48.821 (48.563)	68.520 (68.520)	1.841 (1.581)	1380.85
132.0	9.21	57.301 (57.124)	76.955 (76.955)	2.256 (2.078)	1532.40
148.5	9.27	65.800 (65.747)	85.407 (85.407)	2.708 (2.653)	1684.93
165.0	9.34	74.320 (74.438)	93.877 (93.877)	3.197 (3.311)	1838.46

* - Lower Limit Violation

Table E.5 The Diakoptical Economic Active Dispatch

of the 5 Bus Test System

Bus No.	Load=...5+j1.0MVA		Load=165+j10MVA	
	Voltage p.u.	Angle Degrees	Voltage p.u.	Angle Degrees
1	.0600	0.0	1.0600	0.0
2	.0574	-0.3322	1.0241	-3.8156
3	.0572	-0.3504	1.0234	-4.0651
4	.0511	0.0881	1.0470	-1.2142
5	.0543	-0.3538	1.0175	-4.6680

Table E.6 The Voltage Profiles of the 5 Bus System Based

on the Diakoptical Economic Active Dispatch Solutions

to be evaluated of each of the piecewise submodels and the number of
load flow results required are summarized in Table E.7. From Table

Model	P_{LA}	P_{LIA}	P_{LB}	P_{LIB}	P_{LIAB}	P_{LI}
No. of Parameters	15	15	6	6	15	15
No. of Load Flow	16	16	7	7	16	16

Table E.7 The 11 Bus Piecewise Active Power

Loss Model Parameter Evaluation Requirements
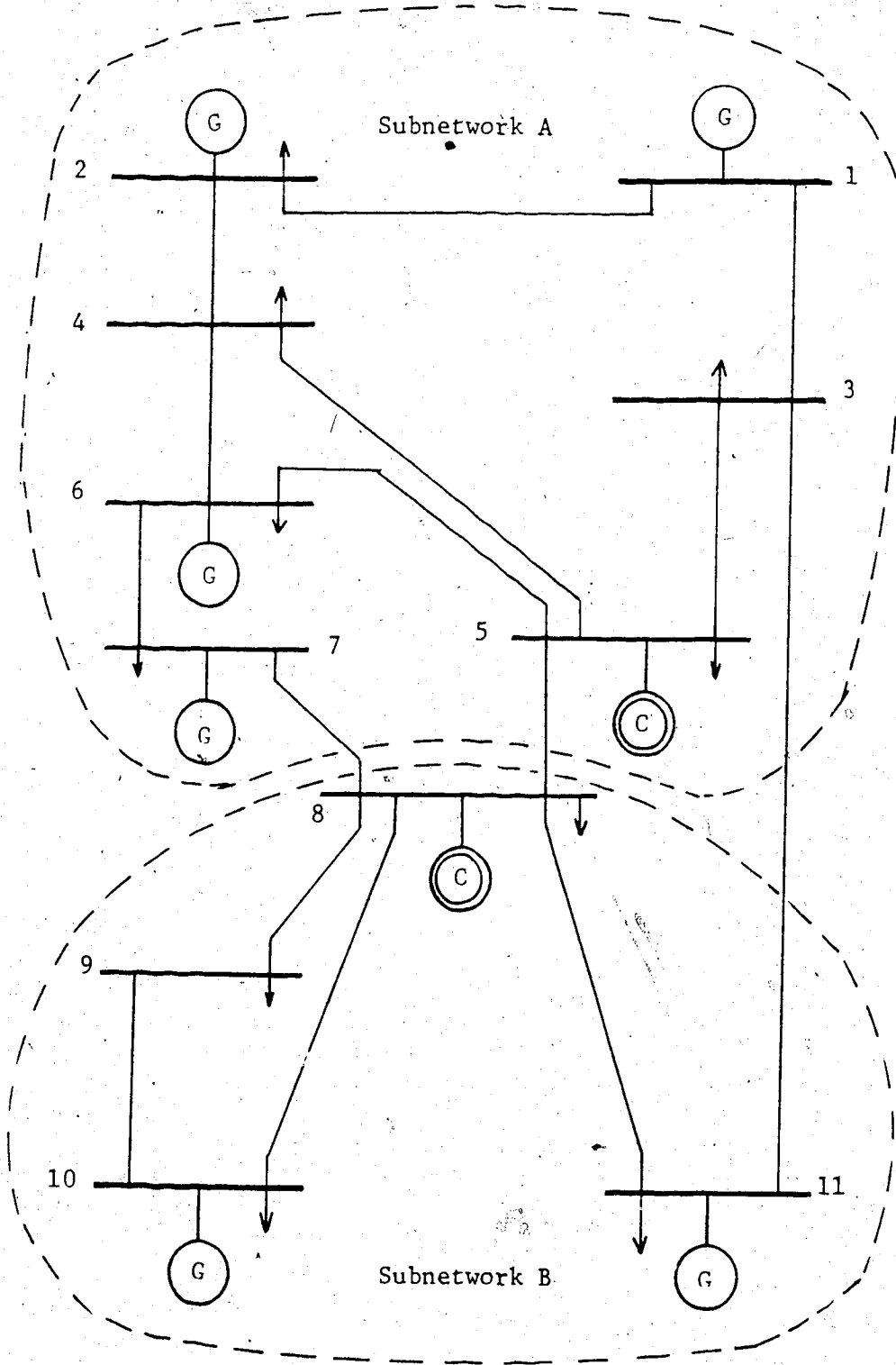
Figure E.2 The 11 Bus Test System Torn into

E.7, the number of parameters of the largest submodel is 15. To evaluate the parameters of all submodels, 16 load flow solutions were carried out covering the entire load range of the system (system nominal load is 420 + j240 MVA). Based on the load flow results obtained, the piecewise loss model parameters were evaluated by the ridge estimator. As in the case of the 5 bus system, the evaluated parameters of P_{LIA}, P_{LIB} and P_{LIAB} resulted in very high mean square errors (of the order of 10^5 and higher). The parameters of P_{LA}, P_{LB} and P_{LI} are only shown here which are presented in Tables E.8, E.9 and E.10.

E.1.4 The 11 Bus Test System – Piecewise Active Power Dispatch

The generator capacities used in the evaluation of the economic dispatch schedules of the 11 bus test system are shown in Table E.11, for coal fired plants. Using the piecewise loss model of this system, the economic active dispatch solution for the nominal loading of 420 + j240 MVA was obtained as shown in Table E.12. The load flow solution based on the economic dispatch result is also shown in Table E.12 for comparison. The load flow voltage profile obtained is shown in Table E.13. In Table E.12, the difference in the active power generation at the slack bus between the two sections is 2.384 MW, which is picked up by the total system losses. The difference between the two solutions in the total active power losses is 2.468 MW. The voltage levels shown in Table E.13 are rather low, but all fall within the limits of the base load flow solutions used in the evaluation of the piecewise active loss model.

	Ridge k = 0.34		
Parameter	P_{LA}	Parameter	P_{LA}
K_{LOA}	0.001549	B_{A14}	0.015025
B_{OA1}	0.024124	B_{A22}	0.006083
B_{OA2}	0.005998	B_{A23}	0.001955
B_{OA3}	0.004551	B_{A24}	0.002690
B_{OA4}	0.005731	B_{A33}	0.000964
B_{A11}	0.050635	B_{A34}	0.001178
B_{A12}	0.013677	B_{A44}	0.003987
B_{A13}	0.013556		

Table E.8 The Parameters of the Active Loss Submodel

P_{LA} of the 11 Bus Test System in p.u. on 100 MVA Base

	Ridge k = 0.0		
Parameter	P_{LB}	Parameter	P_{LB}
K_{LOB}	0.001561	B_{B11}	0.065649
B_{OB1}	-0.009790	B_{B12}	-0.051784
B_{OB2}	0.005283	B_{B22}	0.133209

Table E.9 The Parameters of the Active Loss Submodel

P_{LB} of the 11 Bus Test System in p.u. on 100 MVA Base

	Ridge k = 0.34		
Parameter	P_{LI}	Parameter	P_{LI}
K_{LOI}	0.002065	B_{IAB12}	-0.008041
B_{OIAA1}	-0.002063	B_{IAB21}	0.002568
B_{OIAA2}	0.002227	B_{IAB22}	0.000710
B_{OIAA3}	0.002820	B_{IAB31}	0.003542
B_{OIAA4}	0.002861	B_{IAB32}	0.001404
B_{OIBB1}	0.003282	B_{IAB41}	0.003444
B_{OIBB2}	0.001439	B_{IAB42}	0.001181
B_{IAB11}	-0.005404		

Table E.10 The Parameters of the Active Submodel

P_{LI} of the 11 Bus Test System in p.u. on

100 MVA Base

Generator No.	Generator Size (MW)	Source Constraints		Bus No.
		MW	MVARS	
1	400	$5 \leq P_{G1} \leq 400$	$-60 \leq Q_{G1} \leq 60$	1
2	200	$5 \leq P_{G2} \leq 200$	$-40 \leq Q_{G2} \leq 60$	2
3	200	$5 \leq P_{G3} \leq 200$	$-40 \leq Q_{G3} \leq 50$	6
4	200	$5 \leq P_{G4} \leq 200$	$-40 \leq Q_{G4} \leq 50$	7
5	200	$5 \leq P_{G5} \leq 200$	$-40 \leq Q_{G5} \leq 50$	10
6	400	$5 \leq P_{G6} \leq 400$	$-40 \leq Q_{G6} \leq 50$	11

Table E.11 The 11 Bus Test System Generator Capacities -

Coal (See Table 2.1 for Cost Coefficients)

	System Load = 420 + j240 MVA	
Variable	Economic Solution	Load Flow Solution
P_{G1} MW	36.117	33.733
P_{G2} MW	74.150	74.150
P_{G6} MW	94.211	94.211
P_{G7} MW	77.579	77.579
P_{G10} MW	81.409	81.409
P_{G11} MW	69.805	69.805
P_L MW	13.271	10.803
F_o $/hr	5067.850	
λ_p $/MWh	9.36	

Table E.12 The Diakoptical Economic Active Dispatch

of the 11 Bus Test System

E.1.5 The 23 Bus Test System - Piecewise Active Power Loss Model

The single line diagram of this model system is shown in Figure

8.2. This power system is part of the 275/132 KV British network. The

network is torn into two subnetworks as indicated by the broken line.

Subnetworks A and B, contain four and two generation buses respectively.

The number of parameters to be evaluated for each of the piecewise

loss submodels, and the number of load flow results required are given

in Table E.14. As in the case of the 11 bus test system, the number of

load flow results required to evaluate all the parameters in Table E.14

Load = 420 + j240 MVA					
Bus No.	Voltage p.u.	Angle Degrees	Bus No.	Voltage p.u.	Angle Degrees
1	1.0400	0.00	7	1.000	−3.0277
2	1.0450	−2.4107	8	0.9926	−5.9364
3	0.9592	−2.5338	9	0.9845	−5.0594
4	0.9561	−7.8013	10	1.0500	−2.4278
5	0 9847	−8.9871	11	1.0270	1.9409
6	0.9645	−6.5824			

Table E.13 The Voltage Profile of the 11 Bus Test System

Based on the Diakoptical Economic Active Dispatch

Solution

Model	P_{LA}	P_{LIA}	P_{LB}	P_{LIB}	P_{LIAB}	P_{LI}
No. of Parameters	15	15	6	6	15	15
No. of Load Flows	16	16	7	7	16	16

Table E.14 The 23 Bus Piecewise Active Power

Loss Model Parameter Evaluation Requirements

is 16. These were carried out for different load and voltage levels

of the system. Using these base load flow results, the parameters of

the combined submodels P_{LAA}, P_{LBB} ($P_{LAA} = P_{LA} + P_{LIA}$, $P_{LBB} = P_{LB} + P_{LIB}$)

and the submodel P_{LIAB} of this system were evaluated by the ridge

estimator. The results obtained are shown in Tables E.15, E.16 and

E.17. The validity of the evaluated submodels were verified by computing

the total power system losses using the piecewise loss model and

comparing the results to the base load flow power losses. It was

observed that the differences between the two power losses were very

small.

E.2 Piecewise Active-Reactive Loss Models and Economic Dispatch

Schedules of Model Power Systems

In this section, the piecewise active-reactive loss models and the

economic active-reactive dispatch solutions are presented for the 5 and

11 bus test systems.

	Ridge k = 0.001		
Parameter	P_{LAA}	Parameter	P_{LAA}
K_{LOAA}	6.485778	B_{AA14}	-0.001799
B_{OAA1}	-0.025337	B_{AA22}	0.000073
B_{OAA2}	-0.048513	B_{AA23}	0.000397
B_{OAA3}	-0.025839	B_{AA24}	0.000239
B_{OAA4}	-0.026027	B_{AA33}	0.000285
B_{AA11}	0.020992	B_{AA34}	0.000246
B_{AA12}	-0.000860	B_{AA44}	0.000362
B_{AA13}	-0.001415		

Table E.15 The Parameters of the Active Submodel P_{LAA}

of the 23 Bus Test System in p.u. on 100 MVA Base

	Ridge k = 0.001		
Parameter	P_{LBB}	Parameter	P_{LBB}
K_{LOBB}	6.458704	B_{BB11}	0.000619
B_{OBB1}	-0.018807	B_{BB12}	0.000541
B_{OBB2}	-0.018928	B_{BB22}	0.000407

Table E.16 The Parameters of the Active Submodel

P_{LBB} of the 23 Bus Test System in p.u. on

100 MVA Base

Ridge k = 0.001			
Parameter	P_{LIAB}	Parameter	P_{LIAB}
K_{LOIAB}	-12.913089	B_{IAB12}	-0.002464
B_{OIAB1}	0.039708	B_{IAB21}	0.001465
B_{OIAB2}	0.013553	B_{IAB22}	0.001688
B_{OIAB3}	0.018177	B_{IAB31}	0.002400
B_{OIAB4}	0.019070	B_{IAB32}	0.002203
B_{OIBA1}	0.018831	B_{IAB41}	0.001896
B_{OIBA2}	0.018895	B_{IAB42}	0.001922
B_{IAB11}	-0.002695		

Table E.17 The Parameters of the Active Power Loss Submodel

P_{LIAB} of the 23 Bus Test System in p.u. on 100 MVA Base

E.2.1 The 5 Bus Test System - Piecewise Active-Reactive Loss Model

The 5 bus test system is shown in Figure E.1. As mentioned earlier, subnetworks A and B contain one active-reactive generation bus each. The number of parameters to be evaluated for the piecewise active-reactive loss model and the number of load flow results required are given in Table E.18. The losses in interconnections are represented by the approximate loss submodels (i.e., P_{LI} and Q_{LI}). To evaluate the parameters of all submodels shown in Table E.18, a minimum of eight load flow results were required which were performed for different load levels of the system (system nominal load = 165 + j10 MVA). Using the

Model	P_{LA}	Q_{LA}	P_{LB}	Q_{LB}	P_{LI}	Q_{LI}
No. of Parameters	4	4	4	4	7	7
No. of Load Flows	5	5	5	5	8	8

Table E.18 The 5 Bus Piecewise Active-Reactive Power Loss

Model Parameter Evaluation Requirements

load flow results obtained, the parameters of the piecewise active-

reactive power loss model were evaluated by the ridge estimator. The

parameter estimates obtained are shown in Tables E.19 and E.20 for the

active and reactive parts respectively.

E.2.2 The 5 Bus Test System - Piecewise Active-Reactive Power Dispatch

Using the piecewise active-reactive model with parameters as

given above, the economic dispatch active-reactive dispatch schedules of

the 5 bus test system were obtained for different load levels (this

system has no purely reactive sources). The dispatch results obtained

are given in Tables E.21 and E.22 for the active and reactive parts

respectively. The load flow solutions based on the economic dispatch

results are shown in brackets in Tables E.21 and E.22. The load flow

voltage profiles for light and heavy loads of the system are shown in

Table E.23.

Comparing the results shown in Tables E.21 and E.22, it is seen

that the load flow solutions agree very closely with the economic dispatch

Parameter	P_{LA} k = 0.05	Parameter	k = 0.05	Parameter	P_{LI} k = 0.05
K_{LOPA}	-0.004780	K_{LOPB}	0.006152	K_{LOPI}	0.002115
E_{PPA1}	0.002318	E_{PPB1}	0.006856	E_{PPAA1}	0.005710
E_{PQA1}	0.042057	E_{PQB1}	0.018197	E_{PQAA1}	-0.018991
$A_{P\ell11}$	0.019966	A_{PB11}	0.002432	E_{PPBB1}	0.004137
				E_{PQBB1}	-0.000083
				A_{PIAB11}	0.009500
				B_{PIAB11}	-0.005612

Table E.19 The 5 Bus Piecewise Active-Reactive Power Loss Model

Parameters in p.u. on 100 MVA Base (Active Part)

Parameter	Q_{LA} ($k = 0.05$)	Parameter	Q_{LB} ($k = 0.05$)	Parameter	Q_{LI} ($k = 0.05$)
K_{LOAQ}	-0.092049	K_{LOBQ}	-0.008459	K_{LOQI}	-0.088009
E_{QPA1}	0.008079	E_{QPB1}	0.010500	E_{QPAA1}	-0.064364
E_{QQA1}	0.126523	E_{QQB1}	0.070328	E_{QQAA1}	-0.047628
A_{QA11}	0.034033	A_{QB11}	0.016083	F_{QPBB1}	-0.003727
				E_{QQBB1}	0.278103
				A_{QIAB11}	0.018515
				B_{QIAB11}	0.097693

Table E.20 The 5 Bus Piecewise Active-Reactive Power Loss Model

Parameters in p.u. on 100 MVA Base (Reactive Part)

P_D MW	λ_P $/MWh	P_{GA1} MW	P_{GB4} MW	P_L MW	F_o $/h
16.5	8.80	11.402 (11.596)	5.016 (5.016)	0.007 (0.112)	490.45
33.0	8.86	18.756 (18.760)	14.447 (14.447)	0.203 (0.205)	636.38
49.5	8.91	25.768 (25.683)	24.183 (24.183)	0.451 (0.364)	783.16
66.0	8.97	32.773 (32.565	33.955 (33.955)	0.729 (0.589)	930.88
82.5	9.02	39.772 (39.623)	43.765 (43.765)	1.037 (0.887)	1079.53
99.0	9.08	46.764 (46.642)	53.613 (53.613)	1.377 (1.255)	1229.13
115.5	9.14	53.748 (53.700)	63.498 (63.498)	1.746 (1.697)	1379.67
132.0	9.20	60.725 (60.797)	73.422 (73.422)	2.147 (2.217)	1531.16
148.5	9.26	67.694 (67.934)	83.385 (83.385)	2.579 (2.817)	1683.61
165.0	9.31	74.656 (75.114)	93.387 (93.387)	3.043 (3.500)	1837.03

Table E.21 The Diakoptical Economic Active-Reactive

Dispatch of the 5 Bus System (Active)

Q_D MVAR	λ_q $/MVARh	Q_{GA1} MVAR	Q_{GB4} MVAR	Q_L MVAR
1.0	0.20	10.079 (9.067)	-40.000* (-40.000)	-31.831 (-31.931)
2.0	0.20	10.371 (10.501)	-40.000* (-40.000)	-31.629 (-31.499)
3.0	0.20	11.793 (12.132)	-40.000* (-40.000)	-31.207 (-30.035)
4.0	0.21	13.349 (13.964)	-40.000* (-40.000)	-30.651 (-30.035)
5.0	0.21	15.045 (16.022)	-40.000* (-40.000)	-29.955 (-28.977)
6.0	0.21	16.886 (18.297)	-40.000* (-40.000)	-29.114 (-27.703)
7.0	0.21	18.879 (20.798)	-40.000* (-40.000)	-28.121 (-26.201)
8.0	0.22	21.031 (23.541)	-40.000* (-40.000)	-26.969 (-24.461)
9.0	0.22	23.348 (26.523)	-40.000* (-40.000)	-25.652 (-22.476)
10.0	0.22	25.838 (29.764)	-40.000* (-40.000)	-24.162 (-20.236)

* Lower Limit Violation

Table E.22 The Diakoptical Economic Active-Reactive

patch of the 5 Bus System (Reactive)

Bus No.	Load=16.5+j1 MVA		Load=165.0+j10 MVA	
	Voltage p.u.	Angle Degrees	Voltage p.u.	Angle Degrees
1	1.0600	0.0	1.0600	0.0
2	1.0566	-0.4614	1.0164	-3.7404
3	1.0564	-0.4885	1.0152	-3.9868
4	1.0500	-0.0851	1.0371	-1.0585
5	1.0532	-0.5157	1.0079	-4.5846

Table E.23 The Voltage Profile of the 5 Bus System

Based on the Diakoptical Economic Active-

Reactive Solution

solutions in the active power generations. There are in general some

differences in the reactive powers between the load flow solution and

the economic dispatch solution. For example, in the case of 100% load

level, the reactive powers at the slack bus (bus number 1) of the two

solutions differ by 3.926 MVARS, which is picked up by the total

reactive power losses. If the slack bus voltage in the load flow

solution is allowed to float, it will assume a value of 1.105 p.u., and

the load flow solution would then agree very closely with the dispatch

solution in both the active and reactive power flows. However, this

high slack bus voltage, not only raises the bus voltages in general,

but it is outside the feasible operating range of the base load flow

results used to evaluate the piecewise active-reactive loss model.

Hence from the above discussion, the solutions shown in Tables E.21 and

E.22 are the economic dispatch solutions of the system.

E.2.3 The 11 Bus Test System - Piecewise Active-Reactive Power Loss Model

The 11 bus power system is shown in Figure E.2. The network as

a whole has six active-reactive generation buses 1, 2, 6, 7, 10 and 11,

and two purely reactive sources at buses 5 and 8. The network in

Figures E.2 is torn into two subnetworks A and B along the broken line.

Subnetwork A and B contain four and two generation buses respectively.

The number of parameters to be evaluated of the piecewise-loss model,

and the number of load flow results required are given in Table E.24.

Model	P_{LA}	Q_{LA}	P_{LB}	Q_{LB}	P_{LI}	Q_{LI}
No. of Parameters	25	25	9	9	29	29
No. of Load Flows	26	26	10	10	30	30

Table E.24 The 11 Bus Piecewise Active-Reactive Power

Loss Model Parameter Evaluation Requirements

The purely reactive loss models are dealt with later. The number of

parameters to be evaluated for the largest submodel is 29. A minimum

of 30 load flow solutions were carried out for different load and

voltage levels. Based on the load flow result obtained, the parameters

of the piecewise active-reactive loss model of this system were

evaluated by the ridge estimator. The parameter estimates obtained are shown in Tables E.25 to E.30 for the active and reactive parts.

The purely reactive powers at buses 5 and 8, were modeled in terms of the total reactive load demand of the network (see Chapter II). In the modeling procedure, the reactive limits used are given below:

$$- 40 \leq Q_{GV5} \leq 50 \quad \text{MVARS} \qquad (E.1)$$

$$- 40 \leq Q_{GV8} \leq 50 \quad \text{MVARS} \qquad (E.2)$$

The reactive powers at buses 5 and 8, were expressed as third order polynomials in the total reactive load demand. Using the base load flow results obtained, the parameters of these polynomials were evaluated by the ridge estimator. The results obtained are given in Table E.31.

E.2.4 The 11 Bus Test System - Piecewise Active-Reactive Power Dispatch

The economic active-reactive dispatch solution obtained for this system for 100% load level (i.e. 420 + j240 MVA) is shown in Table E.32. The generation capacities used are given in Table E.11 for coal fired plants. The load flow solution based on the economic dispatch result is also given in Table E.32. The voltage profile that corresponds to the economic solution is shown in Table E.33.

As in the case of the 5 bus test system, it is observed from Table E.32, that both the economic dispatch result and the load flow solution agree very closely in the active power generation. The difference

	Ridge k = 0.00023		
Parameter	P_{LA}	Parameter	P_{LA}
K_{LOPA}	-0.000256	A_{PA22}	0.079209
E_{PPA1}	0.028880	A_{PA23}	-0.013739
E_{PPA2}	-0.002655	A_{PA24}	-0.027041
E_{PPA3}	0.030913	A_{PA33}	0.029591
E_{PPA4}	0.005315	A_{PA34}	-0.016761
E_{PQA1}	0.065364	A_{PA44}	0.003990
E_{PQA2}	-0.022612	B_{PA12}	0.055627
E_{PQA3}	-0.014239	B_{PA13}	-0.025137
E_{PQA4}	0.034934	B_{PA14}	-0.051851
A_{PA11}	0.103770	B_{PA23}	-0.000240
A_{PA12}	0.029862	B_{PA24}	0.039305
A_{PA13}	-0.048961	B_{PA34}	-0.010428
A_{PA14}	0.021178		

Table E.25 The 11 Bus System Piecewise Active-Reactive Loss Model - the Parameters of the Submodel P_{LA} in p.u. on 100 MVA Base

Parameter	k=0.00023 P_{LB}
K_{LOPB}	0.000194
E_{PPB1}	-0.008650
E_{PPB2}	0.029544
E_{PQB1}	-0.037757
E_{PQB2}	-0.002288
A_{PB11}	0.108865
A_{PB12}	-0.062706
A_{PB22}	0.067215
B_{PB12}	0.032553

Table E.26 The 11 Bus System Piecewise Active-

Reactive Loss Model - the Parameters

of the Submodel P_{LB} in p.u. on 100 MVA Base

	Ridge k = 0.00023		
Parameter	P_{LI}	Parameter	P_{LI}
K_{LOPI}	-0.007376	A_{PAB21}	-0.011398
E_{PPIAA1}	0.027200	A_{PAB22}	-0.004686
E_{PPIAA2}	0.000274	A_{PAB31}	-0.003040
E_{PPIAA3}	-0.012536	A_{PAB32}	0.028821
E_{PPIAA4}	-0.004942	A_{PAB41}	0.020329
E_{PQIAA1}	0.044640	A_{PAB42}	0.040464
E_{PQIAA2}	0.025447	B_{PAB11}	-0.015945
E_{PQIAA3}	-0.010715	B_{PAB12}	-0.014240
E_{PQIAA4}	-0.057507	B_{PAB21}	-0.033965
E_{PPIBB1}	0.005619	B_{PAB22}	0.015835
E_{PPIBB2}	0.015427	B_{PAB31}	0.015424
E_{PQIBB1}	-0.025149	B_{PAB32}	0.007925
E_{PQIBB2}	0.056669	B_{PAB41}	0.045359
A_{PAB11}	-0.030333	B_{PAB42}	-0.013600
A_{PAB12}	-0.045088		

Table E.27 The 11 Bus System Piecewise Active-Reactive

Loss Model – the Parameters of the Submodel P_{LI}

in p.u. on 100 MVA Base

	Ridge k = 0.00023		
Parameter	Q_{LA}	Parameter	Q_{LA}
K_{LOQA}	-0.001151	A_{QA22}	0.282171
E_{QPA1}	0.120550	A_{QA23}	-0.031631
E_{QPA2}	-0.020670	A_{QA24}	-0.083420
E_{QPA3}	0.109920	A_{QA33}	0.075480
E_{QPA4}	0.003360	A_{QA34}	-0.068048
E_{QQA1}	0.251792	A_{QA44}	-0.035857
E_{QQA2}	-0.096246	B_{QA12}	0.136346
E_{QQA3}	-0.030552	B_{QA13}	-0.068088
E_{QQA4}	0.165602	B_{QA14}	-0.146759
A_{QQ11}	0.209733	B_{QA23}	-0.022641
A_{QA12}	0.026595	B_{QA24}	0.152332
A_{QA13}	-0.121539	B_{QA34}	-0.016143
A_{QA14}	0.047521		

Table E.28 The 11 Bus System Piecewise Active-Reactive
Loss Model - the Parameters of the Submodel
Q_{LA} in p.u. on 100 MVA Base

Parameter	k = 0.00023 Q_{LB}
K_{LOQB}	0.000107
E_{QPB1}	-0.017775
E_{QPB2}	0.050190
E_{QQB1}	-0.053493
E_{QQB2}	-0.005950
A_{QB11}	0.166789
A_{QB12}	-0.097678
A_{QB22}	0.108988
B_{QB12}	0.052770

Table E.29 The 11 Bus System Piecewise Active-

Reactive Loss Model – the Parameters of

the Submodel Q_{LB} in p.u. on 100 MVA Base

Parameter	Q_{LI}	Parameter	Q_{LI}
		Ridge $k = 0.00023$	
K_{LOQI}	-0.015176	A_{QIAB21}	-0.018730
E_{QPIAA1}	0.053153	A_{QIAB22}	-0.007421
E_{QPIAA2}	0.002139	A_{QIAB31}	-0.008285
E_{QPIAA3}	-0.020813	A_{QIAB32}	0.055125
E_{QPIAA4}	-0.006603	A_{QIAB41}	0.046677
E_{QQIAA1}	0.081682	A_{QIAB42}	0.079653
E_{QQIAA2}	0.049886	B_{QIAB11}	-0.035525
E_{QQIAA3}	-0.023225	B_{QIAB12}	-0.020183
E_{QQIAA4}	-0.129613	B_{QIAB21}	-0.065574
E_{QPIBB1}	0.012002	B_{QIAB22}	0.021681
E_{QPIBB2}	0.028195	B_{QIAB31}	0.032283
E_{QQIBB1}	-0.05875	B_{QIAB32}	0.012161
E_{QQIBB2}	0.11406	B_{QIAB41}	0.075743
A_{QIAB11}	-0.05670	B_{QIAB42}	-0.006540
A_{QIAB12}	-0.08845		

Table E.30 The 11 Bus System Piecewise Active-Reactive

Loss Model - the Parameters of the Submodel

Q_{LI} in p.u. on 100 MVA Base

Parameter	Q_{GV5}	Q_{GV8}
A_0	0.164817	0.148750
A_1	0.095000	0.583942
A_2	0.164441	-0.311074
A_3	-0.061663	0.053551

Table E.31 The Parameters of Q_{GV5} and Q_{GV8}

of the 11 Bus System in p.u. on

100 MVA Base

between the two solutions in the reactive power flow at the slack bus
(bus number 1) is 2.986 MVARS which is picked up by the total losses.
If the slack bus voltage is allowed to float, the two solutions can be
made to agree with one another provided the voltage levels are
maintained within the voltage limits of the base load flow results used
to evaluate the piecewise and the purely reactive models. The voltage
levels shown in Table E.33, all fall within the voltage limits of the
base load flow results. The diakoptical active-reactive dispatch
method gave a lower value for the total fuel cost than the active
dispatch method.

244

| | System Load = 420+j240 MVA | |
Variable	Dispatch Solution	Load Flow Solution
P_{G1} MW	74.377	73.618
Q_{G1} MVAR	-6.259	-9.245
P_{G2} MW	51.400	51.400
Q_{G2} MVAR	54.135	54.135
Q_{GV5} MVAR	48.737	48.740
P_{G6} MW	123.143	123.143
Q_{G6} MVAR	32.040	32.040
P_{G7} MW	58.220	58.220
Q_{G7} MVAR	15.564	15.560
Q_{GV8} MVAR	49.872	49.870
P_{G10} MW	62.786	62.786
Q_{G10} MVAR	45.949	45.950
P_{G11} MW	64.521	64.521
Q_{G11} MVAR	30.336	30.340
P_L MW	14.448	13.666
Q_L MVAR	30.375	27.380
F_o \$/hr	5061.527	
λ_p \$/MWh	9.220	
λ_q \$/MVARh	0.194	

Table E.32 The Diakoptical Economic Active-Reactive Dispatch

of the 11 Bus Test System (Nominal Load)

	Load = 240 + j240 MVA				
Bus No.	Voltage p.u.	Angle Degrees	Bus No.	Voltage p.u.	Angle Degrees
1	1.0400	0.0	7	0.9911	-13.1990
2	1.0450	-7.9180	8	0.9926	-15.9020
3	0.9537	-6.5120	9	0.9745	-16.865
4	0.9700	-13.3320	10	1.0355	-15.017
5	0.9895	-16.044	11	1.0548	-7.9120
6	0.9857	-12.0280			

Table E.33 The Voltage Profile of the 11 Bus System Based

on the Diakoptical Economic Active-Reactive

Dispatch Solution

POWER SYSTEMS OPERATING DATA

The power systems used in this thesis are listed below:

1.   the 5 bus test system (3)

2.   the IEEE 30 bus test system (42)

3.   the 11 bus test system (56)

4.   the 23 bus test system (57)

The transmission network line parameters and operational data of the above power systems are given below.

F.1   The 5 Bus Test System

The operating conditions, voltage regulated bus data and the network line data of this system are given in Tables F.1, F.2 and F.3 respectively.

Bus No.	Voltage* p.u.	Angle* Degrees	Generation Active MW	Load	
				Active MW	Reactive MVAR
1	1.06	0.0	0.0	0.0	0.0
2	1.00	0.0	0.0	45.0	15.0
3	1.00	0.0	0.0	40.0	5.0
4	1.00	0.0	40.0	20.0	-20.0
5	1.00	0.0	0.0	60.0	10.0
* Initial Voltages and Angles					

Table F.1 The Operating Conditions of the 5 Bus Test System

Bus No.	Voltage p.u.	MVAR Capability	
		Min	Max
4	1.047	-40.00	50.00

Table F.2 Voltage Regulated Bus Data of the 5 Bus

Test System

Send Bus	End Bus	Resistance	Reactance	Line Charging
1	4	.02000	.06000	.03000
1	2	.08000	.24000	.02500
4	2	.06000	.18000	.02000
4	3	.06000	.18000	.02000
4	5	.04000	.12000	.01500
2	3	.01000	.03000	.01000
3	5	.08000	.24000	.02500

Table F.3 Line Data of 5 Bus Test System in p.u. on

100 MVA Base

F.2   The IEEE 30 Bus Test System

The system data are given in the following Tables.

Bus No.	Voltage* p.u.	Angle* Degrees	Generation Active MW	Load Active MW	Reactive MVAR
1	1.06	0.0	0.0	0.0	.0
2	1.00	0.0	40.0	21.70	12.70
3	1.00	0.0	0.0	2.40	1.20
4	1.00	0.0	0.0	7.60	1.60
5	1.00	0.0	0.0	94.20	19.00
6	1.00	0.0	0.0	0.0	0.0
7	1.00	0.0	0.0	22.80	10.90
8	1.00	0.0	0.0	30.00	30.00
9	1.00	0.0	0.0	0.0	0.0
10	1.00	0.0	0.0	5.80	2.00
11	1.00	0.0	0.0	0.0	0.0
12	1.00	0.0	0.0	11.20	7.50
13	1.00	0.0	70.45	0.0	0.0
14	1.00	0.0	0.0	6.20	1.60
15	1.00	0.0	0.0	8.20	2.50
16	1.00	0.0	0.0	3.50	1.80
17	1.00	0.0	0.0	9.00	5.80
18	1.00	0.0	0.0	3.20	0.90
19	1.00	0.0	0.0	9.50	3.40
20	1.00	0.0	0.0	2.20	0.70
21	1.00	0.0	0.0	17.50	11.20
22	1.00	0.0	0.0	0.0	0.0
23	1.00	0.0	0.0	3.20	1.60
24	1.00	0.0	0.0	8.70	6.70
25	1.00	0.0	0.0	0.0	0.0
26	1.00	0.0	0.0	3.50	2.30
27	1.00	0.0	0.0	0.0	0.0
28	1.00	0.0	0.0	0.0	0.0
29	1.00	0.0	0.0	2.40	0.90
30	1.00	0.0	0.0	10.60	1.90

* Initial Values

Table F.4 The Operating Conditions of the IEEE 30 Bus Test

System

Bus No.	Voltage p.u.	MVAR Capability	
		Min	Max
2	1.045	-40.000	50.000
5	1.010	-40.000	40.000
8	1.010	-10.000	40.000
11	1.082	-6.000	24.000
13	1.071	-6.000	24.000

Table F.5 Voltage Regulated Bus Data of the IEEE

30 Bus Test System

Send Bus	End Bus	Resistance	Reactance	Line Charging
1	2	.01920	.05750	.02640
1	3	.04520	.18520	.02040
2	4	.05750	.17370	.01840
3	4	.01320	.03790	.00420
2	5	.04720	.19830	.02090
2	6	.05810	.17630	.01870
4	6	.01190	.04140	.00450
5	7	.04600	.11600	.01020
6	7	.02670	.08200	.00850
6	8	.01200	.04200	.00450
6	9	.00000	.20800	.00000
6	10	.00000	.55600	.00000
9	11	.00000	.20800	.00000
9	10	.00000	.11000	.00000
4	12	.00000	.25600	.00000
12	13	.00000	.14000	.00000
12	14	.12310	.25590	.00000
12	15	.06620	.13040	.00000
12	16	.09450	.19870	.00000
14	15	.22100	.19970	.00000
16	17	.08240	.19230	.00000
15	18	.10700	.21850	.00000
18	19	.06390	.12920	.00000
19	20	.03400	.06800	.00000
10	20	.09360	.20900	.00000
10	17	.03240	.08450	.00000
10	21	.03480	.07490	.00000
10	22	.07270	.14990	.00000
21	22	.01160	.02360	.00000
15	23	.10000	.20200	.00000
22	24	.11500	.17900	.00000
23	24	.13200	.27000	.00000
24	25	.18850	.32920	.00000
25	26	.25440	.38000	.00000
25	27	.10930	.20870	.00000
27	28	.00000	.39600	.00000
27	29	.21980	.41530	.00000
27	30	.32020	.60270	.00000
29	30	.23990	.45330	.00000
8	28	.06360	.20000	.02140
6	28	.01690	.05990	.00650

Table F.6 Line Date of the IEEE 30 Bus Test System in p.u.

on 100 MVA Base

Send Bus	End Bus	Tap Setting
4	12	.932
6	9	.978
6	10	.969
28	27	.968

Table F.7 Transformer Data of the IEEE 30 Bus Test System

Bus No.	Suscesptance
10	.19000
24	.04300

Table F.8 The Shunt Data of the IEEE 30 Bus Test System

F.3   The 11 Bus Test System

The data of this system are given in the following Tables.

Bus No.	Voltage* p.u.	Angle* Degrees	Generation Active MW	Load	
				Active MW	Reactive MVAR
1	1.04	0.0	0.0	0.0	0.0
2	1.00	0.0	90.0	40.0	20.0
3	1.00	0.0	0.0	20.0	20.0
4	1.00	0.0	0.0	60.0	20.0
5	1.00	0.0	0.0	40.0	20.0
6	1.00	0.0	80.0	80.0	40.0
7	1.00	0.0	75.0	40.0	20.0
8	1.00	0.0	0.0	40.0	40.0
9	1.00	0.0	0.0	40.0	20.0
10	1.00	0.0	60.0	20.0	20.0
11	1.00	0.0	50.0	40.0	20.0

Table F.9 The Operating Conditions of the 11

Bus Test System

Bus No.	Voltage p.u.	MVAR Capability	
		Min	Max
2	1.000	-40.0000	50.0000
5	1.050	-40.0000	50.0000
6	1.027	-40.0000	50.0000
7	1.009	-40.0000	40.0000
8	1.047	-40.0000	50.0000
10	1.050	-40.0000	50.0000
11	1.027	-40.0000	50.0000

Table F.10 Voltage Regulated Bus Data of

11 Bus Test System

Send Bus	End Bus	Resistance	Reactance	Line Charging
1	2	.14500	.40900	.00000
1	3	.22800	.28300	.00000
2	4	.07800	.25900	.00000
4	6	.05800	.08800	.00000
6	7	.28600	.43500	.00000
7	8	.06900	.19800	.00000
8	9	.20200	.30800	.00000
9	10	.09400	.14800	.00000
3	11	.43000	.81300	.00000
3	5	.28400	.61000	.00000
4	5	.20800	.55000	.00000
5	6	.14800	.39300	.00000
5	8	.10300	.24200	.00000
8	11	.39000	.65700	.00000
8	10	.30200	.41400	.00000

Table F.11 Line Data of the 11 Bus Test System in p.u.

on 100 MVA Base

F.4 The 23 Bus Test System

The data of this power system are given in the following Tables.

Bus No.	Voltage* p.u.	Angle* Degrees	Generation Active MW	Load Active MW	Reactive MVAR
1	1.05	0.0	0.00	64.00	16.00
2	1.00	0.0	125.13	101.00	25.00
3	1.00	0.0	0.0	0.00	0.00
4	1.00	0.0	0.00	47.00	12.00
5	1.00	0.0	0.00	51.00	13.00
6	1.00	0.0	0.00	41.00	10.00
7	1.00	0.0	0.00	48.00	12.00
8	1.00	0.0	0.00	1.00	0.00
9	1.00	0.0	0.00	150.00	38.00
10	1.00	0.0	0.00	177.00	44.00
11	1.00	0.0	232.91	130.00	32.00
12	1.00	0.0	0.00	6.00	0.00
13	1.00	0.0	0.00	-4.00	0.00
14	1.00	0.0	500.00	480.00	120.00
15	1.00	0.0	0.00	201.00	50.00
16	1.00	0.0	0.00	132.00	33.00
17	1.00	0.0	0.00	344.00	86.00
18	1.00	0.0	0.00	104.00	26.00
19	1.00	0.0	0.00	376.00	94.00
20	1.00	0.0	803.00	-100.00	-25.00
21	1.00	0.0	0.00	375.00	94.00
22	1.00	0.0	0.00	-210.00	-52.00
23	1.00	0.0	979.97	129.00	32.00

* Initial Values

Table F.12 The Operating Conditions of the 23 Bus

Test System

Bus No.	Voltage p.u.	MVAR Capability	
		Min	Max
2	1.022	−30.000	194.650
3	1.021	−30.000	40.000
4	1.002	−40.000	50.000
10	0.996	−60.000	60.000
11	1.035	−40.000	189.060
14	1.050	−120.000	430.320
20	1.050	−155.000	514.130
23	1.050	−205.000	774.960

Table F.13 Voltage Regulated Bus Data of 23 Bus Test System

Send Bus	End Bus	Resistance	Reactance	Line Charging
1	3	.02420	.05400	.01180
1	4	.03090	.06930	.01510
2	5	.04040	.08880	.01970
8	5	.03250	.07090	.01570
2	7	.06150	.16200	.03420
3	6	.05760	.15200	.03200
4	9	.02660	.07000	.01480
9	7	.02290	.05040	.01120
8	6	.04460	.10030	.02180
11	10	.02330	.05140	.04560
8	10	.05970	.13150	.02910
9	10	.05970	.13150	.02910
13	14	.00430	.03510	.23730
14	12	.00430	.03510	.23730
15	12	.00380	.03070	.20780
18	15	.00350	.02880	.19510
23	13	.00890	.07200	.48710
16	17	.00100	.00800	.05430
17	18	.00210	.01670	.11330
19	18	.00160	.01270	.08620
20	19	.00450	.03620	.24510
22	18	.00240	.01920	.12980
20	21	.00190	.01560	.10560
21	22	.00140	.01140	.07700
23	16	.00200	.01640	.11090
12	8	.00230	.08390	.00000
13	8	.00230	.08390	.00000
12	9	.00185	.13000	.00000
13	9	.00230	.08390	.00000
1	2	.00250	.20000	.00000

Table F.14 Line Data of 23 Bus Test System in p.u.

on 100 MVA Base

Send Bus	End Bus	Tap Setting
12	8	1.0330
13	8	1.0500
12	9	1.0500
13	9	0.9762

Table F.15 Transformer Data of 23 Bus Test System

Send Bus	End Bus	Tap Setting
12	8	1.0330
13	8	1.0500
12	9	1.0500
13	9	0.9762

Table F.15 Transformer Data of 23 Bus Test System